AFAL-TR-64-339

Technical Report No. 158

Locked Instability and Forced Oscillations in Automatic Phase Control Systems

E. M. Aupperle

COOLEY ELECTRONICS LABORATORY

Department of Electrical Engineering
The University of Michigan

Air Force Avionics Laboratory
Research and Technology Division
Air Force Systems Command
Wright-Patterson Air Force Base, Ohio
Project 4043 Task 404302
Air Force Project Engineer
Lt. Larry J. Baumgardner

December 1964

Technical Report No. 158

LOCKED INSTABILITY AND FORCED OSCILLATIONS IN AUTOMATIC PHASE CONTROL SYSTEMS

by

E. M. Aupperle

Approved by: M. P. Ristenbatt
M. P. Ristenbatt

for

COOLEY ELECTRONICS LABORATORY
Department of Electrical Engineering
The University of Michigan
Ann Arbor, Michigan

Submitted in partial fulfillment of the requirements
for the degree of Instrumentation Engineer
in The University of Michigan

December 1964

engn
UMR0141

FOREWARD

This report was prepared by the Cooley Electronics Laboratory, The University of Michigan, Ann Arbor, Michigan on Air Force Contract No. AF 33(615)-1058, under Task No. 404302 of Project 04043. The work was administered under the direction of the Air Force Systems Command, Wright-Patterson Air Force Base, Ohio. Lt. L. Baumgardner served as the Project Engineer for the Air Force Avionics Laboratory. His assistance and guidance are gratefully acknowledged.

Acknowledgments

The author wishes to thank Professor Lawrence L. Rauch for his comments, technical guidance, and encouragement. Further, the author wishes to thank Mr. Ralph M. Olson for his patient help with the experimental portions of this work.

Special gratitude is owed to Mrs. Martha Lee Barton, Miss Dianne Bloom, and Mr. Gary Greenlee for preparing this manuscript for publication.

Finally, the author is appreciative of the support the Air Force Avionics Laboratory has given this work.

ABSTRACT

This study presents an analysis and expands the understanding of the characteristics of the periodic response from an Automatic Phase Control (APC) system that may result from:

a) A constant-frequency input signal within the system capture range when the system gain is excessive (locked instability oscillations), or

b) A pair of constant-frequency input signals, both of which occur simultaneously within the passband of the APC system (forced oscillations).

The absence of any additive random signal, such as noise, is assumed.

The above cases are treated using the same technique. First, the nonlinear differential equation is determined which describes the APC system under excitation. Second, a periodic system response function is assumed and is expressed as a Fourier series. Third, this periodic series expression is inserted into the system differential equation and the nonlinear term(s) is expanded. Finally, the dependence of the arbitrary coefficients of the assumed response function on the system parameters is found by equating the equal-frequency terms that result. Although only the constant and first harmonic terms of the assumed Fourier series are retained for the complete set of calculations, the relationships thus determined agree closely with experimental observations.

A principal result for the first of the two excitations is that minima of both system gain and phase shift are required for oscillation. The oscillation frequency, if oscillations occur, will be that (constant) frequency at which the transfer function of the system's low-pass filter has a phase shift of $-\pi/2$ radians. The magnitude of the periodic system response is an even function of the difference between the input signal frequency and the system oscillator's open-loop frequency. Its maximum magnitude occurs when the difference in these frequencies is zero, and decreases rapidly for increasing absolute values of the difference frequency. It is also shown that the static system phase error always exceeds in absolute value the error that would exist if no oscillations occurred. Finally, a technique is discussed for determining the APC system gain and the magnitude of the transfer

function of the system's lowpass filter at the frequency of oscillation from three easily performed measurements.

Forced oscillations may occur in any APC system, and the analysis is considerably more complex than with the single excitation. The frequency of oscillation is related to the difference in the frequencies of the two input signals, e.g., it may be equal to an integer multiple or submultiple of this difference. The magnitude of the response is a function of the system lowpass filter characteristic, the system gain, difference in the frequencies of the two input signals and their amplitude ratio, and the difference in the frequencies of the input signal having greater amplitude and the open-loop system oscillator signal. This dependence is portrayed using several computer-evaluated examples since a direct calculation is not feasible. The system phase error is affected somewhat by the second input signal, but is primarily dependent on the initial frequency difference as in the single excitation case.

The applications of this study are a) to provide the designer with a means for analyzing the susceptibility of his APC system to a locked periodic response, and b) to provide guidelines for the control of the locked periodic response. An example of the former is presented in detail in this study, and two examples of the latter are reviewed briefly.

TABLE OF CONTENTS

	Page
ABSTRACT	iii
LIST OF ILLUSTRATIONS	vi
LIST OF SYMBOLS	ix
SECTION 1: INTRODUCTION	1
1.1 Statement of the Problem	1
1.2 Review of the Literature	3
1.3 Method and Topics of Investigation	4
SECTION 2: MATHEMATICAL FORMULATION OF THE SUSCEPTIBILITY PROBLEM	6
2.1 Derivation of the APC System Defining Equation	6
2.2 Alternate APC System Defining Equations	9
2.3 Development of the Interference Susceptibility Equations	11
SECTION 3: LOCKED INSTABILITY OSCILLATIONS OF THE APC SYSTEM	16
3.1 Theoretical Determination of the Instability Characteristics	16
3.1.1 Instability Considerations	16
3.1.2 Characteristics of the Locked Oscillations	20
3.1.3 Stability Analysis for the Locked Oscillations	28
3.2 Experimental Comparisons with the Theoretically Determined Oscillation Characteristics	37
3.3 Comments and Conclusions	44
SECTION 4: SECONDARY SIGNAL INTERFERENCE SUSCEPTIBILITY	46
4.1 Introduction to the Interference Problem	46
4.2 Derivation of the Interference Susceptibility Coefficient Equations	47
4.3 Susceptibility Characteristics of the Ideal Integrator	51
4.4 Susceptibility Characteristics of Three Other Lowpass Filters	59
4.5 Stability Analysis of the Forced Oscillations	80
4.6 Alternate Analytical Approach	81
4.7 Case of System Insensitivity to Target Signal Amplitude	85
SECTION 5: SUPPLEMENTARY EXPERIMENTAL PROGRAM	90
5.1 Summary of the Experimental Program	90
5.2 Experimental APC System	92
5.3 Experimental and Comparative Theoretical Results	96
SECTION 6: CONCLUSIONS AND APPLICATIONS	108
APPENDIX A. Newton-Raphson Method for Simultaneous Nonlinear Equations	113
APPENDIX B. Implementation of the Newton-Raphson Method	115
APPENDIX C. Derivation of Some Fourier Coefficients	119
REFERENCES	123

LIST OF ILLUSTRATIONS

Figure		Page
1.1	The automatic phase control system.	1
3.1	The graphical solution of Eqs. 3.30 and 3.31.	24
3.2	An expansion of Fig. 3.1 near the origin.	25
3.3	β and $\Delta\theta_r$ versus $H^*\Delta\omega_r$ for $H^*G = 1.75$.	26
3.4	Experimental curves of β and $\Delta\theta_r$ versus $\Delta\omega_r$ for three input signal levels.	40
3.5	Theoretical curves of β and $\Delta\theta_r$ versus $\Delta\omega_r$ corresponding to the curves in Fig. 3.4.	41
3.6	Direct comparison of the theoretical curve and experimental points shown for the largest value of input signal levels in Figures 3.4 and 3.5.	42
3.7	Periodic system response waveforms.	43
4.1	The harmonic relation between β and $G_\infty/\tau\omega_f^2$.	53
4.2	The β values for which $G_\infty/\tau\omega_f^2$ is minimum.	54
4.3	The limiting values of β for infinite $G_\infty/\tau\omega_f^2$.	55
4.4	The first subharmonic relationship between β and $G_\infty/\tau\omega_f^2$.	56
4.5	The β characteristics for an APC system with an ideal-integrator lowpass filter.	57
4.6	The system response characteristics for an APC system with an ideal-integrator lowpass filter.	58
4.7	Characteristics of the single pole filter.	61
4.8	System response for the single pole filter with G equal to 0.956×10^5 radians/second.	62
4.9	System response for the single pole filter with G equal to 1.20×10^5 radians/second.	62
4.10	System response for the single pole filter with G equal to 1.35×10^5 radians/second.	63
4.11	Characteristics of the single pole-single zero filter.	64
4.12	System response for the single pole-single zero filter with G equal to 0.956×10^5 radians/second.	65
4.13	System response for the single pole-single zero filter with G equal to 1.20×10^5 radians/second.	65
4.14	System response for the single pole-single zero filter with G equal to 1.35×10^5 radians/second.	66

LIST OF ILLUSTRATIONS (Cont.)

Figure		Page
4.15	Characteristics of the three pole filter.	67
4.16	System response for the three pole filter with G equal to 0.956×10^5 radians/second.	68
4.17	System response for the three pole filter with G equal to 1.20×10^5 radians/second.	68
4.18	System response for the three pole filter with G equal to 1.35×10^5 radians/second.	69
4.19	$\Delta\theta_s$ characteristics for the three pole filter with G equal to 1.35×10^5 radians/second.	70
4.20	$\Delta\theta_r$ characteristics for the three pole filter with G equal to 1.35×10^5 radians/second.	71
4.21	System variables dependence on $\Delta\omega_r$ for $\Delta\omega_s/2\pi$ equal to 3 kc/sec.	73
4.22	System variables dependence on $\Delta\omega_r$ for $\Delta\omega_s/2\pi$ equal to 7 kc/sec.	74
4.23	System variables dependence on $\Delta\omega_r$ for $\Delta\omega_s/2\pi$ equal to 10 kc/sec.	75
4.24	System variables dependence on $\Delta\omega_r$ for $\Delta\omega_s/2\pi$ equal to 12 kc/sec.	76
4.25	System variables dependence on $\Delta\omega_r$ for $\Delta\omega_r/2\pi$ equal to 12.9 kc/sec.	77
4.26	System variables dependence on $\Delta\omega_r$ for $\Delta\omega_s/2\pi$ equal to 15 kc/sec.	78
4.27	System response as a function of $\Delta\omega_r$ and $\Delta\omega_s$.	79
4.28	The harmonic relation between β and $G'_\infty/\tau\Delta\omega_s^2$.	89
5.1	Experimental test configuration.	91
5.2	APC system circuit diagram.	93
5.3	The experimental APC system.	94
5.4	System oscillator frequency versus voltage relation.	95
5.5	System magnitude response for the experimental circuit with G equal to 1.355×10^5 radians/second.	97
5.6	System magnitude response for the experimental circuit with G equal to 1.685×10^5 radians/second.	98
5.7	System magnitude response for the experimental circuit with G equal to 1.89×10^5 radians/second.	99
5.8	Periodic forced system response waveforms.	101
5.9	Periodic forced system response waveforms.	102
5.10	Periodic forced system response waveforms.	103
5.11	Characteristics of the two-pole filter.	104
5.12	System magnitude response for the two-pole filter with G equal to 1.335×10^5 radians/second.	105

LIST OF ILLUSTRATIONS (Cont.)

Figure		Page
5.13	System magnitude response for the two-pole filter with G equal to 1.685×10^5 radians/second.	106
5.14	System magnitude response for the two-pole filter with G equal to 1.89×10^5 radians/second.	107
B.1	Flow chart of the Newton-Raphson method program.	116

LIST OF SYMBOLS

Symbol	Description	First Used on Page
A	A constant matrix	30
E_o	System oscillator signal peak magnitude	6
E_r	Reference signal peak magnitude	6
E_s	Secondary signal peak magnitude	6
E_t	Constant bias voltage	6
F_x	A nxn matrix with columns defined by $\partial\hat{F}/\partial x$; $(i, =1,2, \ldots, n)$	29
$\hat{F}$	A column vector of functions dependent on $\hat{x}$ and possibly t	29
H^*	A real constant defined by $H^* = \lvert\overline{H}(\omega_f)\rvert/\omega_f$	23
$H(s)$	The APC system transfer function	4
$H(\omega)$	The APC system transfer function	7
$\overline{H}(\omega)$	The normalized system transfer function, i.e., $\overline{H}(\omega) = H(\omega)/H(0)$	8
G	The APC system zero frequency gain (input signal amplitude sensitive case)	8
G'	The APC system zero frequency gain (input signal amplitude insensitive case)	10
G_∞	The APC system gain for an ideal integrator lowpass filter	20
$M(\hat{x})$	A matrix with elements $f_{ij}(\hat{x})$, $(i, j=1,2, \ldots, n)$	113
T	The fundamental period of $\hat{\phi}(t)$	30
a	A complex constant	4
$a_1, \ldots, a_4$	Four real constants	31
b	A complex constant	4
c	An arbitrary real constant	30
c_p	$(p=0,1,2,\ldots)$ The unknown amplitude coefficients of the assumed Fourier series representing the system response	11
$f_{ij}(\hat{x})$	The ij-th element of $M(\hat{x})$ defined by $f_{ij}(\hat{x}) = \partial\hat{f}(\hat{x})/\partial x_j$	113

LIST OF SYMBOLS (Cont.)

Symbol	Description	First Used on Page
$\hat{f}$	A column vector of functions dependent on $\hat{x}$	113
i	An integer variable (i=1,2, ..., n) used as a subscript	29
k	As a real variable defined by $2\sqrt{n}/1+n$	82
k	As an integer variable (k=1,2,3,...) used as a subscript	30
k_m	The gain constant of the system multiplier (phase detector)	7
k_m'	A real constant associated with the multiplier (phase detector)	7
k_o	Gain constant of the system oscillator	7
m	An integer variable: (m=1,2,3,...)	49
n	As a constant: a given positive integer	29
n	As an integer variable: (n=1,2,3,...)	49
p	An integer variable (p=1,2,3,...) used as a subscript	11
s	A complex variable	4
t	An independent variable; time in seconds	6
t'	An independent variable: time in seconds	13
t_o	A real constant: dimensionally seconds	13
t_1 and t_2	Two specific values of time	30
$\hat{x}$	A column vector of dependent variables which are functions of time	29
$\hat{y}$	A column vector of dependent variables which are functions of time	
$\Delta\theta_r$	A phase constant defined by $\Delta\theta_r = \theta_r' - \theta_o$	14
$\Delta\theta_{rc}$	The critical value of $\Delta\theta_r$ for which β becomes zero for any fixed value of gain	38
$\Delta\theta_{ro}$	An initial estimate of $\Delta\theta_r$ required by the Newton-Raphson method.	115
$\Delta\theta_s$	A specific phase angle defined by $\Delta\theta_s = \Delta\theta_r - \Delta\omega_s/\omega_f\theta_1$	48
$\Delta\theta_{so}$	An initial estimate of $\Delta\theta_s$ required by the Newton-Raphson method	115

LIST OF SYMBOLS (Cont.)

Symbol	Description	First Used on Page
$\Delta\omega_r$	Essentially the difference in the radian frequencies of the reference and open-loop system oscillator signals. Specifically, $\Delta\omega_r = \omega_r - \omega_o - k'_m G/k_m$	14
$\Delta\omega'_r$	Essentially, the reference and open-loop system oscillator signals. Specifically, $\Delta\omega'_r = \omega_r - \omega_o - k'_m G'/k_m$	15
$\Delta\omega_{rc}$	The critical value of $\Delta\omega_r$ for which β becomes zero for any fixed value of gain	38
$\Delta\omega_s$	The difference in the radian frequencies of the secondary and reference signals, i.e., $\Delta\omega_s = \omega_s - \omega_r$	12
$\Omega(\omega_f)$	A real variable representing phase shift as a function of ω_f	50
α_1 and α_2	A pair of real variables	86
β	A real dimensionless variable defined by $\beta = k_o e_1/\omega_f$	21
β^*	A specific value of β	52
β_{max}	The maximum value of β for any fixed system gain	38
β_o	An initial estimate of β required by the Newton-Raphson method	115
γ	A dimensionless real constant constrained by $0 \leq \gamma \leq 1$	17
ε	An arbitrary real positive constant	30
$\varepsilon(t)$	System response function	2
$\varepsilon(t)_{rms}$	The rms value of $\varepsilon(t)$	37
η	The ratio E_s/E_r	6
η_i	The i-th arbitrary constant (i=1,2,...,n)	35
θ_o	An integration constant	12
θ_p	(p=1,2,3, ...) The unknown phase coefficients of the assumed Fourier series representing the system response	11
θ_r	Reference signal phase angle	6
θ'_r	A real constant: dimensionally radians	13
ϑ_s	Secondary signal phase angle	12

LIST OF SYMBOLS (Cont.)

Symbol	Description	First Used on Page
$\theta_o(t)$	System phase error	6
$\theta_r(t)$	Reference signal phase function	6
$\theta_s(t)$	Secondary signal phase function	6
λ	An unknown complex variable	18
λ_i	The i-th associated multiplier, defined by $\lambda_i = e^{\rho_i T}$ (i=1,2, ..., n)	30
μ	A real variable	30
ρ_i	The i-th characteristic exponent (i=1,2, ..., n)	30
τ	An arbitrary positive time constant	17
τ_1, τ_2	A pair of arbitrary positive time constants	19
ϕ	The singular point values of $\phi(t)$ found from the APC system defining equations	16
ϕ_p	The principal value of ϕ	16
ϕ_{np}	A nonprincipal value of ϕ	17
$\phi(t)$	A phase function defined by $\phi(t) = \theta_r(t) - \theta_o(t)$	8
$\overline{\phi}(t)$	A phase function defined by $\overline{\phi}(t) = \phi(t) - \phi_p$	17
$\hat{\phi}(t)$	A column vector representing the real solution of a system of equations	29
$\hat{\phi}^*(t)$	A column vector representing the real solution of a system of equations	30
$\psi(t)$	A phase function defined by $\psi(t) = \theta_s(t) - \theta_r(t)$	10
ω	Independent variable: radian frequency in radians per second	7
ω_f	The fundamental radian frequency of the periodic response	11
ω_o	System oscillator open-loop radian frequency	6
ω_o'	The zero-bias, radian frequency of the system oscillator	7
ω_r	Reference signal radian frequency	6
ω_s	Secondary signal radian frequency	12

1. INTRODUCTION

1.1 Statement of the Problem

The response of the Automatic Phase Control (APC) system to certain classes of input signals with and without additive wideband noise has been studied extensively. Nevertheless, the many nuances in the analysis of this relatively simple nonlinear feedback system reveal why some questions remain to be answered in greater detail. This study presents an analysis and expands our understanding of the characteristics of the periodic response that may result from:

a) A constant-frequency input signal within the system capture range when the system gain is excessive, or

b) A pair of constant-frequency input signals, both of which occur within the passband of the APC system, i.e., the secondary-signal interference problem.

The absence of any random signal, such as noise, is assumed for the purposes of this study.

Before expanding this statement of the problem, it is helpful to review briefly the operation of the APC system. The elements of the system are shown in the block diagram of Fig. 1.1. In the usual analysis, a single input signal (also referred to as the reference

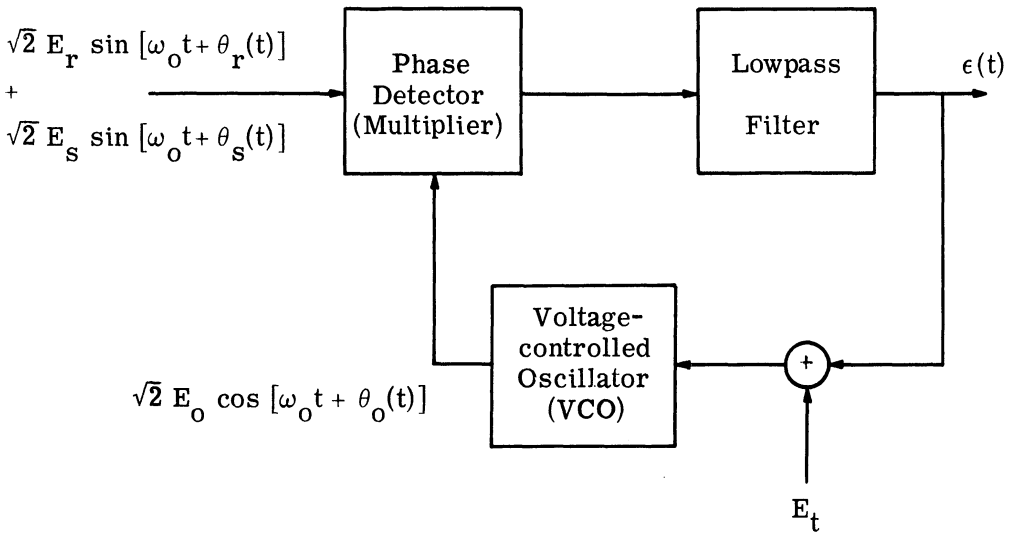

Fig. 1.1 The automatic phase control system

Manuscript released by author December, 1964 for publication as a RTD Technical Report.

signal) is multiplied by the voltage-controlled, system-oscillator signal to produce an error signal proportional to the sine of the phase difference between the two phase-detector input signals. This error signal may then be modified by a linear lowpass filter, and, along with a constant tuning voltage, used to control the system oscillator. When the APC system is operating ideally, the system response function, $\varepsilon(t)$, (i.e., the output from the lowpass filter) is related linearly to the instantaneous frequency of the reference signal. Since the system oscillator is designed to have its instantaneous frequency related linearly to $\varepsilon(t)$, the instantaneous phase difference between the system oscillator and the reference signals must be constant. Thus, the APC system response, $\varepsilon(t)$, is said "to track," "to be synchronized with," or "to be locked to" the reference signal frequency. The characteristics of the lowpass filter greatly influence the performance of the APC system. Among other things, the filter limits the system bandwidth and restricts the type of input signals which the system can track satisfactorily. For further details concerning typical APC system operation, the reader is referred to Refs. 1-12.

It is easy to understand why the APC system may be unstable for large system gains. Since the system oscillator already effects one ideal integration in the feedback loop, it is only necessary for the remainder of the loop to provide, at a finite frequency, an additional phase-shift of $-\pi/2$ radians to produce potential instability. Indeed, the lowpass filter usually introduces a substantial fraction, if not all, of the required, additional, negative phase shift. Stray circuit and/or component capacitance can also be counted on to provide negative phase shift.

If the APC system does have a total phase shift of $-\pi$ radians at a finite frequency, then the same system having sufficiently large gain will be unstable. It is easy to show (see Section 2) that, for some APC system designs, the system gain is proportional to the amplitude of the input signal. Hence, in these cases, the system is large-signal-unstable when sufficient negative phase shift is present.

This study demonstrates that the instability described above results in a periodic system response which will be referred to as "locked-instability oscillations." The relations are determined among this periodic system response, the system phase error, the system gain, the lowpass filter, and the difference in frequencies of the reference and the open-loop system oscillator signals.

A periodic response function is also obtained, in general, when a pair of constant-frequency input signals is present in the passband of an APC system. This oscillation results from the two input signals, in contradistinction to the locked-instability

oscillation of the previous case and as such represents the response to a periodic forcing function. Therefore, no specific amount of phase shift and/or gain is necessary for the periodic system response to occur. It also follows that the response is dependent on the particular lowpass filter transfer function used; as a result, the influence of specific transfer functions must be studied individually.

Several questions concerning the behavior of the APC system to the double input signal case quickly arise. How does the performance of the APC system compare with that of the conventional FM detector (the limiter-discriminator)? Can a periodic response exist at a frequency not equal to the difference in the frequencies of the two input signals? What maximum amplitude (if it exists) can the periodic response have for various ratios of the input signal amplitudes as the difference in input frequencies is varied? How is the periodic response affected by variation in the system gain?

This study analyzes the forced periodic response of the APC system to a pair of constant-frequency input signals and answers the questions raised above. This is accomplished by determining the relationship of the periodic response to the various independent parameters.

1.2 Review of the Literature

In 1949, J. Granlund (Ref. 13) analyzed the interference resulting from the simultaneous reception of two frequency-modulated signals by the limiter-discriminator FM detector. He employed quasi-stationary analysis of this co-channel interference problem to show that the interference signal frequency was equal to the difference in the frequencies of the two input signals. The magnitude of the interference signal was also shown to be proportional to the difference of input frequencies for any fixed ratio of input signal magnitudes. Granlund proved, both analytically and experimentally, that with proper limiter-discriminator design, the stronger signal could substantially suppress the weaker signal (30-db suppression with a 0.5-db difference in input signal strength). Although his paper does not directly apply to the APC system, it is a related device and affords an interesting comparison (see Section 4).

Most of the early applications of the APC system focused on the horizontal-sweep and color subcarrier synchronization circuits in television receivers. Consequently, numerous papers appeared in the early nineteen-fifties treating the acquisition and tracking ability of the APC system to pulsed television synchronization signals (Refs. 1, 2, 14 and 15). Later treatments were concerned with:

a. Precision frequency control of high-power oscillators,

b. spectral purity exceeding the reference; e.g., selecting one of many reference frequency harmonics,

c. tracking frequency changing references.

Papers, which appeared after the mid nineteen-fifties, described the APC system response to signal-plus-noise environments, threshold effects, additional work on acquisition and tracking, and transient behavior (Refs. 3-12 and 16).

The first mention of potential APC system instability for a constant frequency reference with excessive loop gain was made by A. J. Viterbi in 1959 (Ref. 4). He found that, for a lowpass filter transfer function of the form

$$H(s) = 1 + \frac{a}{s} + \frac{b}{s^2}, \tag{1.1}$$

where a and b are appropriate constants, the system would become unstable for sufficiently high values of b. However, he did not pursue the matter to investigate the nature of the system response when it is thus unstable.

In 1960, T. J. Rey published a paper (Ref. 6) in which he demonstrated that a periodic response did occur for a constant frequency input signal within the system capture range. He derived a pair of equations characterizing this oscillation and indicated that the response is nearly sinusoidal for a system gain just in excess of the critical level. In this study the same analytical techniques as Rey used were employed, but a somewhat different pair of equations were found. The significance of these equations has also been expanded.

The secondary signal problem was briefly considered by C. S. Weaver (Ref. 7) in 1961. He asserts, without proof, that an interfering signal affects the APC system preceded by a limiter and a standard FM discriminator similarly. That is, the stronger signal (even if only incrementally) will completely capture the APC system. He shows that when the interference signal is weaker than the signal to be tracked, the loop tracking range is reduced. His results are obtained using standard linear operational techniques on a linearized APC system model. The results here do not overlap his, and are principally concerned with the characteristics of the output response as a function of the various system parameters.

1.3 Method and Topics of Investigation

The following technique is used to analyze both of the problems discussed in this study. First, the differential equation describing the loop operation is written for the

system shown in Fig. 1.1. Second, a periodic response function (in the form of a Fourier series) is assumed and inserted into the system differential equation. Finally, the dependence of the arbitrary coefficients of the response function (the form of which has been assumed) on the system parameters is found by equating terms of equal frequency. (T. J. Rey (Ref. 6) used this technique for a portion of his analysis.) The first and second steps of the above-described mathematical formulation are discussed in Section 2.

Section 3 contains a treatment of the locked-instability problem as a special case of the interference problem, i.e., the case where the magnitude of the second input signal is reduced to zero. The necessary and sufficient conditions for the occurrence of a periodic response are discussed. The magnitude of the response is shown to depend on the system gain, the difference in frequencies of the input and oscillator signals when the system loop is opened, and the frequency at which the lowpass filter has a phase-shift of $-\pi/2$ radians. It is also shown that the static system phase error always exceeds in absolute value the error that would exist if no periodic response occurred. The theoretically derived results are then compared with experimental results for a particular lowpass filter.

The two-input signal problem is examined in Section 4. Since the character of the periodic response is dependent on the transfer function of the lowpass filter, it is necessary to examine specific examples. First the ideal-integrator case is analyzed by a graphical technique. The results of this aid in understanding the influence of other possible lowpass filters. The influences of three other lowpass filters are studied using a digital-computer solution of the coefficient equations derived in part in Section 2 and concluded in the earlier portion of Section 4. This solution is evaluated by means of the Newton-Raphson method for simultaneous non-linear equations.

Sections 5 and 6, respectively, consider experimental details and data (including a comparison between an experimental and analytical study of a fourth filter), and some potential applications and conclusions based on this study.

Appendix A briefly describes the mathematical basis of the Newton-Raphson method used for the computations required in Section 4, while Appendix B provides the implementation details of the particular routine employed in this study. In Appendix C, the two sets of Fourier coefficients required in Section 4 are derived.

2. MATHEMATICAL FORMULATION OF THE SUSCEPTIBILITY PROBLEM

2.1 Derivation of the APC System Defining Equation

The well-known APC system model shown in Fig. 1.1 is characterized by an ordinary, nonlinear, differential equation of arbitrary order, and hence its complete analysis is impossible with present mathematical methods. The characteristics of the lowpass filter can be shown to determine the order of the system differential equation. Thus, system behavior is primarily a function of the lowpass filter.

Let us now consider the form of the system equation when the input signal to the APC system consists of a phase-modulated reference signal of E_r^2 watts and a phase-modulated secondary signal of E_s^2 watts. The combination may be, in general, represented by

$$\sqrt{2}\, E_r \sin[\omega_o t+\theta_r(t)] + \sqrt{2}\, E_s \sin[\omega_o t+\theta_s(t)] \ , \tag{2.1}$$

where ω_o is the radian center frequency of the APC system oscillator under open-loop conditions (when the oscillator input voltage is simply E_t). $\theta_r(t)$ and $\theta_s(t)$, respectively, are phase functions of the reference and secondary signals. For example, if the reference signal has a constant radian frequency of ω_r with an initial phase angle of θ_r, then

$$\theta_r(t) = (\omega_r - \omega_o)\, t+\theta_r \tag{2.2}$$

E_s is set equal to nE_r and the input signal is rewritten as

$$\sqrt{2}\, E_r \left\{ \sin[\omega_o t+\theta_r(t)] + n \sin[\omega_o t+\theta_s(t)] \right\}. \tag{2.3}$$

The APC system oscillator signal may be expressed by

$$\sqrt{2}\, E_o \cos[\omega_o t+\theta_o(t)] \ , \tag{2.4}$$

where $\theta_o(t)$ is the system phase error. This locally generated signal is multiplied by the input signal in the phase detector to yield a voltage expressed by

$$k_m E_r E_o \Big\{ \sin[2\omega_o t + \theta_r(t) + \theta_o(t)] + n \sin[2\omega_o t + \theta_s(t) + \theta_o(t)] + \sin[\theta_r(t) - \theta_o(t)] + n \sin[\theta_s(t) - \theta_o(t)] \Big\} , \tag{2.5}$$

where k_m is the gain (or loss) constant of the multiplier and is dimensionally $(\text{voltage})^{-1}$. Typically, the phase detector output is filtered (prior to the system lowpass filter) to the extent that the sum terms in expression 2.5 may be neglected. It is thus convenient, although not necessary, to view the phase detector as having an ideal lowpass filter output with a gain k_m and a cutoff frequency higher than the highest difference frequency but lower than the least sum frequency. In this event, the APC system lowpass filter input may be expressed by

$$k_m E_r E_o \Big\{ \sin[\theta_r(t) - \theta_o(t)] + n \sin[\theta_s(t) - \theta_o(t)] \Big\} + k_m' E_r E_o , \tag{2.6}$$

where the last term is used to account for any constant offset generated in the multiplier. k_m' is also dimensionally $(\text{voltage})^{-1}$.

Let the system lowpass filter have a transfer function $H(\omega)$. Then the system response, $\varepsilon(t)$, is, in practice, given by

$$\varepsilon(t) = k_m' E_r E_o H(0) + k_m E_r E_o H(\omega) \Big\{ \sin[\theta_r(t) - \theta_o(t)] + n \sin[\theta_s(t) - \theta_o(t)] \Big\} . \tag{2.7}$$

The system response is added to a constant bias voltage, E_t; the resulting sum voltage controls the instantaneous frequency of the voltage-controlled system oscillator (see Fig. 1.1). Since it is possible to design an oscillator whose frequency is linearly proportional to the applied voltage, such a relationship will be assumed. Thus, the instantaneous radian frequency of the system oscillator may be expressed as (from expression 2.4)

$$\omega_o + \dot{\theta}_o(t) = k_o[E_t + \varepsilon(t)] + \omega_o' , \tag{2.8}$$

where k_o is the gain constant of the system oscillator expressed in radians/volt and ω_o' is the zero-bias, radian frequency. Consequently, ω_o, the radian frequency of the system oscillator under open-loop conditions, is equal to

$$\omega_o = k_o E_t + \omega_o' \quad , \tag{2.9}$$

and so

$$\dot{\theta}_o(t) = k_o \varepsilon(t) \quad . \tag{2.10}$$

Substitution of Eq. 2.7 into Eq. 2.10 produces

$$\dot{\theta}_o(t) = k_o k_m' E_r E_o H(0) + k_o k_m E_r E_o H(\omega) \Big\{ \sin[\theta_r(t) - \theta_o(t)] + \eta \sin[\theta_s(t) - \theta_o(t)] \Big\} \quad . \tag{2.11}$$

If a differential phase function, $\phi(t)$, is defined by

$$\phi(t) = \theta_r(t) - \theta_o(t) \quad , \tag{2.12}$$

then Eq. 2.11 can be expressed alternately as

$$\dot{\theta}_r(t) - k_o k_m' E_r E_o H(0) = \dot{\phi}(t) + k_o k_m E_r E_o H(\omega) \Big\{ \sin[\phi(t)] + \eta \sin[\phi(t) + \theta_s(t) - \theta_r(r)] \Big\} , \tag{2.13}$$

and, further defining,

$$G = k_o k_m E_r E_o H(0) \quad , \tag{2.14}$$

$$\overline{H}(\omega) = H(\omega)/H(0) \quad , \tag{2.15}$$

Then Equation 2.13 becomes

$$\dot{\theta}_r(t) - \frac{k_m'}{k_m} G = \dot{\phi}(t) + G \overline{H}(\omega) \Big\{ \sin[\phi(t)] + \eta \sin[\phi(t) + \theta_s(t) - \theta_r(t)] \Big\} . \tag{2.16}$$

Equation 2.16 is the fundamental differential equation for the operation of the APC system when all noise effects except the interfering secondary signal are neglected.

In concluding this section, it is useful to point out that the order of Eq. 2.16 exceeds by one the degree of the denominator of $H(\omega)$. Thus, the second-degree transfer function given by Eq. 1.1 and analyzed by Viterbi (Ref. 4) results in a third-order differential equation. Even this complexity precludes analysis by the conventional phase-plane technique. The APC system properties with various lowpass filter combinations and with η equal to zero have been extensively studied (see, for example, Refs. 3, 4, 5, 9 and 17).

2.2 Alternate APC System Defining Equations

In certain applications of the APC system, a balanced phase detector is used which is nearly insensitive to input-signal amplitude variation (Refs. 1 and 2). In this case, Eq. 2.16 is invalid because the loop gain constant expressly contains the reference-signal amplitude, and the secondary-signal amplitude is seen to modulate the loop gain periodically. To account for these effects, another treatment of the input signal can be employed; this is shown by the following development.

The input signal given by expression 2.3 is repeated here for convenience

$$\sqrt{2}\, E_r \left\{ \sin[\omega_o t + \theta_r(t) + \eta \sin[\omega_o t + \theta_s(t)] \right\} . \tag{2.17}$$

By applying trigonometric identities, it is not difficult to show (see, for example, Ref. 18) that Eq. 2.17 is equivalent to

$$\sqrt{2}\, E_R \sqrt{1+\eta^2+2\eta \cos[\theta_s(t) - \theta_r(t)]}\, \sin\left\{ \omega_o t + \theta_r(t) + \tan^{-1} \right.$$

$$\left. \frac{\eta \sin[\theta_s(t) - \theta_r(t)]}{1+\eta\cos[\theta_s(t) - \theta_r(t)]} \right\}. \tag{2.18}$$

This expression for the input signal is illuminating in two ways. First, the dependence of the input signal amplitude variation on η and on the instantaneous phase <u>difference</u> of the two signals is seen more specifically than in expression 2.17. Second, the instantaneous frequency of expression 2.18 is obtained by differentiating the argument of the sine function to yield

$$\omega_o + \dot{\theta}_r(t) + \eta[\dot{\theta}_s(t) - \dot{\theta}_r(t)] \; \frac{\eta + \cos[\theta_s(t) - \theta_r(t)]}{1+\eta^2+2\eta \cos[\theta_s(t) - \theta_r(t)]} . \tag{2.19}$$

Expression 2.19 indicates that the instantaneous frequency is influenced, as is the amplitude, by η and the differences in phase and frequency of the input signals. These observations suggest introducing another phase function $\psi(t)$ defined by

$$\psi(t) = \theta_s(t) - \theta_r(t) \tag{2.20}$$

which permits rewriting expressions 2.18 and 2.19, respectively, as

$$\sqrt{2}\, E_r \sqrt{1+\eta^2+2\eta\cos\psi(t)}\, \sin\left[\omega_o t + \theta_r(t) + \tan^{-1}\frac{\eta\sin\psi(t)}{1+\eta\cos\psi(t)}\right] \tag{2.21}$$

and

$$\omega_o + \dot{\theta}_r(t) + \eta\dot{\psi}(t)\,\frac{\eta+\cos\psi(t)}{1+\eta^2+2\eta\cos\psi(t)}\,. \tag{2.22}$$

If the APC system is made insensitive to the input-signal amplitude, expression 2.21 may be replaced by

$$\sqrt{2}\,\sin\left[\omega_o t + \theta_r(t) + \tan^{-1}\frac{\eta\sin\psi(t)}{1+\eta\cos\psi(t)}\right], \tag{2.23}$$

where $\sqrt{2}$ is retained for subsequent convenience. Observe that this modified input-signal expression is equivalent to a single, phase-modulated reference signal expression. The implications of this equivalence are discussed in Section 4.

The two input-signal expressions, 2.21 and 2.23, can now be used in conjunction with the APC system oscillator signal expression (2.4) to obtain alternate system equations. Since the procedure of these derivations is identical to that of the derivation given in Section 2.1, only the results are presented here.

The defining equation for an input-signal-amplitude insensitive system is

$$\dot{\theta}_r(t) - \frac{k'_m}{k_m}G' = \dot{\phi}(t) + G'\,\overline{H}(\omega)\,\sin\left[\phi(t) + \tan^{-1}\frac{\eta\sin\psi(t)}{1+\eta\cos\psi(t)}\right], \tag{2.24}$$

where

$$G' = k_o k_m E_o H(0)\,. \tag{2.25}$$

and k_m and k_m' are dimensionless.

The defining equation for a system with gain proportional to the input-signal amplitude is

$$\dot{\theta}_r(t) - \frac{k_m'}{k_m} G = \dot{\phi}(t) + G\,\overline{H}(\omega)\sqrt{1 + \eta^2 + 2\eta\cos\psi(t)}$$

$$\cdot \sin\left[\phi(t) + \tan^{-1}\frac{\eta\sin\psi(t)}{1 + \eta\cos\psi(t)}\right], \tag{2.26}$$

which is equivalent to (repeating Eq. 2.16)

$$\dot{\theta}_r(t) - \frac{k_m'}{k_m} G = \dot{\phi}(t) + G\,\overline{H}(\omega)\left\{\sin\phi(t) + \eta\sin[\phi(t) + \psi(t)]\right\}. \tag{2.27}$$

In concluding this section it is worthwhile to review briefly the assumptions implicit in Eqs. 2.24, 2.26 and 2.27.

1. The phase detector has a constant gain over the entire frequency range of the system response.
2. The system response consists only of the difference-frequency-signal terms resulting from the multiplication action of the phase detector. This may be thought of as a consequence of the phase detector and/or the system lowpass filter characteristics.
3. The voltage-controlled system oscillator has a linear frequency variation as a function of applied voltage.

These assumptions are neither particularly restrictive nor difficult to achieve in practice.

2.3 Development of the Interference Susceptibility Equations

Under certain conditions, a periodic response occurs in the APC system while the system is locked in average frequency to the reference signal. The characteristics of the steady-state solution can then be determined from the system equation in the following way. Let

$$\varepsilon(t) = e_o + \sum_{p=1}^{\infty} e_p \cos\,(p\omega_f t + \theta_p) \quad , \tag{2.28}$$

where ω_f is the fundamental radian frequency of the periodic response and the e_p and θ_p are constants to be determined from the system equation. Dimensionally, the e_p are expressed

in volts and the θ_p in radians. From Eq. 2.10, it follows that

$$\dot{\theta}_o(t) = k_o e_o + k_o \sum_{p=1}^{\infty} e_p \cos (p\omega_f t + \theta_p) \quad , \tag{2.29}$$

and, upon integration,

$$\theta_o(t) = \theta_o + k_o e_o t + k_o \sum_{p=1}^{\infty} \frac{e_p}{p\omega_f} \sin (p\omega_f t + \theta_p) \quad , \tag{2.30}$$

where θ_o is the integration constant.

From this point on, it is mathematically convenient to restrict the two input signals to sinusoids. Let

$$\sqrt{2}\, E_r \sin[\omega_o t + \theta_r(t)] = \sqrt{2}\, E_r \sin[\omega_r t + \theta_r] \quad , \tag{2.31}$$

$$\sqrt{2}\, E_s \sin[\omega_o t + \theta_s(t)] = \sqrt{2}\, E_s \sin[\omega_s t + \theta_s], \tag{2.32}$$

where ω_r and ω_s are the respective radian frequencies, and θ_r and θ_s are the respective phase angles of the two input signals. This requires that

$$\theta_r(t) = (\omega_r - \omega_o)\, t + \theta_r \quad , \tag{2.33}$$

$$\theta_s(t) = (\omega_s - \omega_o)\, t + \theta_s \quad . \tag{2.34}$$

Thus, in this case, the instantaneous phase difference between the two input signals becomes (see Eq. 2.20)

$$\psi(t) = \Delta\omega_s t + \theta_s - \theta_r \quad , \tag{2.35}$$

where

$$\Delta\omega_s = \omega_s - \omega_r \quad . \tag{2.36}$$

A linear transformation in the independent variable t simplifies some of the subsequent

equations. Let

$$t' = t + t_o \quad , \tag{2.37}$$

where t_o is such that

$$\psi(t') = \Delta\omega_s(t' - t_o) + \theta_s - \theta_r = \Delta\omega_s t' \tag{2.38}$$

or

$$t_o = \frac{\theta_s - \theta_r}{\Delta\omega_s} \quad . \tag{2.39}$$

Equation 2.33 then becomes

$$\theta_r(t') = (\omega_r - \omega_o)\, t' - \left(\frac{\omega_r - \omega_o}{\Delta\omega_s}\right)(\theta_s - \theta_r) + \theta_r \tag{2.40}$$

or

$$\theta_r(t') = (\omega_r - \omega_o)\, t' + \theta_r' \quad , \tag{2.41}$$

where

$$\theta_r' = \theta_r - \left(\frac{\omega_r - \omega_o}{\Delta\omega_s}\right)(\theta_s - \theta_r) \quad . \tag{2.42}$$

In the following equations, the system time reference will be t', though the prime will be dropped from t' for convenience.

From Eqs. 2.12, 2.30, and 2.41, $\phi(t)$ is found to be[1]

$$\phi(t) = (\omega_r - \omega_o)\, t + \theta_r' - \theta_o - k_o\, e_o t - k_o \sum_{p=1}^{\infty} \frac{e_p}{p\omega_f} \sin(p\omega_f t + \theta_p) \quad , \tag{2.43}$$

from which $\dot{\phi}(t)$ is obtained by differentiation

[1]Note that Eq. 2.30 may be substituted here without a time translation, since its coefficients are yet to be determined.

$$\dot{\phi}(t) = \omega_r - \omega_o - k_o e_o - k_o \sum_{p=1}^{\infty} e_p \cos(p\omega_f t + \theta_p) \quad . \tag{2.44}$$

When the APC system is locked in average frequency to the reference signal, it follows, from Eq. 2.44, that

$$e_o = \frac{\omega_r - \omega_o}{k_o} \, . \tag{2.45}$$

Under this last condition, Eqs. 2.38, 2.43, and 2.44, and the derivative of Eq. 2.41 may be substituted into Eq. 2.27 to yield

$$\begin{aligned} \Delta\omega_r = {} & -k_o \sum_{p=1}^{\infty} e_p \cos(p\omega_f t + \theta_p) \\ & + G\,\overline{H}(\omega) \left\{ \sin\left[\Delta\theta_r - k_o \sum_{p=1}^{\infty} \frac{e_p}{p\omega_f} \sin(p\omega_f t + \theta_p)\right] \right. \\ & \left. + \eta \sin\left[\Delta\theta_r - k_o \sum_{p=1}^{\infty} \frac{e_p}{p\omega_f} \sin(p\omega_f t + \theta_p) + \Delta\omega_s t\right] \right\} , \end{aligned} \tag{2.46}$$

where

$$\Delta\omega_r = \omega_r - \omega_o - \frac{k'_m}{k_m} G \quad , \tag{2.47}$$

$$\Delta\theta_r = \theta'_r - \theta_o \quad . \tag{2.48}$$

The same substitutions into the equivalent equation (2.26) lead to

$$\begin{aligned} \Delta\omega_r = {} & -k_o \sum_{p=1}^{\infty} e_p \cos(p\omega_f t + \theta_p) + G\,\overline{H}(\omega) \sqrt{1+\eta^2+2\eta\cos(\Delta\omega_s t)} \\ & \cdot \sin\left[\Delta\theta_r - k_o \sum_{p=1}^{\infty} \frac{e_p}{p\omega_f} \sin(p\omega_f t + \theta_p) + \tan^{-1} \frac{\eta \sin(\Delta\omega_s t)}{1+\eta\cos(\Delta\omega_s t)}\right] , \end{aligned} \tag{2.49}$$

and into the input-amplitude-insensitive system equation (2.24) lead to

$$\Delta\omega_r' = -k_o \sum_{p=1}^{\infty} e_p \cos(p\omega_f t + \theta_p) + G' \overline{H}(\omega) \sin\left[\Delta\theta_r - k_o \sum_{p=1}^{\infty} \frac{e_p}{p\omega_f} \right.$$

$$\left. \cdot \sin(p\omega_f t + \theta_p) + \tan^{-1} \frac{\eta \sin(\Delta\omega_s t)}{1+\eta \cos(\Delta\omega_s t)} \right], \qquad (2.50)$$

where

$$\Delta\omega_r' = \omega_r - \omega_o - \frac{k_m'}{k_m} G' \quad . \qquad (2.51)$$

Equations 2.46, 2.49, and 2.50 are the general, interference-susceptibility equations for the APC system. It will be recalled that the arbitrary constants, e_p and θ_p, are to be determined by equating equal-frequency terms of these equations. Note that e_o has already been found (Eq. 2.45) and that θ_o is contained in $\Delta\theta_r$. Further consideration of these equations will be presented in Sections 3 and 4.

The additional assumptions implicit in Eqs. 2.46, 2.49, and 2.50, relative to the more general system equations 2.24, 2.25, and 2.27, are:

1. The possible existence of a steady-state system response.
2. The ability to express the steady-state solution in terms of a Fourier series.
3. Restriction of the two input signals to sinusoidal (constant frequency) waveforms.
4. The ability of the APC system to lock to the reference signal in average frequency simultaneously with the occurrence of a periodic response.

The third assumption above is imposed to facilitate the mathematical formulation. Granlund (Ref. 13) used the same technique in his treatment of the interference problem for the conventional FM discriminator. The first and fourth assumptions will be discussed in Sections 3 and 4. The second assumption follows from the first and the fact that the system response is continuous.

3. LOCKED INSTABILITY OSCILLATIONS OF THE APC SYSTEM

3.1 Theoretical Determination of the Instability Characteristics

The existence of a periodic response, when only a single, constant-frequency input signal is present, is dependent on both the APC system lowpass filter characteristic and loop gain. This dependence is characterized in this section by analyzing first the conditions necessary for system instability (failure to maintain a constant voltage proportional to the constant frequency of the input signal). Then it is shown that, for small oscillations and with a particular filter, the same conditions are compatible with a stable periodic response. In the process, the characteristics of the APC system periodic response are found, and the general technique for determining the stability of a periodic response is discussed.

3.1.1 Instability Considerations. Under the condition that the input signal to the APC system is a constant frequency sinusoid, the system defining equations, (2.26) and (2.27), both reduce to

$$\Delta\omega_r = \dot{\phi}(t) + G\,\overline{H}(\omega)\,\sin\phi(t) \quad , \tag{3.1}$$

where $\Delta\omega_r$ is obtained from Eqs. 2.41 and 2.47. For the analysis in this section the gain, G, may be thought of as either dependent or independent of the reference-signal amplitude since only the value of gain and not its origin is significant. In this sense, Eq. 2.24 is equivalent to Eqs. 2.26 and 2.27 and also has the reduced form given by Eq. 3.1.

When the lowpass filter transfer function has a finite value at zero frequency, Eq. 3.1 has singular points at (all) the solutions of

$$\phi = \sin^{-1}\frac{\Delta\omega_r}{G} \tag{3.2}$$

and with all of the derivatives of ϕ identically equal to zero. Let the principal value, ϕ_p, of Eq. 3.2 be defined by the requirement that

$$|\phi_p| \leq \pi/2 \quad . \tag{3.3}$$

Define ϕ_{np} as the only nonprincipal value of Eq. 3.2 that satisfies the conditions

$$\frac{\pi}{2} \leq |\phi_{np}| < \pi \quad \text{or} \quad \phi_{np} = \pi \quad . \tag{3.4}$$

All other nonprincipal values of Eq. 3.2 are then displaced from either ϕ_p or ϕ_{np} by plus and minus integer multiples of 2π. Thus, to demonstrate system instability, it is sufficient to show that both ϕ_p and ϕ_{np} are unstable singularities. It is convenient to define

$$\overline{\phi}(t) = \phi(t) - \phi_p \quad . \tag{3.5}$$

Substitution of the equation into Eq. 3.1 yields

$$\Delta\omega_r = \dot{\overline{\phi}}(t) + G\,\overline{H}(\omega)\,[\sin\overline{\phi}(t)\cos\phi_p + \cos\overline{\phi}(t)\sin\phi_p] \quad . \tag{3.6}$$

Note that $\cos\phi_p$ is nonnegative due to the inequality (3.3). The equation analogous to Eq. 3.6 for ϕ_{np} has a factor $\cos\phi_{np}$ which is nonpositive.

At this point it is necessary to assign a particular form to the lowpass filter transfer function. Initially, let

$$H(s) = \frac{1 + \gamma\tau s}{1 + \tau s} \quad , \tag{3.7}$$

where γ is a dimensionless constant constrained to values

$$0 \leq \gamma \leq 1 \quad , \tag{3.8}$$

and τ is an arbitrary, positive time constant. This transfer function represents a filter with a real zero to the left of a negative real pole. The limiting cases, γ equal to 0 and 1, respectively, correspond to a simple RC integrator and no filter at all. Substitution of Eq. 3.7 into Eq. 3.6 results in the following second-order differential equation

$$\begin{aligned}\Delta\omega_r = {} & \dot{\overline{\phi}}(t) + \tau\ddot{\overline{\phi}}(t) + G(\sin\overline{\phi}(t)\cos\phi_p + \cos\overline{\phi}(t)\sin\phi_p \\ & + \gamma\tau\cos\overline{\phi}(t)\dot{\overline{\phi}}(t)\cos\phi_p - \gamma\tau\sin\phi(t)\dot{\overline{\phi}}(t)\sin\phi_p) \quad .\end{aligned} \tag{3.9}$$

For $\overline{\phi}(t) \ll 1$, this equation is equivalent to

$$\ddot{\overline{\phi}}(t) + \left(\frac{1}{\tau} + G\gamma \cos\phi_p\right)\dot{\overline{\phi}}(t) + \frac{G}{\tau}\cos\phi_p\,\overline{\phi}(t) - G\gamma \sin\phi_p\,\overline{\phi}(t)\dot{\overline{\phi}}(t) = 0 \quad . \tag{3.10}$$

The question of the stability of the solution

$$\ddot{\overline{\phi}}(t) = \dot{\overline{\phi}}(t) = \overline{\phi}(t) = 0 \quad , \tag{3.11}$$

for nonlinear differential equations such as Eq. 3.10, is discussed in Chapter 13 of Ref. 19. The following theorem is proven in that reference.

Theorem: Let at least one characteristic root of the characteristic polynomial of the linear portion of the differential equation have its real part positive. Let the nonlinear portion have an order not greater than the linear portion and be real, continuous, and of "order zero" as its arguments approach zero. Then the identically zero solution is not stable.

It follows that the conditions for instability of Eq. 3.10 depend on values of λ which are solutions to

$$\lambda^2 + \left(\frac{1}{\tau} + G\gamma \cos\phi_p\right)\lambda + \frac{G}{\tau}\cos\phi_p = 0 \tag{3.12}$$

or

$$\lambda = -\frac{1 + G\gamma\tau\cos\phi_p}{2\tau} \pm \sqrt{\left(\frac{1 + G\gamma\tau\cos\phi_p}{2\tau}\right)^2 - \frac{G}{\tau}\cos\phi_p} \quad . \tag{3.13}$$

Since $\cos\phi_p$ is nonnegative, both roots are clearly negative for all values of γ and τ, and the singular point ϕ_p is not unstable. Indeed, it may be shown to be asymptotically stable for all $\phi_p < |\pi/2|$. Notice also that the singular point ϕ_{np} is always unstable when $\phi_p < |\pi/2|$ since $\cos\phi_{np}$ is then negative, and one root will be positive. One concludes from the above discussion that no filters of the form given in Eq. 3.7 will exhibit instability oscillations for any value of loop gain.

As an extension of the lowpass filter transfer function given by Eq. 3.7, consider the class of filters with an additional pole

$$H(s) = \frac{1 + \gamma\tau_1 s}{(1+\tau_1 s)\ (1+\tau_2 s)} \quad , \tag{3.14}$$

where γ, as before, is defined by Eq. 3.8, and τ_1 and τ_2 are arbitrary, positive time constants. In this case, the equation analogous to (3.10) is

$$\dddot{\bar{\phi}}(t) + \left(\frac{\tau_1+\tau_2}{\tau_1\tau_2}\right) \ddot{\bar{\phi}}(t) + \left(\frac{1 + G\gamma\tau_1 \cos\phi_p}{\tau_1\tau_2}\right) \dot{\bar{\phi}}(t) + \left(\frac{G\cos\phi_p}{\tau_1\tau_2}\right) \bar{\phi}(t)$$

$$- \left(\frac{G\gamma \sin\phi_p}{\tau_2}\right) \bar{\phi}(t)\ \dot{\bar{\phi}}(t) = 0 \quad , \tag{3.15}$$

with the third-degree characteristic polynomial

$$\lambda^3 + \left(\frac{\tau_1+\tau_2}{\tau_1\tau_2}\right) \lambda^2 + \left(\frac{1 + G\gamma\tau_1 \cos\phi_p}{\tau_1\tau_2}\right) \lambda + \frac{G\cos\phi_p}{\tau_1\tau_2} \quad . \tag{3.16}$$

By applying Routh's criterion to this polynomial, it may be shown that instability at the ϕ_p singular point requires that

$$G > \frac{\tau_1 + \tau_2}{\cos\phi_p\ [(1-\gamma)\ \tau_1\tau_2 - \gamma\ \tau_1^2]} \tag{3.17}$$

and that the factor in brackets be positive. The singular point, ϕ_{np}, is again unstable for all values of G. Thus, APC systems with filters of the form given in Eq. 3.14 will exhibit instability oscillations, provided γ is not too large and the loop gain is sufficient.

The most significant point of the above discussion, and the examples, is that the question of APC system stability for a constant-frequency, sinusoidal input signal can be determined solely from the linear portion of the system equation, provided the appropriate linear portion exists. This fact permits the use of all the various linear techniques on the characteristic polynomial for the determination of system stability. Consequently, the Nyquist requirement discussed intuitively in Section 1.1 is appropriate; i.e., if the lowpass filter contributes an additional phase shift of $-\pi/2$ radians, the APC system is potentially unstable.

The instability question is essentially the same if the lowpass filter transfer function is infinite at zero frequency. In this case, the input to the lowpass filter must

be identically zero when the system is stably locked to a constant-frequency reference. Notice that this requires k_m' (see, for example, Eq. 2.6) to be zero and zero phase difference between the reference and local signals. Thus, in Eq. 3.1, $\Delta\omega_r$ is zero, and the singular points occur at values of ϕ equal to 0, $\pm\pi$, $\pm 2\pi$, ... Here,

$$\phi_p = 0 \quad \text{and} \quad \phi_{np} = \pi \quad . \tag{3.18}$$

For the class of filters given by

$$H(s) = \frac{1+\gamma\tau s}{\tau s} \quad , \tag{3.19}$$

where γ and τ have the same definition as in Eq. 3.7, the equation analogous to (3.10) is

$$\ddot{\overline{\phi}}(t) + \gamma G_\infty \dot{\overline{\phi}}(t) + \frac{G_\infty}{\tau} \overline{\phi}(t) = 0 \quad , \tag{3.20}$$

where $G_\infty = k_o k_m E_o E_r$ for amplitude-sensitive phase detectors or $G_\infty = k_o k_m E_o$ for amplitude-insensitive phase detectors. Clearly, the system is stable for positive γ. When γ is zero, the characteristic polynomial has two purely imaginary roots. For completeness, the singular point, ϕ_{np}, is unstable for all values of γ. It follows that periodic oscillations may exist for the H(s) given in Eq. 3.19 when γ is zero. Again, the possibility of instability oscillations can be determined readily from linear analysis.

3.1.2 Characteristics of the Locked Oscillations. In this section, periodic response, $\varepsilon(t)$, will be assumed for all APC systems whose equations have an appropriate linear portion and do not have any stable singular points. The frequency of this response will be assumed equal to the frequency at which the system has a total phase shift of π radians. The justification for the existence of such a stable periodic solution is postponed until Section 3.1.3. In this section, the characteristics of the assumed periodic response characteristics are determined.

In Section 2.3, three equations were developed from the system defining equations under the condition that $\varepsilon(t)$ has the general periodic form given in Eq. 2.28. For the case of a single input signal, (recall that here G includes G') the Eqs. 2.46, 2.49 and 2.50 reduce to

$$\Delta\omega_r = -k_o \sum_{p=1}^{\infty} e_p \cos(p\omega_f t + \theta_p) + G\,\overline{H}(\omega) \sin\left[\Delta\theta_r - k_o \sum_{p=1}^{\infty} \frac{e_p}{p\omega_f} \sin(p\omega_f t + \theta_p)\right] , \tag{3.21}$$

where ω_f is the fundamental radian frequency of the oscillation. Implicit in Eq. 3.21 is the condition that the average frequency of the periodic response is equal to the reference frequency (see Eq. 2.45). This may be justified in the present case if the periodic solution is indeed stable. Clearly, if some average frequency difference existed, the consequent change in phase would preclude the continued encirclement of a singular point. Thus, the legitimacy of the results of this section rests solely on the stability of the periodic solution.

The presence of the final term of Eq. 3.21 makes the solution of this equation using the general periodic form extremely difficult. When only the first term of the sum is retained, Eq. 3.21 becomes

$$\Delta\omega_r = -k_o e_1 \cos(\omega_f t + \theta_1) + G\,\overline{H}(\omega) \left[\Delta\theta_r - \frac{k_o e_1}{\omega_f} \cdot \sin(\omega_f t + \theta_1)\right] . \tag{3.22}$$

Since the choice of the origin of the time scale is entirely arbitrary here, we selected t such that θ_1 is zero. Also, let

$$\beta = \frac{k_o e_1}{\omega_f} . \tag{3.23}$$

Equation 3.22 can be written as

$$\Delta\omega_r = -\omega_f \beta \cos(\omega_f t) + G\,\overline{H}(\omega) \sin\left[\Delta\theta_r - \beta \sin(\omega_f t)\right] . \tag{3.24}$$

The Bessel function expansion of the sine factor yields

$$\sin [\Delta\theta_r - \beta \sin (\omega_f t)] =$$

$$\sin (\Delta\theta_r) [J_o(\beta) + 2J_2(\beta) \cos (2\omega_f t) + \ldots] \tag{3.25}$$

$$- \cos (\Delta\theta_r) [2J_1(\beta) \sin (\omega_f t) + 2J_3(\beta) \sin (3\omega_f t) + \ldots] \quad .$$

Only the constant and fundamental terms of this expansion may be retained meaningfully when substituting back into Eq. 3.24, since higher-order harmonics were dropped previously. The following pair of equations results, for filters with a finite gain at zero frequency

$$\Delta\omega_r = G\, J_o(\beta) \sin (\Delta\theta_r) \quad , \tag{3.26}$$[2]

$$\omega_f \beta = 2G\, |\overline{H}(\omega_f)|\, J_1(\beta) \cos (\Delta\theta_r) \quad , \tag{3.27}$$

when the constant and fundamental terms of Eq. 3.24 are equated. Recall that $\overline{H}(\omega_f)$ has, by assumption, an amount of phase shift consonant with equating the fundamental coefficients as indicated.

For filters with an infinite zero frequency gain, $\Delta\omega_r$ and $\Delta\theta_r$ are equal to zero and the single equation required is

$$\omega_f \beta = 2\, G_\infty\, |H(\omega_f)|\, J_1(\beta) \quad . \tag{3.28}$$

Since Eq. 3.28 is a special case of the finite-gain equations, consider now the information available from the pair 3.26, 3.27. When the APC system is locked to an unmodulated sinusoidal reference signal (recall that these equations were derived under this assumption), and is not oscillating (β=0), only Eq. 3.26 has any significance. For this special case,

$$\Delta\omega_r = G \sin (\Delta\theta_r) \quad . \tag{3.29}$$

Notice that, here, $\Delta\theta_r$ is equal to ϕ_p in Section 3.11; i.e., $\Delta\theta_r$ is the static, system phase error. This equation shows that the phase error is dependent on the zero frequency loop gain,

---

[2] Rey (Ref. 6) indicates that $\sin (\Delta\theta_r)$ is identically zero; however, this is necessary only when $\Delta\omega_r$ is zero.

G, and reference frequency offset, $\Delta\omega_r$. Several authors (e.g., Refs. 1, 2, 4, 6) have shown that the loop will remain locked under the above conditions for $\Delta\theta_r < \pi/2$ radians. Hence, $\Delta\omega_r$ must be less than G to insure maintenance of lock, and 2G is defined as the loop "holding range." It follows that the greater G is made, the greater the holding range becomes. This is true up to a point for lowpass filters which provide a total system phase shift of π radians, at a finite frequency. For these filters, the system will begin to oscillate as G is increased.

The characteristics of the periodic system response can be determined from the dependence of β and $\Delta\theta_r$ on $\Delta\omega_r$, G, and $|\overline{H}(\omega_f)|$. Equations 3.26 and 3.27 cannot be solved directly for β and $\Delta\theta_r$, but these equations can easily be solved for the independent variables in terms of β and $\Delta\theta_r$ as shown below:

$$H^* G = \frac{\beta}{2J_1(\beta) \cos(\Delta\theta_r)} \tag{3.30}$$

and

$$H^* \Delta\omega_r = \frac{\beta J_0(\beta) \tan(\Delta\theta_r)}{2J_1(\beta)}, \tag{3.31}$$

where the factor H* is a constant completely determined by the specific lowpass filter used and is defined by

$$H^* = \frac{|\overline{H}(\omega_f)|}{\omega_f} . \tag{3.32}$$

The solution of Eqs. 3.30 and 3.31 is accomplished graphically. (See Figs. 3.1 and 3.2, for plots of these equations.) Observe that Fig. 3.2 is an enlarged plot of Fig. 3.1 near the origin. From these plots, for example, curves showing the dependence of β and $\Delta\theta_r$ on $H^*\Delta\omega_r$ can be determined for constant values of H*G. This is done by selecting a value of H*G and reading the values of β and $H^*\Delta\omega_r$ for each value of $\Delta\theta_r$ from the curves in Figs. 3.1 and 3.2. One example is given in Fig. 3.3 for H*G equal to 1.75. Only half of the curve is shown here since the curve is symmetric about the β axis. The dashed line indicates the values that $\Delta\theta_r$ would assume for this gain if no locked instability oscillations existed.

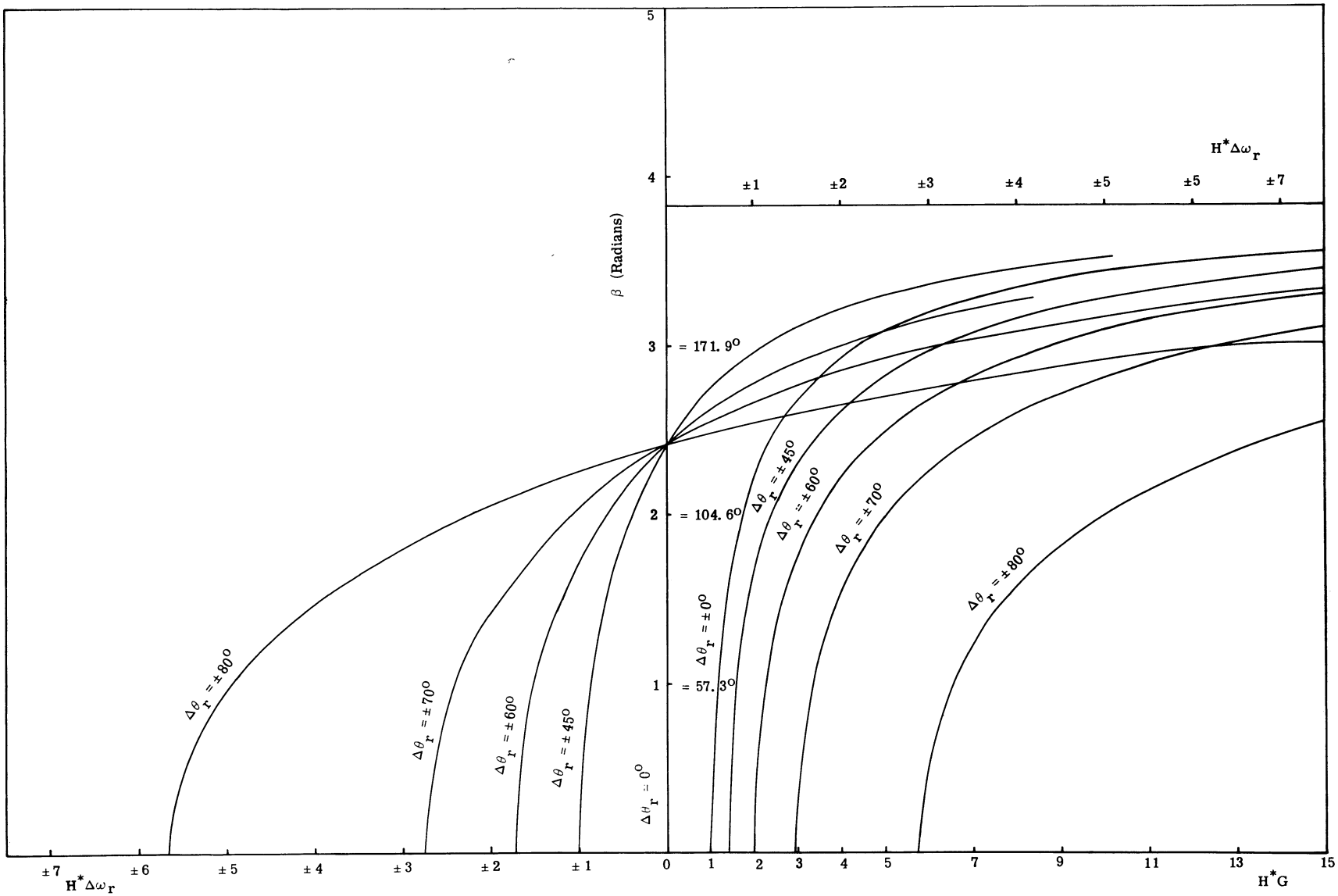

Fig. 3.1 The graphical solution of Eqs. 3.30 and 3.31.

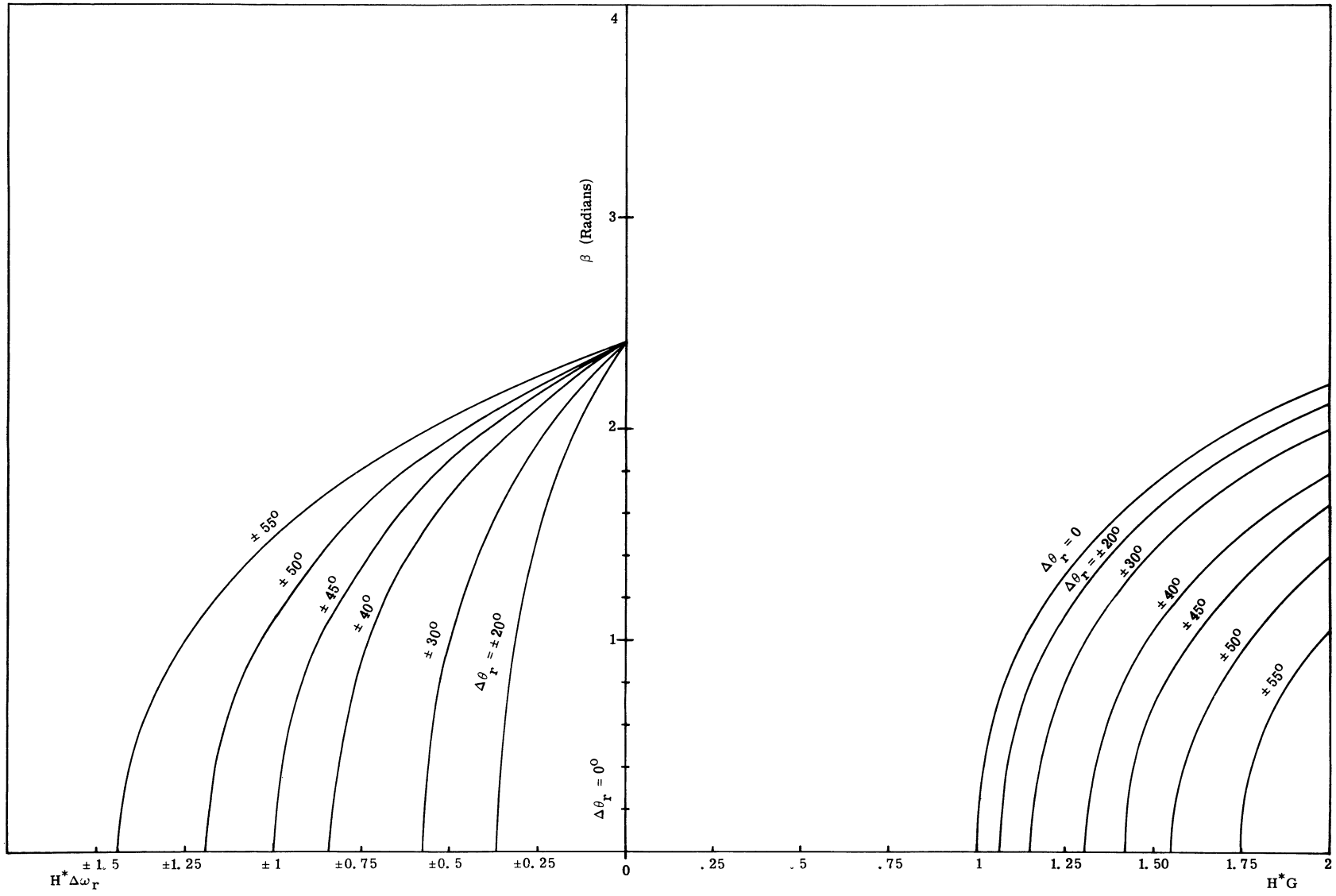

Fig. 3.2. An expansion of Fig. 3.1 near the origin.

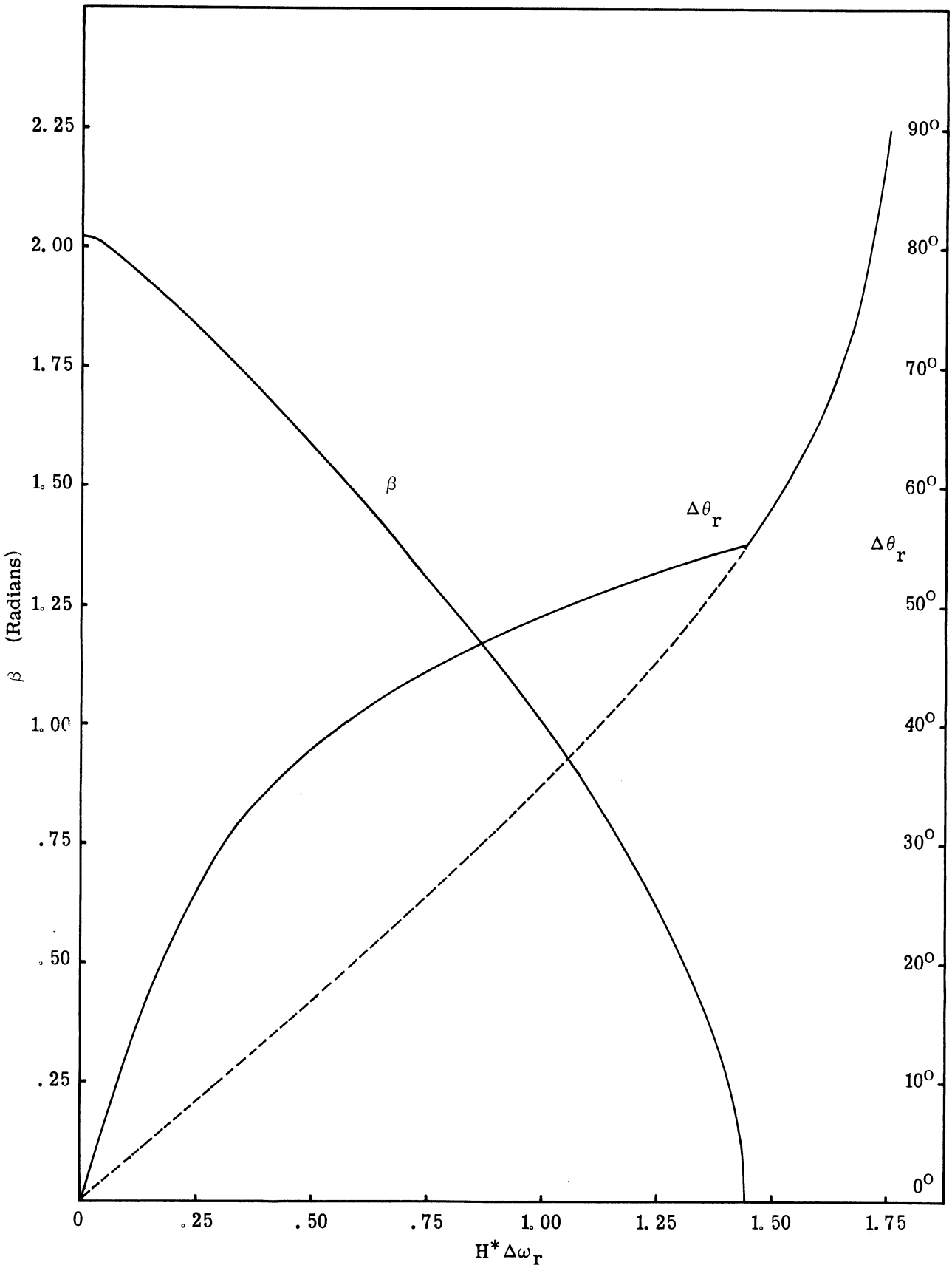

Fig. 3.3. β and $\Delta\theta_r$ versus $H^*\Delta\omega_r$ for H*G = 1.75.

It is worthwhile at this point to write the system response and system oscillator phase in terms of β and $\Delta\theta_r$. For the assumptions made in this section, Eq. 2.28 becomes

$$\epsilon(t) = \frac{\omega_r - \omega_o}{k_o} + \frac{\omega_f \beta}{k_o} \cos \omega_f t \tag{3.33}$$

and Eq. 2.30 becomes

$$\theta_o(t) = \theta_r - \Delta\theta_r + (\omega_r - \omega_o)\, t + \beta \sin \omega_f t \quad . \tag{3.34}$$

Note that here θ_r is equal to θ_r'. Since β and $\Delta\theta_r$ are functions of $\Delta\omega_r$, G, and H*, the APC system's oscillation is completely characterized in terms of the independent variables.

We conclude this treatment of the case of finite system gain at zero frequency with some observations on Figs. 3.1 - 3.3. The peak value of the locked instability oscillations occurs for $\Delta\omega_r$ equal to zero (see Fig. 3.3). For increasing $|\Delta\omega_r|$, β decreases and eventually becomes zero. For still greater $|\Delta\omega_r|$, the system remains stably locked until $|\Delta\theta_r|$ reaches 90°, just as if no oscillation had existed. Notice the abrupt transition in the $\Delta\theta_r$ vs. $|H^*\Delta\omega_r|$ curve just as β becomes zero. For the larger values of $|H^*\Delta\omega_r|$, the $\Delta\theta_r$ curve is simply the inverse sine relation (Eq. 3.29), whereas for the smaller values of the independent variable the effect of $J_o(\beta)$ (see Eq. 3.26) is quite pronounced.

By reference to Figs. 3.1 and 3.2, the question of when oscillations begin can be answered readily. Since the peak value of β occurs when $\Delta\theta_r(\Delta\omega_r = 0)$ is zero, clearly β must be zero for all values of H*G less than unity. Once H*G exceeds unity, β varies continuously with $\Delta\omega_r$. It should be remarked that the holding range continues to increase as H*G increases above unity. The first-order theory developed above indicates that for any finite gain, G, there should be a finite region of $H^*\Delta\omega_r$ in which the locked instability oscillations cease before the loop loses lock. This can be seen from the following. From Eq. 3.31 the frequency at which β goes to zero is simply

$$H^*\Delta\omega_r\Big|_{\beta\to 0} = \frac{\beta J_o(\beta) \tan(\Delta\theta_r)}{2J_1(\beta)}\Bigg|_{\beta\to 0} = \tan(\Delta\theta_r) \quad . \tag{3.35}$$

From Eq. 3.30 the gain, H*G, at this point is

$$H^*G\Big|_{\beta\to 0} = \frac{\beta}{2J_1(\beta)\cos(\Delta\theta_r)}\Bigg|_{\beta\to 0} = \frac{1}{\cos(\Delta\theta_r)} \quad . \tag{3.36}$$

Hence,

$$H^*\Delta\omega_r\Big|_{\beta\to 0} = \tan(\Delta\theta_r) \leq \frac{1}{\cos(\Delta\theta_r)} = H^*G\Big|_{\beta\to 0} \quad . \tag{3.37}$$

The implication of these observations is that the holding range can be made arbitrarily large at the expense of loop oscillation, with the magnitude of oscillation decreasing to zero prior to the loop losing lock. Due to the truncations made in developing the first-order equations these large-gain results are of questionable validity. Furthermore, this result has not been observed experimentally; actually, abrupt jumps are observed between locked and unlocked oscillations.

Finally, a few brief comments are in order concerning the behavior of systems with filters having infinite gain at zero frequency. When $H(\omega)$ has a unique frequency at which the APC system has a total phase shift of π radians, the value of β is found from the $G_\infty H^*$ product and the curve for $\Delta\theta_r = 0$ in the way discussed previously. Here, of course, there is just the single value of β which is independent of the reference signal frequency. Ideally, the holding range is infinite.

For $H(s) = 1/\tau s$, the system has a phase shift of π at all real frequencies and Eq. 3.28 becomes

$$\frac{G_\infty}{\tau} = \frac{\beta}{2J_1(\beta)}\,\omega_f^2 \quad . \tag{3.38}$$

The indication is that as the magnitude of oscillation increases, the frequency of oscillation decreases for a constant value of G_∞.

3.1.3 Stability Analysis for the Locked Oscillations. The validity of the analysis made in Section 3.1.2 is primarily dependent on the existence of a stable periodic response around the unstable singular point at $\phi = \phi_p$ (or any of the other singular points displaced from ϕ_p by an integer multiple of 2π). Although the mathematical theory necessary to investigate this validity is available, the required calculations are very lengthy for all but the simplest filters. In this section, the general stability analysis technique is

outlined briefly. An example calculation is also carried out for the lowpass filter transfer function given in Eq. 3.14.

The question of orbital stability may be examined by the first variation technique (see Ref. 19 for additional details). The theory for this analysis, discussed in the literature, is concerned with a system of n first-order differential equations. The same formulation is presented here. If the column vector $\hat{\phi}(t)$ is a real solution of the system of equations

$$\dot{\hat{x}} = \hat{F}(t,\hat{x}) \tag{3.39}$$

for $0 \leq t < \infty$, where the column vector $\hat{F}$ is analytic in $\hat{x}$ for each t, then the first variation equation is

$$\dot{\hat{y}} = F_x[t, \hat{\phi}(t)]\, \hat{y} \quad , \tag{3.40}$$

where $F_x[t, \hat{\phi}(t)]$ is a matrix composed of the columns $\partial\hat{F}/\partial x_i$ (i=1,2,..., n). A special case of Eq. 3.39 occurs when $\hat{F}$ does not depend on t. In this case, the first variation equation becomes

$$\dot{\hat{y}} = F_x[\hat{\phi}(t)]\, \hat{y} \quad . \tag{3.41}$$

Notice that both Eqs. 3.40 and 3.41 are linear equations with, in general, time-dependent coefficients. The APC system equation for the case of a single input signal of constant frequency does not depend on time and hence takes the latter form.

If $\hat{\phi}(t)$ is a periodic solution of Eq. 3.39, it follows that Eq. 3.41 represents a system of linear differential equations with periodic coefficients. The stability characteristics of the solutions can be shown to depend on the real parts of the characteristic exponents for this system. Since $\hat{\phi}(t)$ satisfies the variation equation, the characteristic exponent associated with it may be taken as zero. Thus, for an n-th order system, the remaining n-1 characteristic exponents determine the orbital stability of $\hat{\phi}(t)$.

The solution $\hat{x} = \hat{\phi}(t)$ may be regarded as a closed curve, or orbit in $\hat{x}$ space with t as a parameter. If n-1 characteristic exponents of Eq. 3.41 have negative real parts, then the closed orbit is asymptotically stable in the sense that any solution of Eq. 3.39 which comes near a point of the orbit tends to the orbit as t approaches infinity. This is called asymptotic orbital stability. The following theorem is proved in Ref. 19.

Theorem: Let n-1 characteristic exponents of Eq. 3.41 have negative real parts. Then, there exists an $\epsilon > 0$ such that if a solution $\hat{\phi}^*(t)$ of Eq. 3.39 satisfies $|\hat{\phi}^*(t_2) - \hat{\phi}^*(t_1)| < \epsilon$ for some t_1 and t_2, there exists a constant c such that

$$\lim_{t\to\infty} |\hat{\phi}^*(t) - \hat{\phi}^*(t + c)| = 0 \quad . \tag{3.42}$$

Thus, not only is there asymptotic orbital stability but each solution near the orbit possesses an asymptotic phase c.

Although the technique just outlined provides the desired answer to the stability question, its application is hindered by the two requirements:

1. That a periodic solution already has been found.
2. That the remaining n-1 characteristic exponents can be found.

For the present application, the first of these is at least approximately met. The second requirement can be fulfilled only with considerable effort. However, a method does exist that permits determining each characteristic exponent from the known elements of the matrix, $F_x[\hat{\phi}(t)]$. This method is described in detail in Chapter XVII of Ref. 20 and applies to those cases where each element of $F_x[\hat{\phi}(t)]$ can be expanded in the power series form

$$F_x[\hat{\phi}(t)] = A + \sum_{k=1}^{\infty} F_x^{(k)}[\hat{\phi}(t)]\mu^k \quad , \tag{3.43}$$

where A is a constant matrix independent of μ, and μ is sufficiently small. A perturbation technique is employed to determine each characteristic exponent in the form of

$$\rho_i = \rho_i^{(0)} + \rho_i^{(1)}\mu + \rho_i^{(2)}\mu^2 + \ldots \quad . \tag{3.44}$$

A noteworthy feature of this method is that any one root can be approximated to an arbitrary degree without carrying along any approximations to the other roots.

One additional fact is helpful in determining the characteristic exponents. There is an associated multiplier, λ_i, for each characteristic exponent, ρ_i, defined by

$$\lambda_i = e^{\rho_i T} \quad , \tag{3.45}$$

where T is the fundamental period of $\hat{\phi}(t)$. It is proven in Ref. 19 that

$$\prod_{i=1}^{n} \lambda_i = \exp \int_0^T t_r F_x[\hat{\phi}(s)]\, ds \quad . \tag{3.46}$$

Since one of the λ_i is known to have unity value, only n-2 characteristic exponents need be found by the perturbation method. The remaining λ_i can be found from Eq. 3.46. The characteristic exponent associated with the unity value λ_i equals zero. The requirement that each of the remaining ρ_i have a negative real part is equivalent to requiring that each associated λ_i be less than unity in absolute value.

The remainder of this section, an example of the above stability analysis is carried out for the lowpass filter transfer function given in Eq. 3.14. The third-order differential equation that results for this choice of filter is

$$\tau_1\tau_2\dddot{\phi}(t) + (\tau_1 + \tau_2)\,\ddot{\phi}(t) + [1 + G\gamma\tau_1 \cos \dot{\phi}(t)]\,\dot{\phi}(t)$$

$$+ G \sin \phi(t) = \tau_1\tau_2\Delta\omega_r \quad . \tag{3.47}$$

For simplicity, $\Delta\omega_r$ will be assumed to have zero value. This avoids making the change of variables defined by Eq. 3.5, but does not limit the generality of the following results.

Using the definitions

$$a_1 = \frac{\tau_1 + \tau_2}{\tau_1\tau_2} \qquad a_2 = \frac{1}{\tau_1\tau_2}$$

$$a_3 = \frac{G}{\tau_1\tau_2} \qquad a_4 = \frac{G\gamma}{\tau_2} \tag{3.48}$$

and

$$\phi_o(t) = \phi(t) \quad , \tag{3.49}$$

then, Eq. 3.47 reduces to the following system of equations:

$$\dot{\phi}_o(t) = \phi_1(t) \quad ,$$

$$\dot{\phi}_1(t) = \phi_2(t) \quad ,$$

$$\dot{\phi}_2(t) = -a_3 \sin \phi_o(t) - [a_2 + a_4 \cos \phi_o(t)]\, \phi_1(t) - a_1 \phi_2(t) \quad . \tag{3.50}$$

This system has the form of Eq. 3.39. The first variation equation is thus

$$\begin{vmatrix} \dot{y}_1(t) \\ \dot{y}_2(t) \\ \dot{y}_3(t) \end{vmatrix} = \begin{vmatrix} 0 & 1 & 0 \\ 0 & 0 & 1 \\ -a_3\cos \phi_o(t) + a_4 \sin \phi_o(t)\phi_1(t) & -a_2 - a_3 \cos \phi_o(t) & -a_1 \end{vmatrix} \cdot \begin{vmatrix} y_1(t) \\ y_2(t) \\ y_3(t) \end{vmatrix} . \tag{3.51}$$

The next step in the stability analysis is to insert the known solution into this coefficient matrix. From Eqs. 2.12, 2.41, and 3.34, it may be shown that

$$\phi(t) = -\beta \sin \omega_f t \tag{3.52}$$

for any lowpass filter. Substitution of this solution into the coefficient matrix of Eq. 3.51 yields the periodic matrix:

$$\begin{vmatrix} 0 & 1 & 0 \\ 0 & 0 & 1 \\ -a_3\cos[\beta\sin(\omega_f t)] - a_4 \sin[\beta\sin(\omega_f t)]\beta\omega_f \cos(\omega_f t) & -a_2 - a_4 \cos[\beta\sin(\omega_f t)] & -a_1 \end{vmatrix} \tag{3.53}$$

This matrix has a period of π/ω_f. If the periodic terms are now replaced by their Bessel function expansion and the Bessel functions are, in turn, expanded in terms of β, the matrix takes the required form, i.e., that of Eq. 3.43 with $\mu = \beta^2$. The constant matrix A and the first $F_x^{(k)}[\hat{\phi}(t)]$ matrix are

$$A = \begin{vmatrix} 0 & 1 & 0 \\ 0 & 0 & 1 \\ -a_3 & -(a_2 + a_4) & -a_1 \end{vmatrix}, \tag{3.54}$$

$$F_x^{(1)} = \begin{vmatrix} 0 & 0 & 0 \\ 0 & 0 & 0 \\ \frac{a_3}{4}[1 - \cos(2\omega_f t)] - \frac{a_4 \omega_f}{2} \sin(2\omega_f t) & \frac{a_4}{4}[1 - \cos(2\omega_f t)] & 0 \end{vmatrix}. \tag{3.55}$$

The method given in Ref. 20 for determining the characteristic exponents may now be initiated. Before this is done, however, recall that one of the ρ_i may be taken as zero since $\phi(t)$ is a solution of Eq. 3.51. Let ρ_1 equal zero and hence λ_1 is unity. From Eq. 3.46,

$$\lambda_2 \lambda_3 = \exp \int_0^{\pi/\omega_f} -a_1 \, ds = \exp\left(-\frac{\pi a_1}{\omega_f}\right). \tag{3.56}$$

Since ω_f is the radian frequency at which the APC system has a phase shift of $-\pi$ radians, ω_f is uniquely determined by the lowpass filter time constants. Indeed, it is easy to show that Eq. 3.14 (the transfer function of the lowpass filter) will provide the necessary additional phase shift ($-\pi/2$ radians) in the APC system when

$$\omega_f = \frac{1}{\sqrt{(1 - \gamma)\,\tau_1 \tau_2 - \gamma \tau_1^2}}. \tag{3.57}$$

Substitution back into Eq. 3.56 yields (see also Eq. 3.48)

$$\lambda_2\lambda_3 = \exp\left[-\pi \frac{(\tau_1 + \tau_2)\sqrt{(1 - \gamma)\,\tau_1\tau_2 - \gamma\tau_1^2}}{\tau_1\tau_2}\right] . \tag{3.58}$$

It will be recalled from Section 3.1.1 that the expression under the radical sign must be positive for system instability. It follows that the product $\lambda_2\lambda_3$ is equal to some number less than unity. Since both $|\lambda_2|$ and $|\lambda_3|$ must be less than unity, it is necessary to find only one or the other to answer the question of orbital stability.

In determining any characteristic exponent using the method given in Ref. 20, the initial step is to find the roots of the characteristic polynomial of the constant coefficient matrix, A. This polynomial is simply the polynomial 3.16 with cos ϕ_p equal to unity. Let G be chosen so that the loci of two of the roots of this polynomial are imaginary, in the light of their dependence on G. This requires that

$$G = \frac{\tau_1 + \tau_2}{[(1 - \gamma)\,\tau_1\tau_2 - \gamma\tau_1^2]} , \tag{3.59}$$

and the three roots for this gain are

$$\rho_1^{(0)} = j\sqrt{a_3/a_1} = j\sqrt{a_2 + a_4} = j\,\omega_f ,$$

$$\rho_2^{(0)} = -\rho_1^{(0)} = -j\,\omega_f ,$$

$$\rho_3^{(0)} = -a_1 . \tag{3.60}$$

The superscript zero is used here to denote the zero-order approximation to ρ_i.

The next step in the method is to select a particular ρ_i and solve the appropriate system of linear, constant-coefficient equations to determine the associated $y_i^{(0)}$. For ρ_3, this system is

$$\dot{y}_1^{(0)} - a_1 y_1^{(0)} - y_2^{(0)} = 0 \quad ,$$

$$\dot{y}_2^{(0)} - a_1 y_2^{(0)} - y_3^{(0)} = 0 \quad , \tag{3.61}$$

$$\dot{y}_3^{(0)} + a_3 y_1^{(0)} + (a_2 + a_4)\, y_2^{(0)} = 0 \quad .$$

The superscript zero again indicates that this system is the zero-order approximation. The general solution of this system has the form

$$\begin{vmatrix} y_1^{(0)} \\ y_2^{(0)} \\ y_3^{(0)} \end{vmatrix} = \begin{vmatrix} c_{11} & c_{12} & c_{13} \\ j\omega_f c_{11} & -j\omega_f c_{12} & -a_1 c_{13} \\ -\omega_f^2 c_{11} & -\omega_f^2 c_{12} & a_1^2 c_{13} \end{vmatrix} \cdot \begin{vmatrix} \eta_1 e^{(a_1 + j\omega_f)t} \\ \eta_2 e^{(a_1 - j\omega_f)t} \\ \eta_3 \end{vmatrix} \quad , \tag{3.62}$$

where the η_i are arbitrary constants. It is necessary, however, that the $y_i^{(0)}$ be periodic, and consequently, η_1 and η_2 are set equal to zero. Since c_{13} is also arbitrary, let η_3 be unity in value, whereupon

$$y_1^{(0)} = c_{13} \quad ,$$

$$y_2^{(0)} = -a_1 c_{13} \quad ,$$

$$y_3^{(0)} = a_1{}^2 c_{13} \quad . \tag{3.63}$$

The next step in the perturbation method is to solve the appropriate first-order system. The result for our example is given below:

$$\dot{y}_1^{(1)} - a_1 y_1^{(1)} - y_2^{(1)} = -\rho_3^{(1)}\, c_{13}$$

$$\dot{y}_2^{(1)} - a_1 y_2^{(1)} - y_3^{(1)} = \rho_3^{(1)}\, a_1 c_{13}$$

$$\dot{y}_3^{(1)} + a_3 y_1^{(1)} + (a_2 + a_4)\, y_2^{(1)} = -\rho_3^{(1)}\, a_1^2 c_{13} + \frac{a_3}{4}\,[1 - \cos(2\omega_f t)]\, c_{13}$$

$$- \frac{a_4 \omega_f}{2} \sin(2\omega_f t)\, c_{13} - \frac{a_4}{4}\,[1 - \cos(2\omega_f t)]\, a_1 c_{13} \quad . \tag{3.64}$$

Notice that the zero-order solutions, together with the nonzero elements of the $F_x^{(1)}$ matrix, are used as forcing functions on the $y_i^{(1)}$ system. This system may now be solved, and the values of $\rho_3^{(1)}$ and the $y_i^{(1)}$ determined as periodic functions of time as well as functions of the constants of the A matrix. This general procedure is repeated for higher-order approximations to the characteristic exponent and to the associated periodic y_i functions.

For the purposes of this study, only $\rho_3^{(1)}$ will be determined. This is accomplished through solution of Eq. 3.64, using the variation-of-parameters technique. It is not difficult to show that

$$\rho_3^{(1)} = \frac{a_3 - a_1 a_4}{4(\omega_f^2 + a_1^2)} \quad . \tag{3.65}$$

Thus, $\rho_3^{(1)}$ is positive provided

$$a_3 - a_1 a_4 > 0 \quad , \tag{3.66}$$

which requires that (see Eq. 3.48)

$$\tau_1 \tau_2 (1-\gamma) - \gamma \tau_1^2 > 0 \quad . \tag{3.67}$$

This last condition is also necessary for the instability of an APC system subject to a constant-frequency input signal (see Eq. 3.17).

From Eq. 3.44, the value of ρ_3 is given by

$$\rho_3 = -a_1 + \frac{a_3 - a_1 a_4}{4(\omega_f^2 + a_1^2)}\, \beta^2 + \ldots \quad . \tag{3.68}$$

Clearly, ρ_3 becomes less negative as β increases, and λ_3 becomes larger. Consequently, λ_2 must decrease (from Eq. 3.58). It can also be seen that λ_2 is equal to unity (since $\rho_2^{(0)}$ equals $-j\omega_f$) when β is equal to zero. Both λ_2 and λ_3 are less than unity, for positive

β which provides the criterion for orbital stability when this filter is employed.

The purpose of this section has been to establish the conditions for orbital stability. As is apparent, the required calculations are lengthy, particularly for higher-order APC systems where it is necessary to calculate several of the roots. All of the details for handling the perturbation calculations may be found in Chapter XVII of Ref. 20.

3.2 Experimental Comparisons with the Theoretically Determined Oscillation Characteristics

Experimentation with an APC system has confirmed the analysis of locked instability oscillation characteristics presented in Section 3.1.2. Experimental data pertinent to these instability oscillations are given in this section for an APC system having finite gain at zero frequency. Details concerning the experimental circuit and procedure are discussed in Section 5.

According to the theory of Section 3.1.2, the APC system response, $\epsilon(t)$, is given by

$$\epsilon(t) = \frac{\omega_r - \omega_0}{k_o} + \frac{\omega_f \beta}{k_o} \cos \omega_f t \tag{3.69}$$

for small values of β and for all lowpass filters providing sufficient phase shift. The response, $\epsilon(t)$, may easily be measured experimentally for various input conditions. Since the instability oscillation frequency, ω_f, and the system oscillator gain constant, k_o, may also be found easily, β may be calculated directly from the experimental data. Assuming that the periodic term of Eq. 3.69 is measured with an rms-reading voltmeter, then β is found by

$$\beta = (1.414) \frac{k_o}{\omega_f} \epsilon(t)_{rms} \quad , \tag{3.70}$$

where $\epsilon(t)_{rms}$ is the measured rms value. When this equation is used, a plot of β versus the frequency offset, $\Delta\omega_r$, can be drawn from experimental data on any APC system. The reader will recall that β is a function of G and $|\overline{H}(\omega_f)|$, as well as $\Delta\omega_r$. $|\overline{H}(\omega_f)|$ is a constant for any given APC system. Thus, a family of β vs. $\Delta\omega_r$ curves may be drawn for a specific system with the system gain, G, as a parameter.

The angle $\Delta\theta_r$ may also be found experimentally. A direct way to determine $\Delta\theta_r$ is based on Eq. 2.48, which indicates that $\Delta\theta_r$ is the difference in phase of the reference and system oscillator signals. An alternate method, based on Eq. 3.26, is as follows. Let

$\Delta\omega_{rc}$ be the smallest frequency offset at which β is zero. This value may be found accurately by experiment. From Eq. 3.26, $\Delta\theta_{rc}$ is given by

$$\Delta\omega_{rc} = G \sin(\Delta\theta_{rc}) \quad . \tag{3.71}$$

Dividing Eq. 3.26 by Eq. 3.71 yields

$$\frac{\Delta\omega_r}{\Delta\omega_{rc}} = J_o(\beta) \frac{\sin(\Delta\theta_r)}{\sin(\Delta\theta_{rc})} \quad . \tag{3.72}$$

Finally, solving for $\Delta\theta_r$ yields

$$\Delta\theta_r = \sin^{-1}\left[\frac{\sin(\Delta\theta_{rc})\ \Delta\omega_r}{J_o(\beta)\ \Delta\omega_{rc}}\right] . \tag{3.73}$$

This last equation permits $\Delta\theta_r$ to be plotted, given the $\varepsilon(t)_{rms}$ values. Again, a family of $\Delta\theta_r$ vs. $\Delta\omega_r$ curves exists, with parameter G, for each APC system.

Another useful relationship may be found from Eq. 3.30. β assumes some maximum value when $\Delta\theta_r$ is equal to zero. Let this value be defined as β_{max}. Thus,

$$H^*G = \frac{\beta_{max}}{2J_1(\beta_{max})} \quad . \tag{3.74}$$

Since $\beta/2J_1(\beta)$ equals unity when β equals zero, it follows from Eqs. 3.30 and 3.74 that

$$\cos\Delta\theta_{rc} = \frac{2J_1(\beta_{max})}{\beta_{max}} \quad . \tag{3.75}$$

This permits determining $\Delta\theta_{rc}$ without measuring the system gain. Furthermore, if Eq. 3.75 is used to find $\Delta\theta_{rc}$, then Eq. 3.71 can be used to determine G, since

$$G = \frac{\Delta\omega_{rc}}{\sin(\Delta\theta_{rc})} \quad . \tag{3.76}$$

Finally substitution of Eq. 3.76 and Eq. 3.75 into Eq. 3.74 yields

$$|\overline{H}(\omega_f)| = \frac{\omega_f\beta_{max}\sin\Delta\theta_{rc}}{2\,\Delta\omega_{rc}J_1(\beta_{max})} = \frac{\omega_f}{\Delta\omega_{rc}}\tan\Delta\theta_{rc} \quad . \tag{3.77}$$

These relations among the system parameters are useful in checking the results of various measurements and evaluating those quantities that are difficult to measure directly.

Three sets of values of $\varepsilon(t)_{rms}$ versus $\Delta\omega_r$ were obtained, for three values of reference-signal magnitude, on the APC system shown in Fig. 5.2 of Section 5. Because this system is sensitive to input amplitude, the three sets of data correspond to different values of system gain, G. As shown in Fig. 5.4, the system oscillator gain, k_o, has a value of 42.8 kc/volt. The instability frequency was measured to be 12.94 kc. The values of β as a function of $\Delta\omega_r$ were found from Eq. 3.70 and plotted in Fig. 3.4. Also shown in Fig. 3.4 are the $\Delta\theta_r$ curves which were found with aid of Eqs. 3.73 and 3.75.

The three theoretical curves shown in Fig. 3.5 were constructed for comparison. H*G was determined from Eq. 3.74 for each value of system gain. The curves shown in Fig. 3.2 were then used to find β and $\Delta\theta_r$ in the manner that the curves in Fig. 3.3 were constructed. The close agreement between the two sets of curves shown in Figs. 3.4 and 3.5 is demonstrated in Fig. 3.6 which further substantiates the validity of the theoretical results. In Fig. 3.6, the solid curves are taken directly from Fig. 3.5 (the theoretical prediction for the highest value of input signal) and the points represent actual data values from which were constructed the experimental curves in Fig. 3.4.

The three photographs shown in Fig. 3.7 portray the periodic portion of the system response. Notice that though the first two of these responses are essentially sinusoidal with time in appearance, the third definitely contains some energy in the higher-order harmonics. The high-frequency ripple evident in these photographs is introduced by the system oscillator and is at the reference-signal frequency of approximately 450 kc.

A check on the experimental values of β found from k_o, ω_f, and $\varepsilon(t)_{rms}$ can be made by measuring $J_o(\beta)$ [or $J_1(\beta)$] directly. This can be done conveniently with an appropriate spectrum (or waveform) analyzer. As an example, the three values of β_{max} found with the aid of Eq. 3.70 (see Fig. 3.4) are 0.69, 1.01, and 1.38. The corresponding values of β_{max} found from $J_o(\beta_{max})$ are 0.70, 0.96, and 1.33.

Finally, the experimentally determined values of H*G, G, and $|\overline{H}(\omega_f)|$, found from Eqs. 3.74, 3.76 and 3.77, respectively, are listed below for the three gain levels.

Input Signal Level (volts rms)	H*G	G (kc)	$\lvert\overline{H}(\omega_f)\rvert$
0.320	1.06	32.75	0.427
0.350	1.14	34.0	0.434
0.400	1.28	38.5	0.430

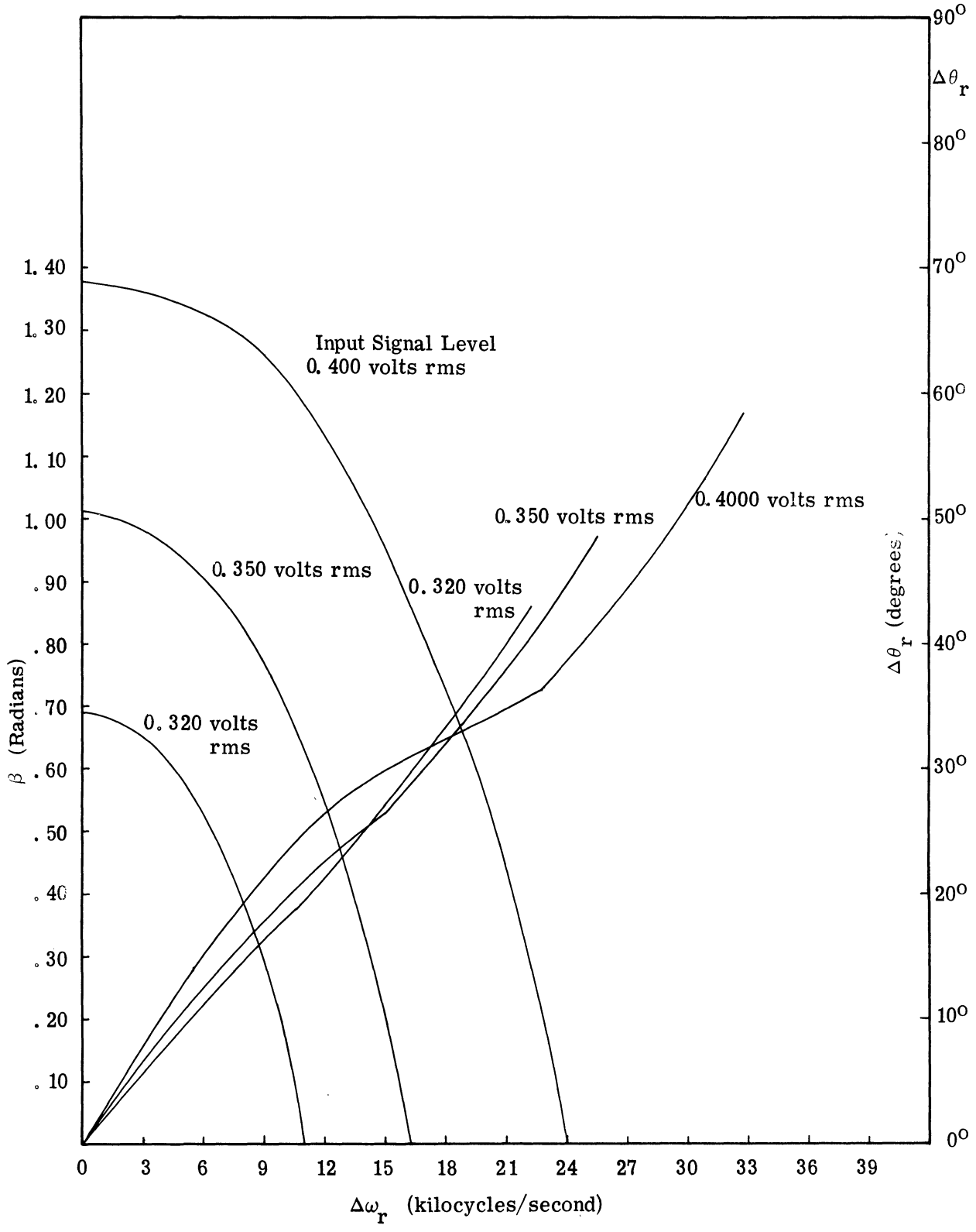

Fig. 3.4 Experimental curves of β and $\Delta\theta_r$ versus $\Delta\omega_r$ for three input signal levels.

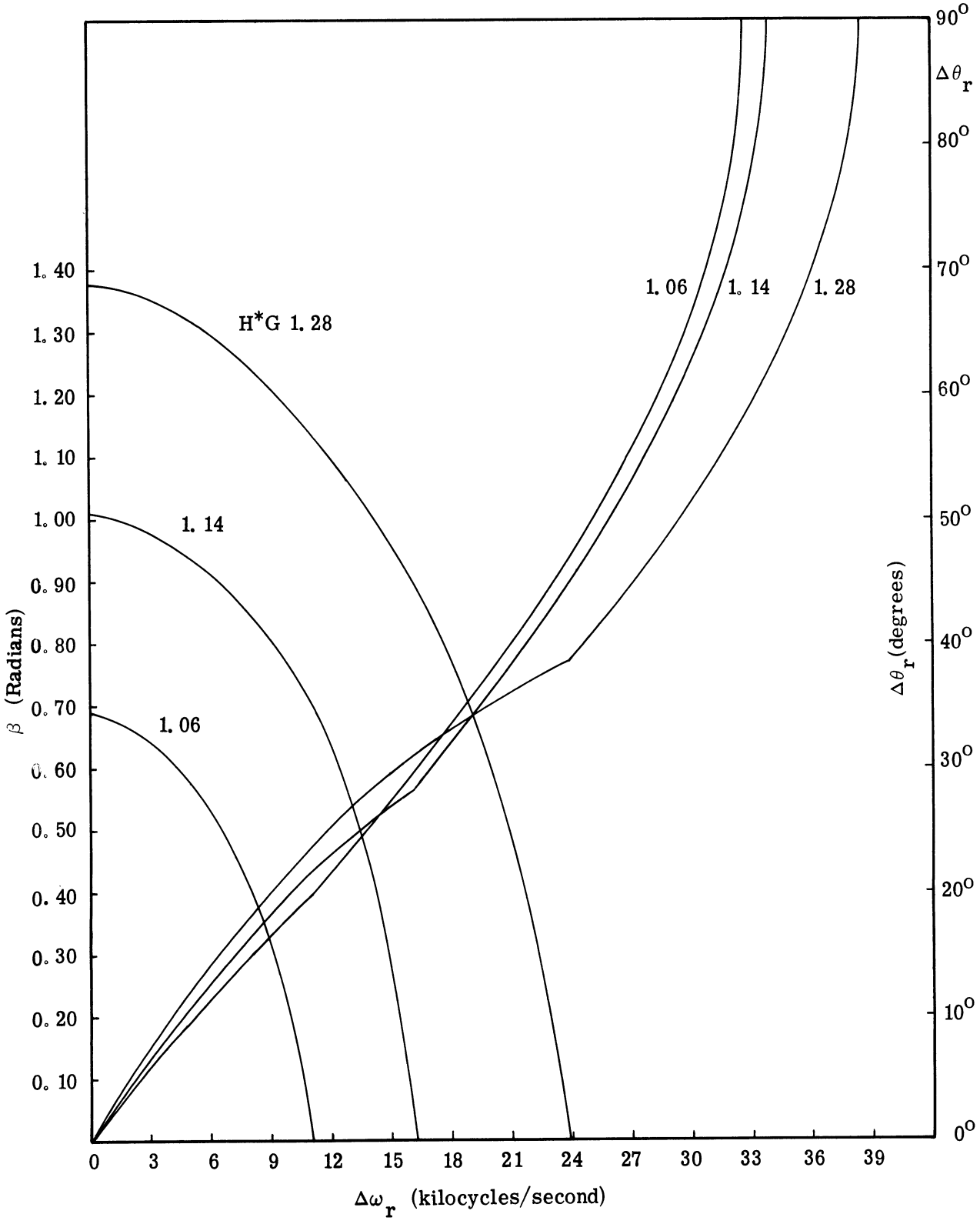

Fig. 3.5. Theoretical curves of β and $\Delta\theta_r$ versus $\Delta\omega_r$ corresponding to the curves in Fig. 3.4.

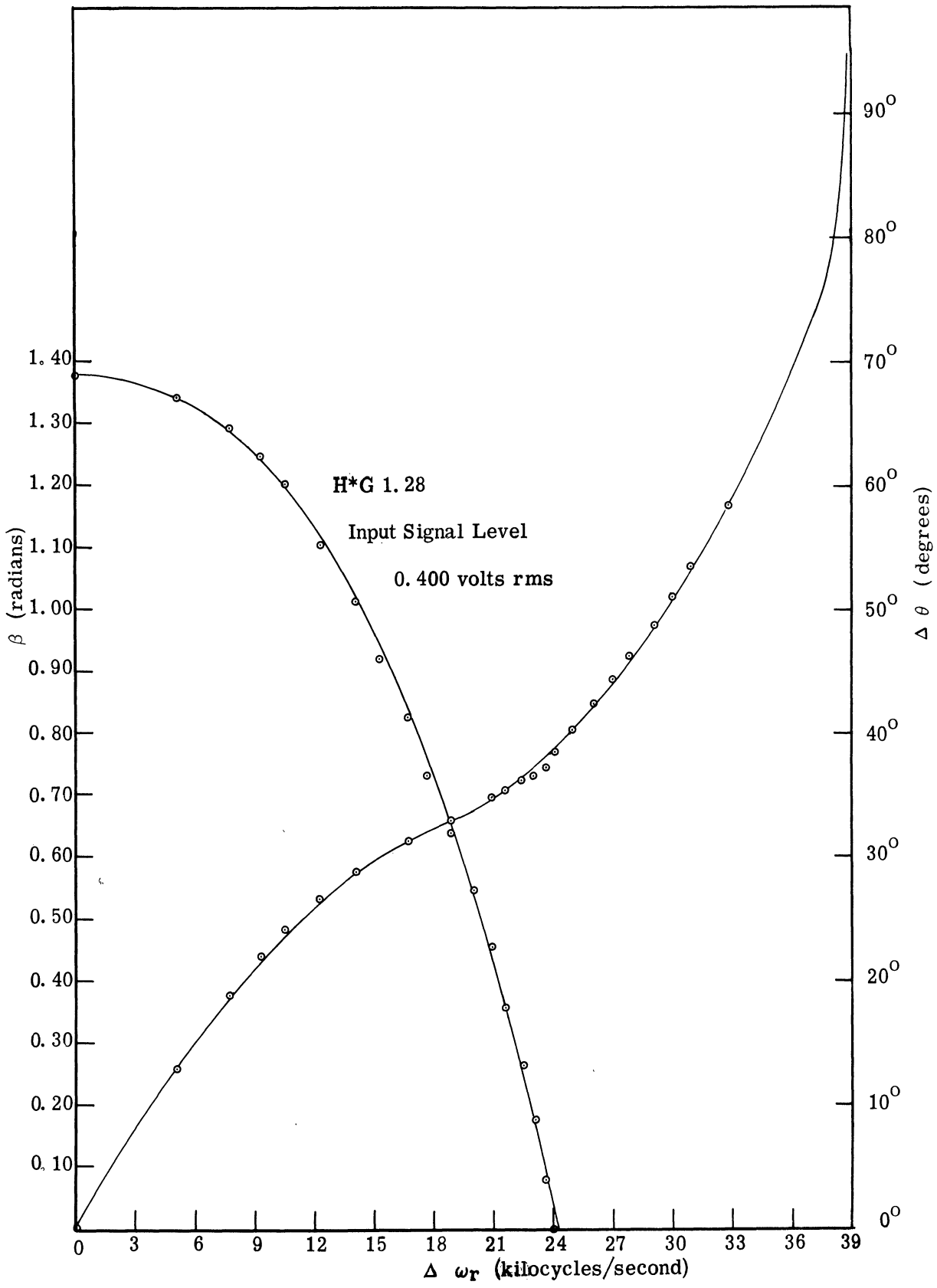

Fig. 3.6. Direct comparison of the theoretical curve and experimental points shown for the largest value of input signal level in Figures 3.4 and 3.5.

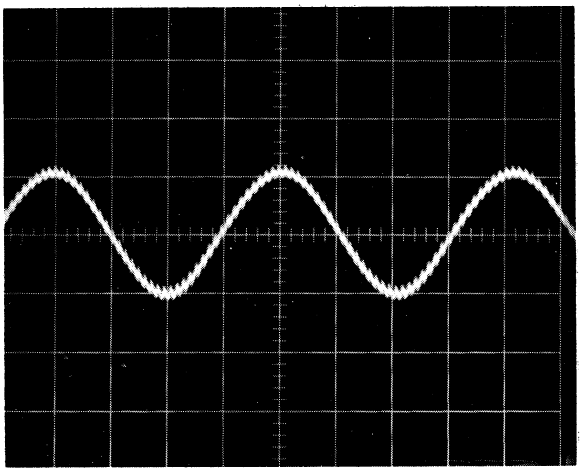

a) Input signal level 0.320 volt rms
Zero frequency offset
Vertical scale 0.20 volt/division
Horizontal scale 20 μs/division

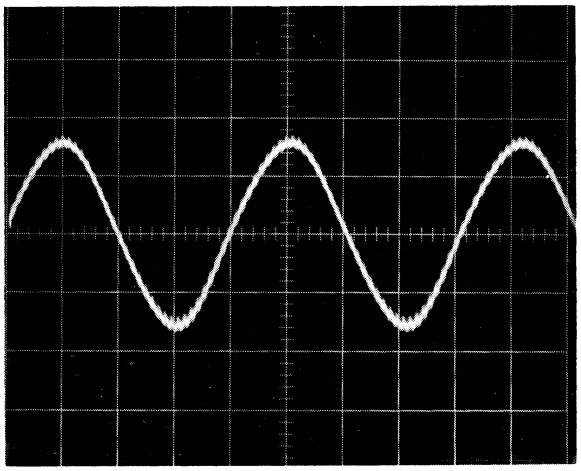

b) Input signal level 0.350 volt rms
Zero frequency offset
Vertical scale 0.20 volt/division
Horizontal scale 20 μs/division

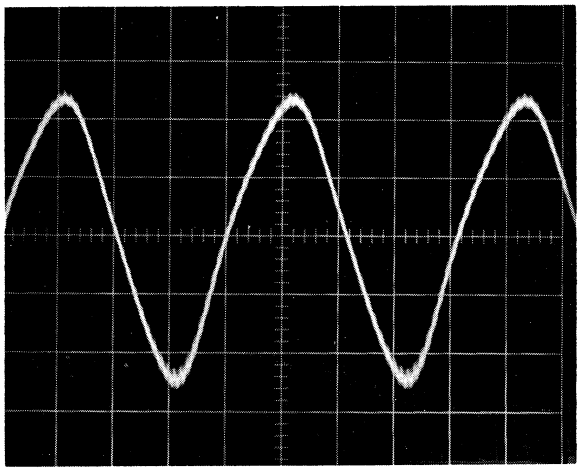

c) Input signal level 0.400 volt rms
Zero frequency offset
Vertical scale 0.20 volt/division
Horizontal scale 20 μs/division

Fig. 3.7. Periodic system response waveforms.

Notice that $|H(\omega_f)|$ is nearly independent of the input signal level, as was expected. The values of G shown above also represent the maximum frequency offset at which the APC system will remain locked (see Section 3.1.2). Although a linear relationship between G and the input signal level was assumed in the analysis, this is not quite appropriate to the experimental circuit. The nonlinearity was introduced by the experimental phase detector, where diodes were employed as envelope detectors. These diodes influence the phase detector gain. Since the diode characteristics are sensitive to the input signal level, then the phase detector gain and, hence, G, varies nonlinearly with the input signal level.

3.3 Comments and Conclusions

The most significant result of this section is the relatively simple expression for system response for the locked instability oscillations given by Eq. 3.33. This equation relates $\varepsilon(t)$ to the input signal parameters and the appropriate APC system constants. The simplicity and general applicability of Eq. 3.33 stems from the fact that knowledge of only the constant H* is necessary to predict behavior, rather than detailed knowledge of the system lowpass filter characteristics. This fact permits the designer of APC systems to determine rapidly the possibility of instability oscillations as a function of system gain, G.

It is worthwhile to compare here the requirement found in Section 3.1.2, i.e., that H*G must be greater than unity for oscillation to exist, with the gain requirements necessary for system instability with an input signal of constant frequency as found in Section 3.1.1. This can be done conveniently, for the example lowpass filter transfer function given by Eq. 3.14, by setting γ equal to zero. In this case, H* is given by

$$H^* = \left. \frac{\tau_1+\tau_2}{1 + (\tau_1^2 + \tau_2^2)\omega^2 + \tau_1^2\tau_2^2\omega^4} \right|_{\omega=\omega_f} , \tag{3.78}$$

where ω_f is found from Eq. 3.57 as

$$\omega_f = \frac{1}{\sqrt{\tau_1\tau_2}} . \tag{3.79}$$

Hence, the product H*G is given by

$$H^*G = \frac{\tau_1\tau_2(\tau_1 + \tau_2)\, G}{\tau_1^2+2\tau_1\tau_2+\tau_2^2} = \frac{\tau_1\tau_2\, G}{\tau_1 + \tau_2} . \tag{3.80}$$

Since H*G must have a value greater than unity for oscillations to exist, it follows that

$$G > \frac{\tau_1 + \tau_2}{\tau_1 \tau_2} \tag{3.81}$$

As expected, inequality 3.81 is identical to inequality 3.17 in Section 3.1.1 when γ and θ_p are zero. It is also possible to show that the same result holds for nonzero γ and θ_p; however, the calculations are considerably more involved.

Note that, although the theoretical development of this chapter is premised on an input signal of constant frequency, the results appear to apply also for slowly modulated input signals. That is, it has been experimentally observed that the same instability oscillations occur when the input signal is (slowly) modulated. Indeed, if an audio modulation signal is present and the system gain is then increased until oscillations result, the audio signal may still be successfully demodulated. In this case, the system response consists of the audio signal and some oscillations. Assuming that the oscillation frequency is sufficiently high, it may be filtered out without appreciably affecting the audio information. Since the system holding range increases with gain, a trade-off between the oscillation amplitude and the system bandwidth may be considered.

4. SECONDARY SIGNAL INTERFERENCE SUSCEPTIBILITY

4.1 Introduction to the Interference Problem

In contrast to the specific requirements for the occurrence of locked instability oscillations, the simple existence of a second periodic input signal leads to a periodic response of an APC system. Although neither special gain nor phase conditions are necessary for the existence of oscillations, both the system gain and phase shift substantially influence the character of the periodic response. In fact, the frequency dependence of the transfer function of the lowpass filter over a wideband must be accounted for in the analysis presented in this section. In the treatment of locked stability oscillations in Section 3, it was sufficient to know only the value, $|H(\omega_f)|$. Indeed, as will be demonstrated, provision for the effect of the secondary signal in the interference susceptibility equations precludes a relatively simple analytical treatment of this problem.

In this section, an extension of the theoretical techniques of Section 3.1.2, which yielded the dependence of the periodic response on system parameters and input signal characteristics, are applied to the secondary signal problem. The initial work makes use of the first of the three interference susceptibility equations derived in Section 2, i.e., Eq. 2.46. The reader will recall that this equation is premised on the assumption that the APC system is sensitive to the input signal amplitude. A set of three equations in three unknowns is found by equating the appropriate coefficients of Eq. 2.46. These "coefficient equations" are used to determine the dependence of the periodic response on the various significant system and signal parameters. This dependence can be examined in detail only for particular choices of lowpass transfer functions.

The initial choice of lowpass transfer characteristic selected is that of the ideal integrator. The three coefficient equations for this characteristic reduce to a single equation which can be solved graphically. This example provides useful insight into the general character of the solutions for more practical system filters. Next, three other APC systems are studied for selected lowpass transfer characteristics. For these studies, the three coefficient equations were solved using a digital computer.

This section continues by considering briefly the stability question of these "forced" oscillations. The procedure is very similar to that presented in Section 3. Also included is a discussion of an alternate approach to the determination of the response characteristics in terms of the input signal and system parameters using the second of the interference-susceptibility equations. This section concludes with a short treatment of the case when the system is insensitive to input signal amplitude.

4.2 Derivation of the Interference Susceptibility Coefficient Equations

In Section 2.3, three equations were developed from the defining equations of the system under the restriction that $\varepsilon(t)$ has the general periodic form given by Eq. 2.28. The first of these, Eq. 2.46, will be considered further in this section, and is repeated below for the reader's convenience.

$$\begin{aligned}\Delta\omega_r = &-k_o \sum_{p=1}^{\infty} e_p \cos(p\omega_f t + \theta_p) \\ &+ G\overline{H}(\omega)\left\{\sin[\Delta\theta_r - k_o \sum_{p=1}^{\infty} \frac{e_p}{p\omega_f} \sin(p\omega_f t + \theta_p)]\right. \\ &\left.+ \eta \sin[\Delta\theta_r - k_o \sum_{p=1}^{\infty} \frac{e_p}{p\omega_f} \sin(p\omega_f t + \theta_p) + \Delta\omega_s t]\right\}\end{aligned} \tag{4.1}$$

Implicit in Eq. 4.1 is the condition that the average frequency of the periodic response is equal to the reference frequency (see Eq. 2.45). As in Section 3, this assumption is justified when the periodic solution is stable. Clearly, if some average frequency difference existed, the consequent increasing (decreasing) phase value would cause a spiraling solution path as opposed to the required closed-loop path. The validity of the calculations made in this section thus rests solely on the stability of the periodic solution.

Following the same approach as employed in the last chapter, we will simplify Eq. 4.1 by retaining only the first term of the sum expressions; i.e., we assume that the waveform of the periodic response is sinusoidal. The simplified equation may be written as

$$\begin{aligned}\Delta\omega_r = &-\beta\omega_f \cos(\omega_f t + \theta_1) + G\overline{H}(\omega)\left\{\sin[\Delta\theta_r - \beta \sin(\omega_f t + \theta_1)]\right. \\ &\left.+ \eta \sin[\Delta\theta_r - \beta \sin(\omega_f t + \theta_1) + \Delta\omega_s t]\right\},\end{aligned} \tag{4.2}$$

where β is defined as before by Eq. 3.23. If we replace the independent variable t by

$$t = t' - \frac{\theta_1}{\omega_f} \quad , \tag{4.3}$$

and define

$$\Delta\theta_s = \Delta\theta_r - \frac{\Delta\omega_s}{\omega_f}\,\theta_1 \quad , \tag{4.4}$$

after the prime notation is dropped, Eq. 4.2 becomes

$$\Delta\omega_r = -\beta\,\omega_f \cos(\omega_f t) + G\bar{H}(\omega)\left\{\sin[\Delta\theta_r - \beta \sin(\omega_f t)] + \eta \sin[\Delta\theta_s + \Delta\omega_s t - \beta \sin(\omega_f t)]\right\} . \tag{4.5}$$

The Bessel function expansion of the sine terms in Eq. 4.5 is

$$\begin{aligned}
&\sin[\Delta\theta_r - \beta \sin(\omega_f t)] + \eta \sin[\Delta\theta_s + \Delta\omega_s t - \beta \sin(\omega_f t)] \\
&= [\sin(\Delta\theta_r) + \eta \sin(\Delta\theta_s + \Delta\omega_s t)] \cos[\beta \sin(\omega_f t)] \\
&- [\cos(\Delta\theta_r) + \eta \cos(\Delta\theta_s + \Delta\omega_s t)] \sin[\beta \sin(\omega_f t)] \\
&= [\sin(\Delta\theta_r) + \eta \sin(\Delta\theta_s + \Delta\omega_s t)]\,[J_o(\beta) + 2J_2(\beta)\cos(2\omega_f t) + \ldots] \\
&- [\cos(\Delta\theta_r) + \eta \cos(\Delta\theta_s + \Delta\omega_s t)]\,[2J_1(\beta)\sin(\omega_f t) + 2J_3(\beta)\sin(3\omega_f t) + \ldots] \quad .
\end{aligned} \tag{4.6}$$

Substitution of this expansion into Eq. 4.5 yields

$$\begin{aligned}
\Delta\omega_r + \beta\omega_f \cos(\omega_f t) = G\bar{H}(\omega)\Big\{ &[\sin(\Delta\theta_r) + \eta \sin(\Delta\theta_s + \Delta\omega_s t)] \\
&\cdot [J_o(\beta) + 2J_2(\beta)\cos(2\omega_f t) + \ldots] \\
&- [\cos(\Delta\theta_r) + \eta \cos(\Delta\theta_s + \Delta\omega_s t)] \\
&\cdot [2J_1(\beta)\sin(\omega_f t) + 2J_3(\beta)\sin(\omega_f t) + \ldots]\Big\} .
\end{aligned} \tag{4.7}$$

Again following the procedures employed in the last chapter, we retain only those terms in Eq. 4.7 which are constant or vary with the fundamental periodic response radian frequency, ω_f. This truncation is justified for APC systems having sufficient attenuation of higher frequencies. The decision of which terms of Eq. 4.7 are to be retained is based on the relationship between $\Delta\omega_s$ and ω_f.

In Ref. 21, Stoker states that four relationships may exist between the forcing-function frequency and the natural system frequency in nonlinear systems. In general, one may expect that

$$\omega_f = \frac{m}{n} \Delta\omega_s \quad , \tag{4.8}$$

where m and n are integers. When m and n are both unity, the system response oscillation is said to be harmonic. When m equals one and n is greater than one, the oscillation is termed subharmonic. When n equals one and m is greater than one, the oscillation is called ultraharmonic. When neither m nor n are equal to unity, the system oscillation is said to be ultra-subharmonic.

In the experimental circuit discussed in Section 5, all but the last of the above forms of oscillation have been observed. However, the harmonic and subharmonic cases predominate. For this reason, the relations between ω_f and $\Delta\omega_s$ in the remainder of this analysis is assumed to be given by

$$\Delta\omega_s = n\omega_f \qquad n = 1, 2, 3, \ldots \quad . \tag{4.9}$$

Substituting Eq. 4.9 into Eq. 4.7, and retaining only the constant and fundamental terms, we obtain

$$\begin{aligned} \Delta\omega_r + \beta\omega_f \cos(\omega_f t) = G\bar{H}(\omega) \Big\{ & J_o(\beta) \sin(\Delta\theta_r) - 2J_1(\beta) \cos(\Delta\theta_r) \sin(\omega_f t) \\ & + n \left[J_{n-1}(\beta) \sin(\omega_f t + \Delta\theta_s) + J_n(\beta) \sin(\Delta\theta_s) \right. \\ & \left. - J_{n+1}(\beta) \sin(\omega_f t - \Delta\theta_s) \right] \Big\} \qquad n = 1, 2, 3, \ldots \quad . \end{aligned} \tag{4.10}$$

Separately equating the constant and fundamental terms of Eq. 4.10 yields the following pair of equations

$$\Delta\omega_r = G[J_o(\beta) \sin(\Delta\theta_r) + \eta J_n(\beta) \sin(\Delta\theta_s)] \quad , \tag{4.11}$$

$$\begin{aligned}\beta\omega_f \cos(\omega_f t) = G\overline{H}(\omega_f) [&-2J_1(\beta) \cos(\Delta\theta_r) \sin(\omega_f t) \\ &+ \eta J_{n-1}(\beta) \sin(\omega_f t + \Delta\theta_s) \\ &- \eta J_{n+1}(\beta) \sin(\omega_f t - \Delta\theta_s)] \quad .\end{aligned} \tag{4.12}$$

It is now noted that for small β, $J_{n+1}(\beta)$ is small compared with $J_{n-1}(\beta)$. Thus, Eq. 4.12 can then be approximated by

$$\begin{aligned}\beta\omega_f \cos(\omega_f t) = G\overline{H}(\omega_f) \Big\{ &[-2J_1(\beta) \cos(\Delta\theta_r) + \eta J_{n-1}(\beta) \cos(\Delta\theta_s)] \sin(\omega_f t) \\ &+ [\eta J_{n-1}(\beta) \sin(\Delta\theta_s)] \cos(\omega_f t) \Big\} \quad .\end{aligned} \tag{4.13}$$

Now, if $\overline{H}(\omega_f)$ is written in the form

$$\overline{H}(\omega_f) = |\overline{H}(\omega_f)| \exp[j\Omega(\omega_f)] \quad , \tag{4.14}$$

Eq. 4.13 can be written as

$$\begin{aligned}\beta\omega_f \cos(\omega_f t) = G|\overline{H}(\omega_f)| \Big\{ &[-2J_1(\beta) \cos(\Delta\theta_r) + \eta J_{n-1}(\beta) \cos(\Delta\theta_s)] \\ &\cdot \sin[\omega_f t + \Omega(\omega_f)] \\ &+ [\eta J_{n-1}(\beta) \sin(\Delta\theta_s)] \cos[\omega_m t + \Omega(\omega_f)] \Big\} \quad .\end{aligned} \tag{4.15}$$

Equating coefficients in Eq. 4.15 yields the following two equations

$$\cot \Omega(\omega_f) = \frac{\eta J_{n-1}(\beta) \sin(\Delta\theta_s)}{\eta J_{n-1}(\beta) \cos(\Delta\theta_s) - 2J_1(\beta) \cos(\Delta\theta_r)} \quad , \tag{4.16}$$

$$\begin{aligned}\beta\omega_f = G|\overline{H}(\omega_f)| [&4J_1^2(\beta) \cos^2(\Delta\theta_r) - 4J_1(\beta) \cos(\Delta\theta_r) \\ &\cdot \eta J_{n-1}(\beta) \cos(\Delta\theta_s) + \eta^2 J_{n-1}^2(\beta)]^{1/2} .\end{aligned} \tag{4.17}$$

Equations 4.11, 4.16 and 4.17 are the coefficient equations from which the dependence of $\Delta\theta_r$, $\Delta\theta_s$, and β on η, $\Delta\omega_r$, $\Delta\omega_s$, G and $\overline{H}(\omega)$ can be found. This dependence information in turn permits predicting the secondary signal interference susceptibility characteristics of the APC system, at least for small β. Unfortunately, these three coefficient equations are quite complex and cannot be solved conveniently even by graphical techniques. In Sections 4.3 and 4.4, solutions of these equations will be found for various lowpass filter characteristics.

In concluding this section it is necessary to emphasize a fact that is implicit in the development above. The reader will recall that there are neither special gain nor phase-shift requirements for the existence of oscillations in the present case. Nevertheless, the applicability of this study is limited to values of APC system gain such that locked instability oscillations will not occur. This restriction prevents the simultaneous occurrence of two distinct modes of oscillation and, consequently, permits writing the form of the oscillatory system response in terms of a single Fourier series, as was assumed originally.

4.3 Susceptibility Characteristics of the Ideal Integrator

In the previous section, three coefficient equations in three unknowns were derived for those APC systems whose gain is proportional to the input signal level. If, in addition, an ideal integrator[3] is assumed for the system's lowpass transfer characteristic, then these three equations reduce to the following single equation,

$$\frac{G_\infty}{\tau\omega_f^2} = \frac{\beta}{2J_1(\beta) \mp \eta J_{n-1}(\beta)} \quad , \tag{4.18}$$

where G_∞ is equal to $k_o k_m E_o E_r$ as before (see Eq. 3.20) and τ is the integrator time constant. This single equation follows from the fact that $\Delta\theta_s$ must be equal to either 0 or π radians

---

[3] In Section 3.1.1 it was shown that the assumption of an ideal integrator lowpass filter characteristic produced an unstable system and, consequently, the coefficient equations developed in Section 4.2 do not apply. With an arbitrary, small amount of damping, however, the integrator system is stable (see the comments following Eq. 3.20). The reader may choose to view this section as either an approximate solution to an almost-ideal integrator case, or an exact solution to the ideal integrator case with an approximate model. In either case, the purpose of this section is to illustrate the basic susceptibility characteristics for this particularly simple case. In the following section, rigor is achieved at the expense of considerable additional complexity.

as required by Eq. 4.13 whenever the lowpass transfer characteristic has a phase shift of $\pi/2$ radians, and the fact that $\Delta\theta_r$ must be equal to zero, since $\Delta\omega_r$ is zero (see Eq. 4.11). Thus, Eqs. 4.11 and 4.16 are identically equal to zero, and Eq. 4.17 reduces to Eq. 4.18. Notice also that Eq. 4.18 reduces to Eq. 3.38 when η becomes equal to zero.

The solution of Eq. 4.18 for β can be obtained graphically for each value of n. Figure 4.1 is a plot of β versus $G_\infty/\tau\omega_f^2$ for various values of η and for n equal to one (the harmonic solution). The three values of η shown (0.1, 0.2, and 0.355) correspond, respectively, to secondary reference signal power levels of -20 db, -14 db, and -9 db. Three aspects of these curves warrant comment. The first, which aids in constructing these curves, concerns the intersection of all curves for the various values of η. It is easy to determine the point of intersection. Let β^* be the value of the ordinate at this point and equate

$$\frac{\beta^*}{2J_1(\beta^*) + \eta J_0(\beta^*)} = \frac{\beta^*}{2J_1(\beta^*) - \eta J_0(\beta^*)} \quad . \tag{4.19}$$

The solution of this equation for nonzero η requires that $J_0(\beta^*)$ equal zero. The first zero of $J_0(\beta)$ occurs for β^* equal to 2.4048. The corresponding abscissa value is given by $\beta^*/2J_1(\beta^*)$ and is equal to 2.317.

The second aspect concerns the curves in Fig. 4.1 that result from subtracting the $\eta J_0(\beta)$ term in the denominator of Eq. 4.18. All of these curves have a minimum value of $G_\infty/\tau\omega_f^2$. The coordinates of this minimum point may be determined by equating the following expression to zero

$$\frac{d[G_\infty/\tau\omega_f^2]}{d\beta} = \frac{3J_1(\beta) - \eta J_0(\beta) - \beta[2J_0(\beta) + \eta J_1(\beta)]}{[2J_1(\beta) - \eta J_0(\beta)]^2} = 0 \tag{4.20}$$

and solving for η

$$\eta = \frac{2[2J_1(\beta) - \beta J_0(\beta)]}{J_0(\beta) + \beta J_1(\beta)} \quad . \tag{4.21}$$

A graphical solution of Eq. 4.21 is presented in Fig. 4.2. As η increases, the value of β at which the minimum value of $G_\infty/\tau\omega_f^2$ is reached also increases. The corresponding value of $G_\infty/\tau\omega_f^2$ is again found from Eq. 4.18 once the value of β has been found. The locations

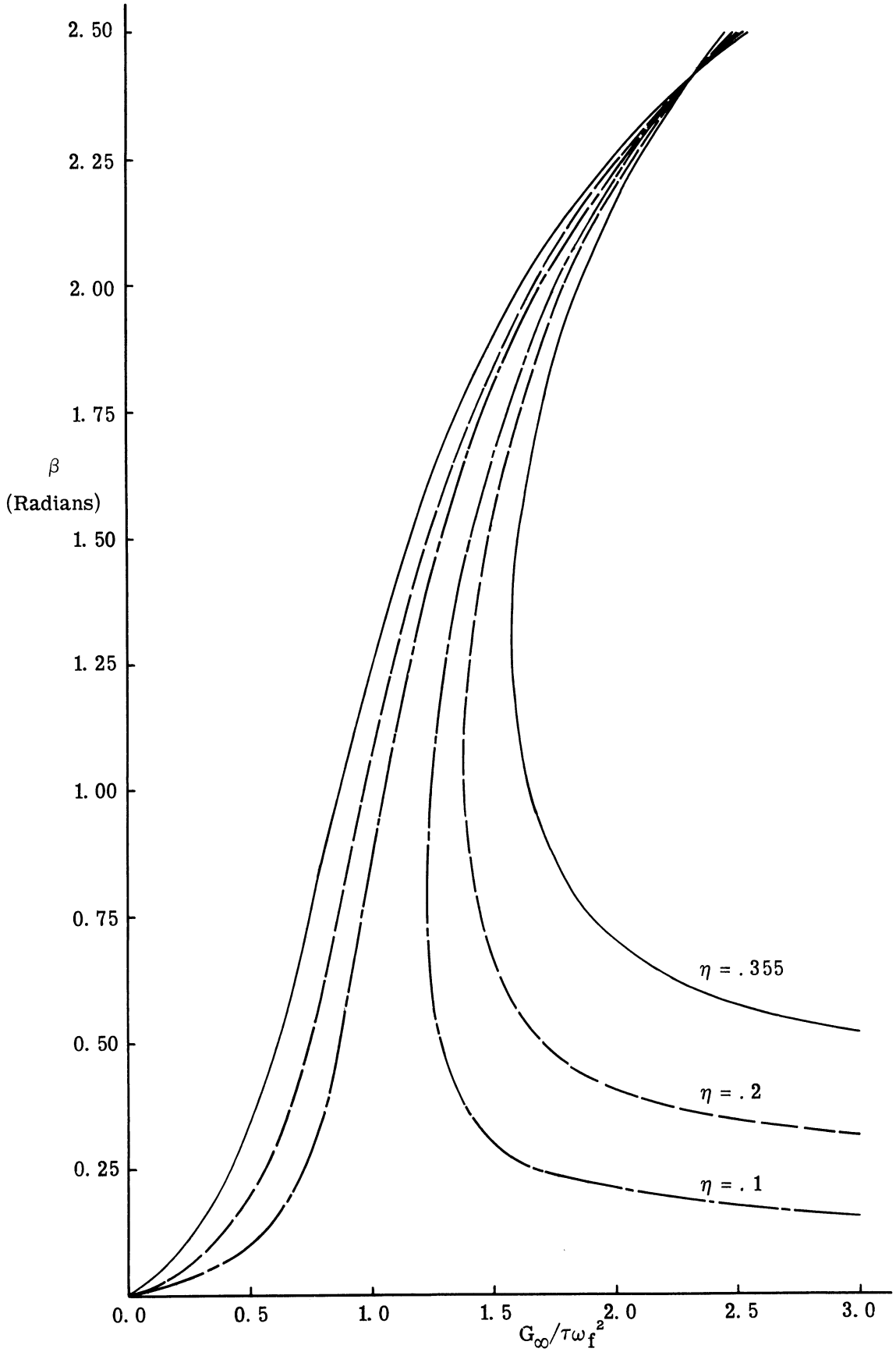

Fig. 4.1. The harmonic relation between β and $G_\infty/\tau\omega_f^2$.

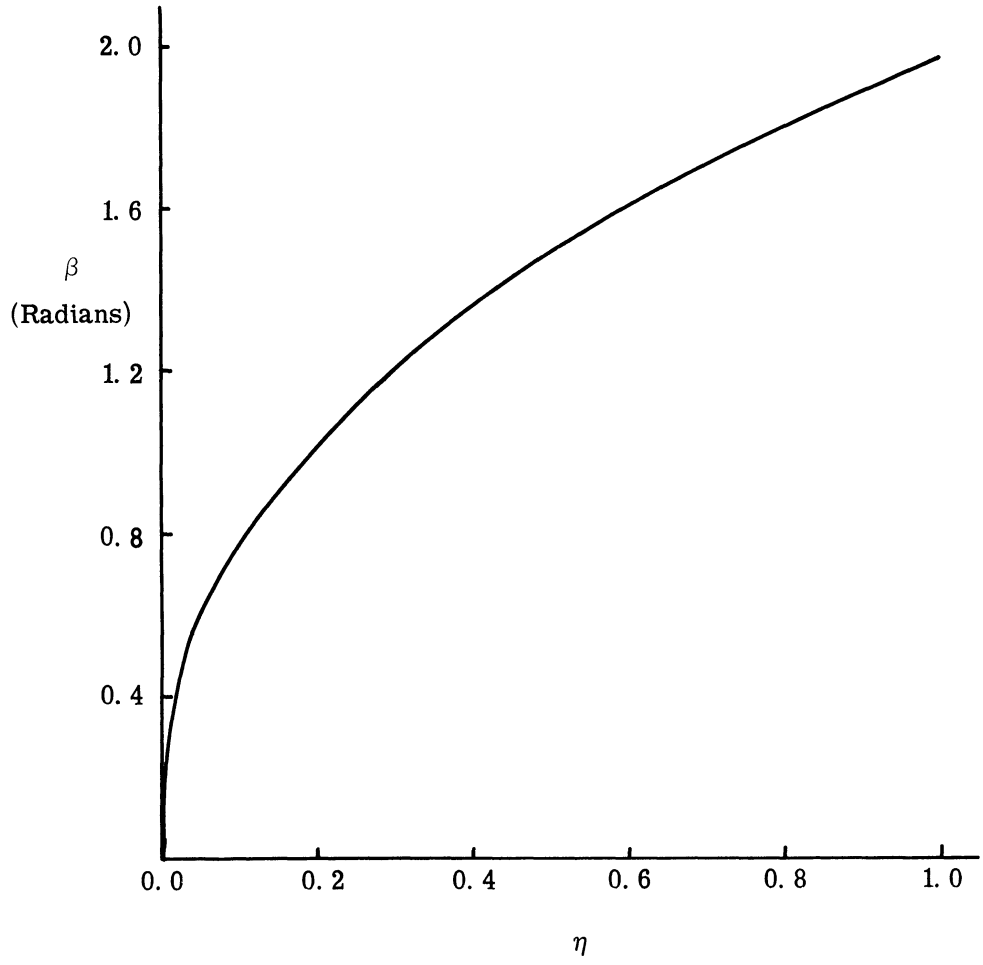

Fig. 4.2. The β values for which $G_\infty/\tau\omega_f^2$ is minimum.

of these minimum values are useful for constructing the graph shown in Fig. 4.1. A further significance to these minima is that as $G_\infty/\tau\omega_f^2$ is decreased, β must exhibit a jump discontinuity for each fixed value of η. This point will be seen more clearly in the construction of Fig. 4.5 below.

The third aspect concerns the limiting value of the curves in Fig. 4.1 for high values of $G_\infty/\tau\omega_f^2$. From Eq. 4.18 it is clear that this occurs for values of β such that

$$2J_1(\beta) - \eta J_0(\beta) = 0 \quad . \tag{4.22}$$

The solution of β as a function of η for this equation is given in Fig. 4.3. Again this information is useful in constructing the original graph shown in Fig. 4.1.

The next step in determining the interference susceptibility characteristics of an APC system with an ideal-integrator lowpass filter is to plot β versus $G_\infty/\tau\omega_f^2$ for various values of η, and for n equal to two (the first subharmonic solution). These curves, shown in Fig. 4.4, lack distinctive features due to the relatively simple form of the denominator in Eq. 4.18. In principle, one next can construct the appropriate curves for n equal to three, etc.; however, the contribution from these higher order subharmonic solutions will be relatively negligible. This statement follows from two facts. First, the secondary signal will now be essentially outside the passband of the APC system, and second, the shape of the higher-order theoretical curves restricts any appreciable contribution.

Using the curves given in Figs. 4.1 and 4.4, β can be plotted as a function of $\Delta\omega_s$ (the difference in the frequencies of the reference and secondary signals) with η as a parameter. The dependence of $\Delta\theta_s$, $\Delta\theta_r$, and β on $\Delta\omega_s$, $\Delta\omega_r$, η, G, and $H(\omega)$ is then

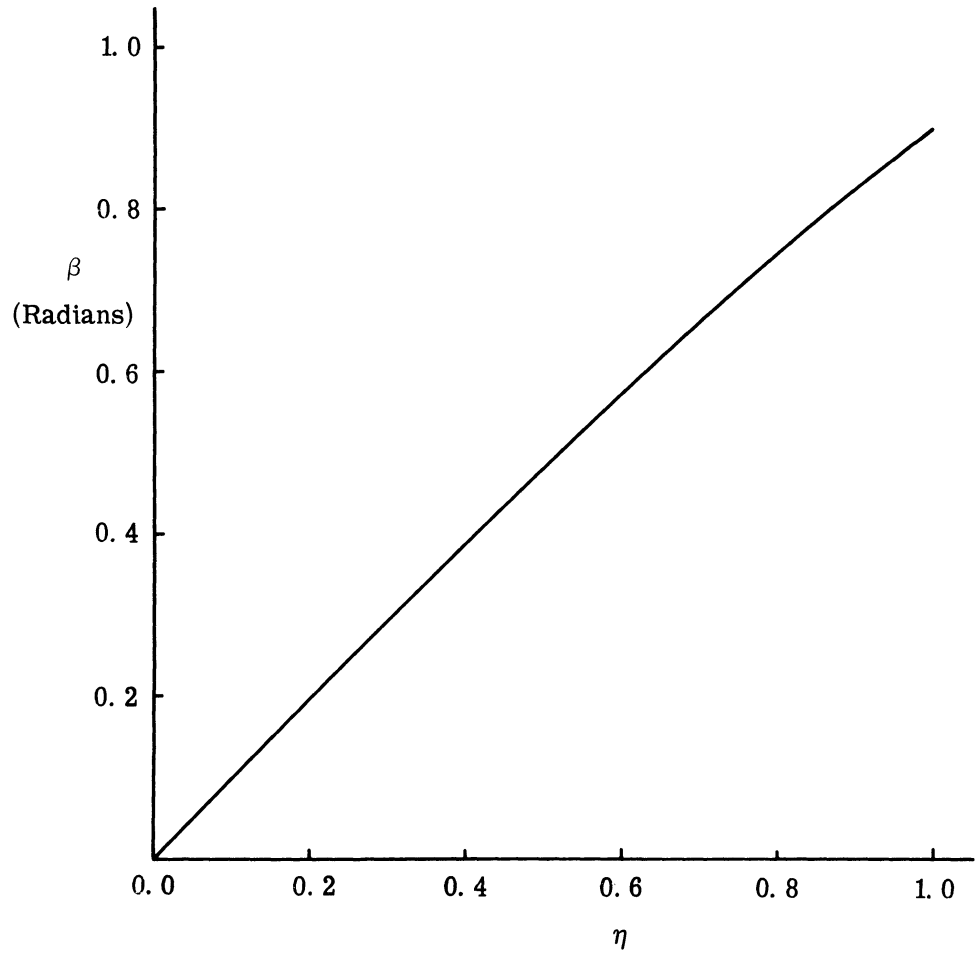

Fig. 4.3. The limiting values of β for infinite $G_\infty/\tau\omega_f^2$.

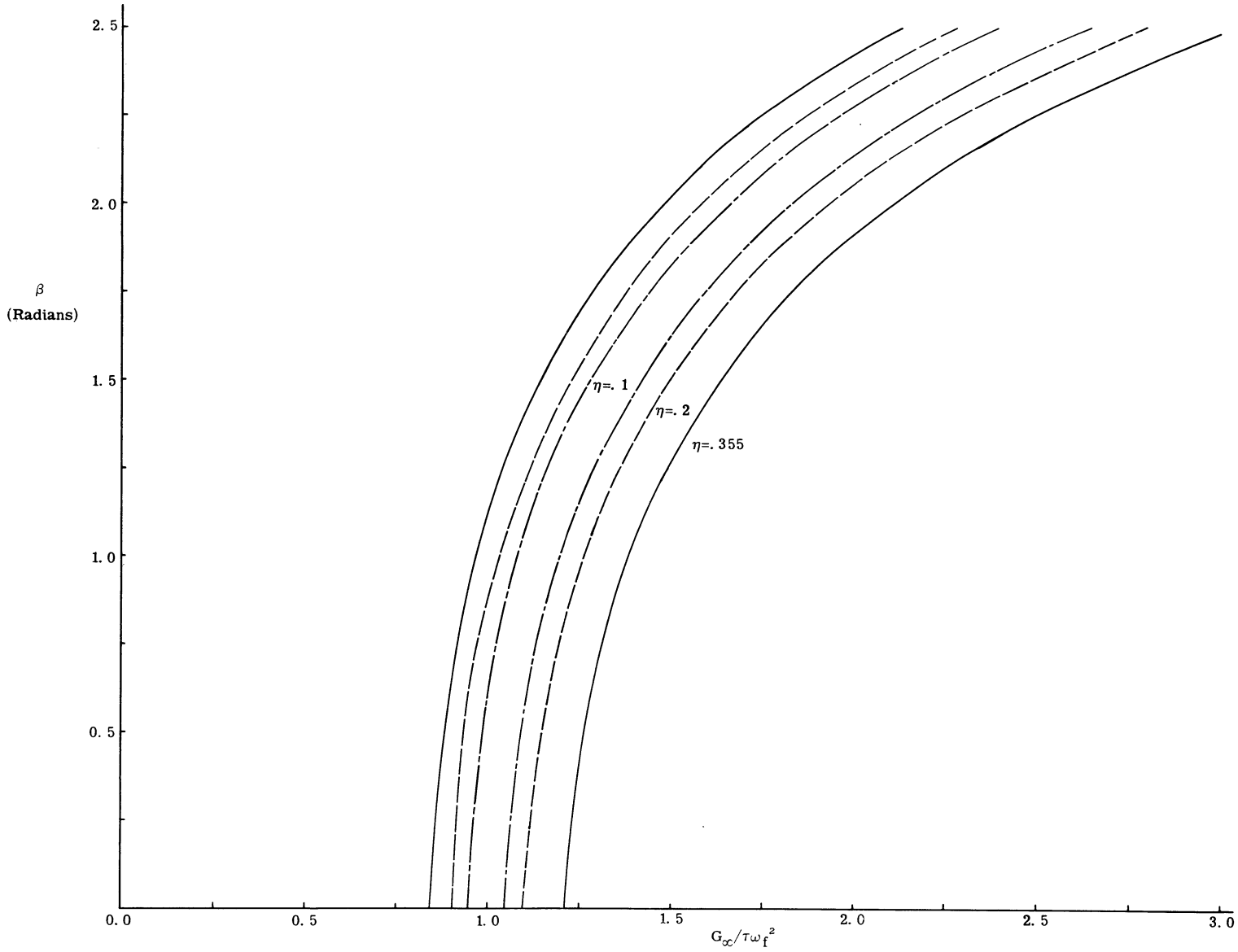

Fig. 4.4. The first subharmonic relationship between β and $G_\infty/\tau\omega_f^2$.

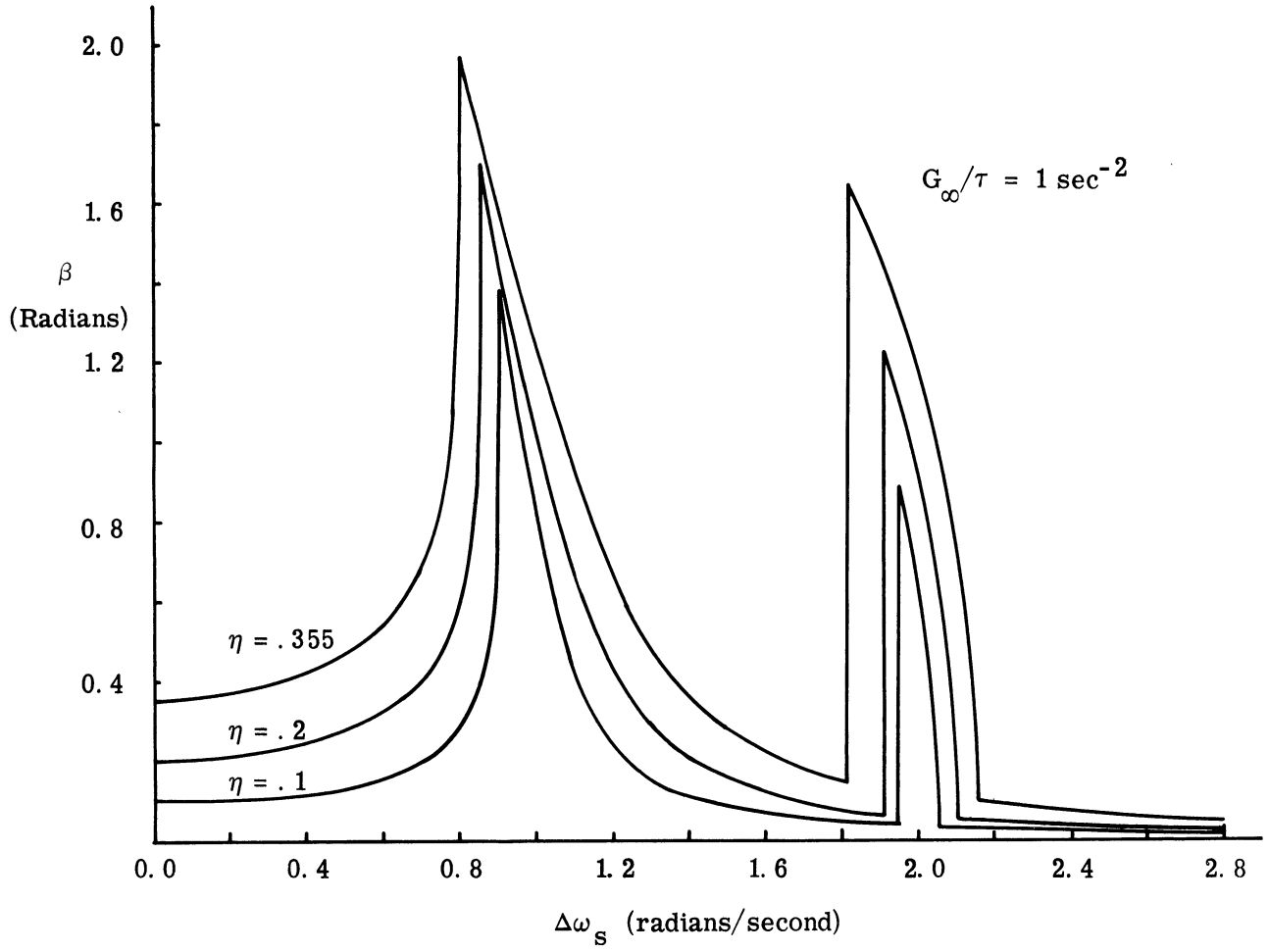

Fig. 4.5. The β characteristics for an APC system with an ideal-integrator lowpass filter.

established for this particular lowpass filter. From $\Delta\theta_s$, $\Delta\theta_r$, and β, the values of θ_1, θ_o, and e_1 can be determined to complete the solution. The reader will recall that both $\Delta\omega_r$ and $\Delta\theta_r$ are zero for the ideal-integrator lowpass transfer characteristic, while $\Delta\theta_s$ is equal to either zero or π radians. The value of $\Delta\theta_s$ is dependent on $\Delta\omega_s$, as will be seen shortly.

Figure 4.5 shows β versus $\Delta\omega_s$ for the three values of η. It was constructed as follows. The ratio G_∞/τ was assigned unity value, and $\Delta\omega_s$ was allowed to range between 0 and 2.8 radians per second. With $\Delta\omega_s$ equal to ω_f, Fig. 4.1 was used to find β as a function of $\Delta\omega_s$ over its range for each value of η. The limiting values of β, for $\Delta\omega_s$ equal to zero, were read from Fig. 4.3. Superimposed on this plot (the second group of peaks) are the values of β obtained from Fig. 4.4 (first subharmonic solution) with $\Delta\omega_s$ equal to $2\omega_f$. The

periodic system response frequency is equal to $\Delta\omega_s$ except within the range of the second peaks, where ω_f is half of $\Delta\omega_s$.

In Section 3, it was sufficient to plot β, e_1 being known immediately since β and e_1 are proportional when the system oscillation frequency is constant (see Eq. 3.23). In the present case, ω_f is not constant. The curves of $k_o e_1$ versus $\Delta\omega_s$, shown in Fig. 4.6, are obtained directly from Fig. 4.5 by multiplying each ordinate value by the appropriate value of ω_f. These two sets of curves differ in one important aspect--the periodic system response amplitude decreases to zero (nearly linearly for low frequencies) with decreasing $\Delta\omega_s$, whereas β approaches a limiting value.

The variable $\Delta\theta_s$ is equal to 0 radian for the negative sign in Eq. 4.18 and π radians for the positive sign. Translating this to either Fig. 4.5 or 4.6, it can be seen that $\Delta\theta_s$ is equal to zero for values of $\Delta\omega_s$ from zero to the occurrence of the first jump, i.e., 0.8 cps for $\eta = 0.355$. For all higher frequencies, $\Delta\theta_s$ is equal to π.

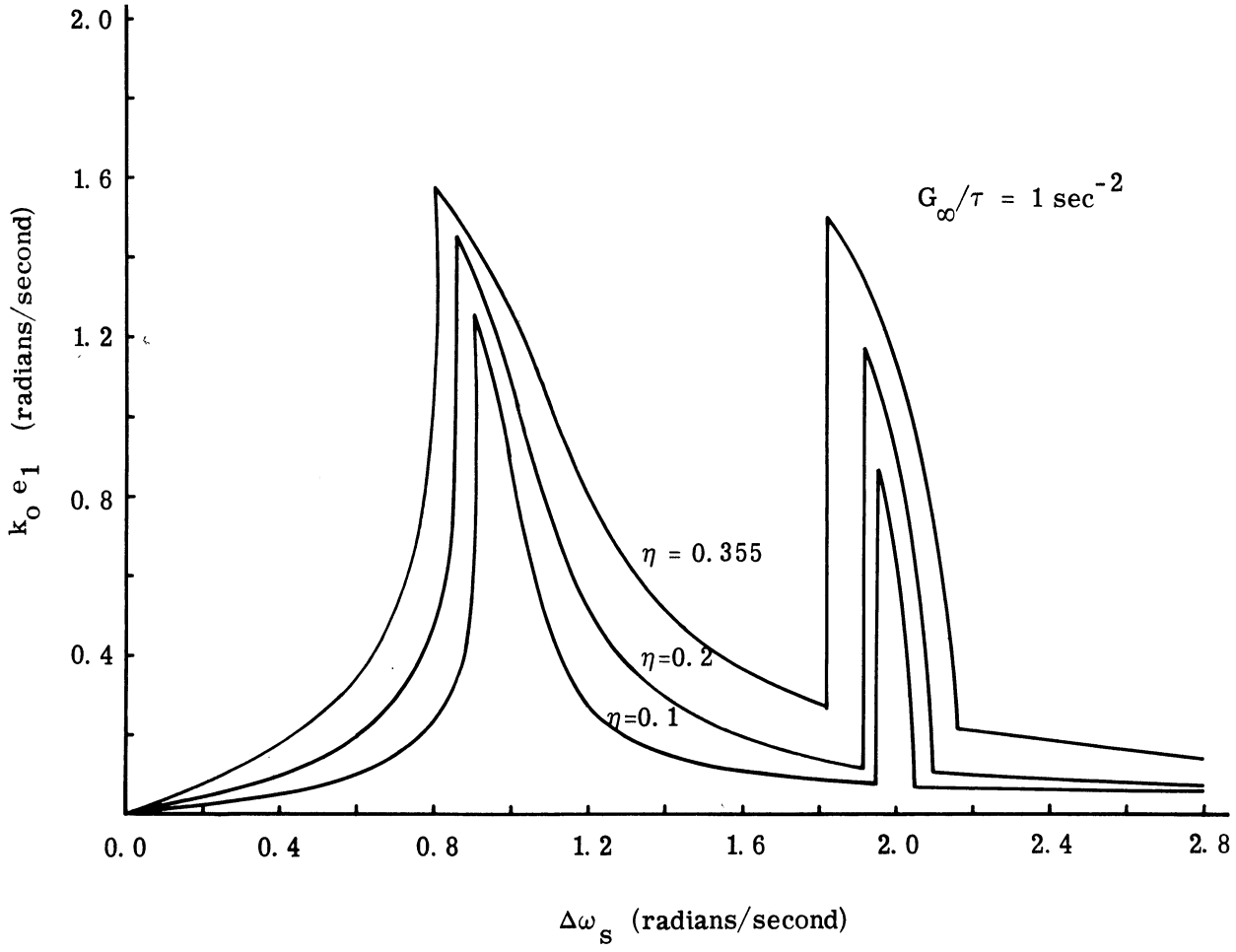

Fig. 4.6. The system response characteristics for an APC system with an ideal-integrator lowpass filter.

In conclusion, the reader is reminded that the purpose of this section has been to introduce the basic characteristics of secondary-signal susceptibility interference. As will be seen theoretically in Section 4.4, and experimentally in Section 5, these results, although somewhat extreme, show qualitative similarity to the results for other transfer characteristics. One indeed finds essentially abrupt jumps in the system response amplitude, and rapid changes in $\Delta\theta_s$, for certain lowpass filters.

A more complex graphical analysis of the three, original, coefficient equations can be carried out for any $H(\omega)$ that has a negative $\pi/2$ radian phase shift at a finite frequency. This analysis is applicable to only a narrow range of frequencies about the critical frequency above. Here the original three equations reduce to

$$\frac{\overline{H}(\omega_f)G}{\omega_f} = \frac{\beta}{2J_1(\beta)\cos(\Delta\theta_r) \mp \eta J_{n-1}(\beta)} \tag{4.23}$$

and

$$\frac{\overline{H}(\omega_f)\Delta\omega_r}{\omega_f} = \frac{\beta J_o(\beta)\sin(\Delta\theta_r)}{2J_1(\beta)\cos(\Delta\theta_r) \mp \eta J_{n-1}(\beta)} \ . \tag{4.24}$$

The procedure for solving these equations is very similar to that used previously in this section and in Section 3.

4.4 Susceptibility Characteristics of Three Other Lowpass Filters

In this section, we return to the problem of the effect of more practical lowpass filter characteristics. For such filters, none of the three coefficient equations developed in Section 4.2 is identically equal to zero. The first step in the analysis procedure for any given filter is the specification of $H(\omega)$ in terms of a magnitude and phase function of frequency. The sequence of subsequent steps is somewhat arbitrary. We have chosen to specify next the system gain, G. Finally, the three dependent variables ($\Delta\theta_r$, $\Delta\theta_s$, and β) are solved for in terms of $\Delta\omega_r$ and $\Delta\omega_s$, with η serving as a parameter.

The technique for solving the three coefficient equations used in this study is an extension of Newton's method for finding the zeros of a function in one variable. This extension, known as the Newton-Raphson method, is discussed in Appendix A. Both of these methods are iterative procedures and thus are easily implemented for solution on a digital computer. A flow chart for the Newton-Raphson method solution to Eqs. 4.11, 4.16, and 4.17,

along with the derivation of the required matrix coefficients for the method, are presented in Appendix B. In the remainder of this section, the computer solution for three specific lowpass filters are presented as examples.

The first solution is for a stable APC system with a lowpass filter having a single real pole at -6.06×10^4 radians/sec. This value corresponds to the design value for the particular lowpass filter incorporated in the experimental circuit shown in Fig. 5.2. The square of the magnitude of the filter transfer function and the cotangent of the filter phase characteristic were computed, and are plotted over a portion of their range in Fig. 4.7. These two filter properties are required in the program based on the Newton-Raphson method (see Appendix B). Notice that the system is necessarily stable, since the cotangent never reaches zero at a finite frequency.

The three sets of curves shown in Figs. 4.8-4.10 correspond, respectively to three distinct selections of system gain. Each of these sets shows $k_o e_1$ (equal to $\Delta\omega_s \beta$) plotted versus $\Delta\omega_s$, for $\Delta\omega_r$ equal to zero and for the values of η indicated. Only the harmonic solution has been calculated from theoretical considerations and plotted here. All of these curves are far less peaked, and lack the abrupt jumps, obtained with the ideal integrator characteristic. Nevertheless, there is a maximum value to the periodic system response, which increases both in amplitude and frequency with increasing loop gain, for each value of η. The same general characteristics are observed for nonzero values of $\Delta\omega_r$, as will be seen in a later example.

For the second example solution, a zero located at -19.15×10^4 radians/sec. is added to the pole of the first example in the filter characteristic. This type of filter frequently is found in practical APC systems, the zero being located to optimize the system's signal-to-noise characteristics (see Ref. 4 for the appropriate design equations). The squared magnitude of the transfer function, and the cotangent of its phase angle for this filter are shown for this in Fig. 4.11. This system is also stable; indeed, it is more so since the cotangent always has a smaller value than in the last example.

The same system gains were chosen for this example to facilitate comparison. The Figs. 4.12-4.14 are the curves of $k_o e_1$ versus $\Delta\omega_s$ with $\Delta\omega_r$ equal to zero. The curves are even less peaked and of lower amplitude in this example than in the previous one. Notice, however, that as before, the maximum system response amplitude, and its frequency of occurrence along the $\Delta\omega_s$ axis, increase with increasing system gain.

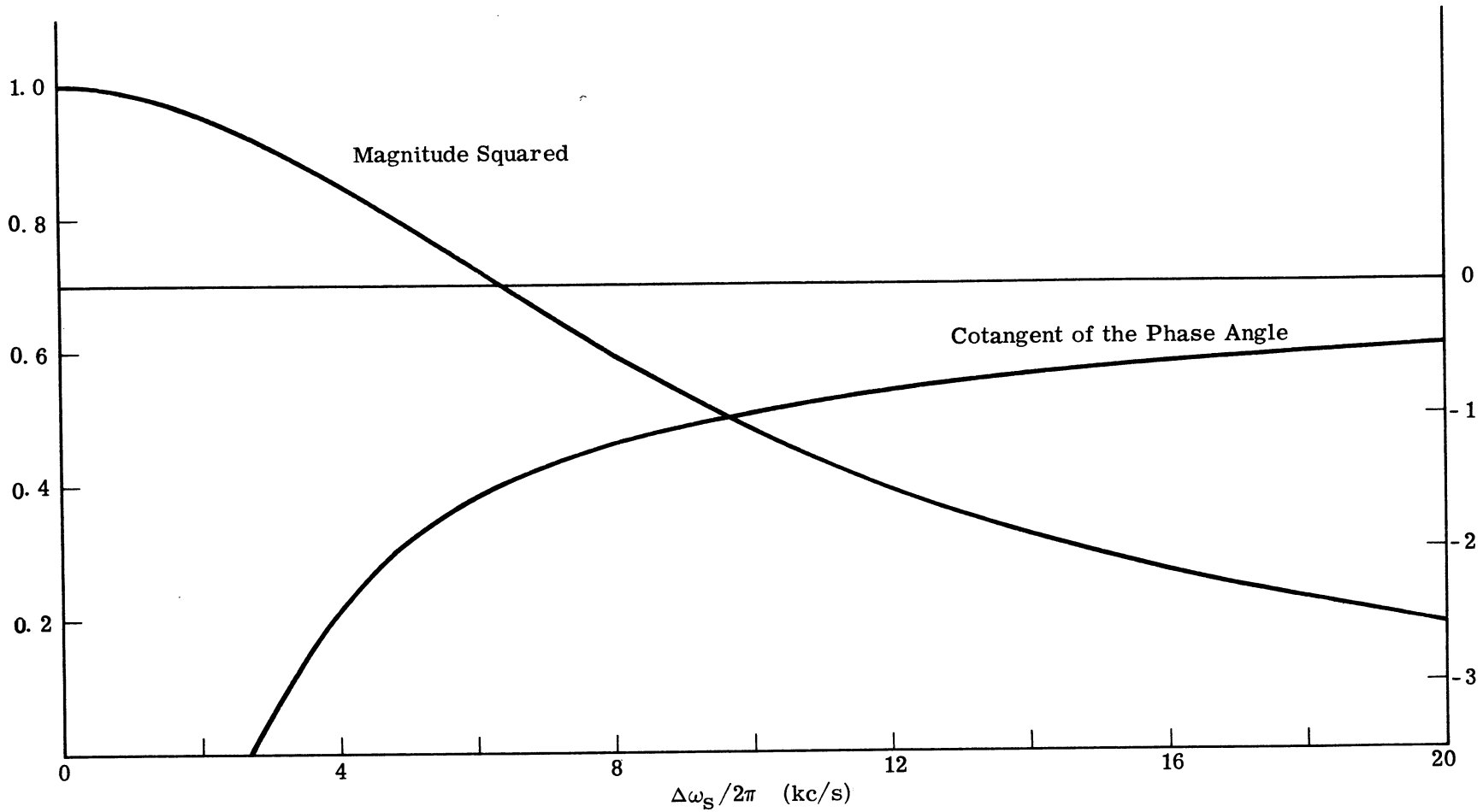

Fig. 4.7. Characteristics of the single pole filter.

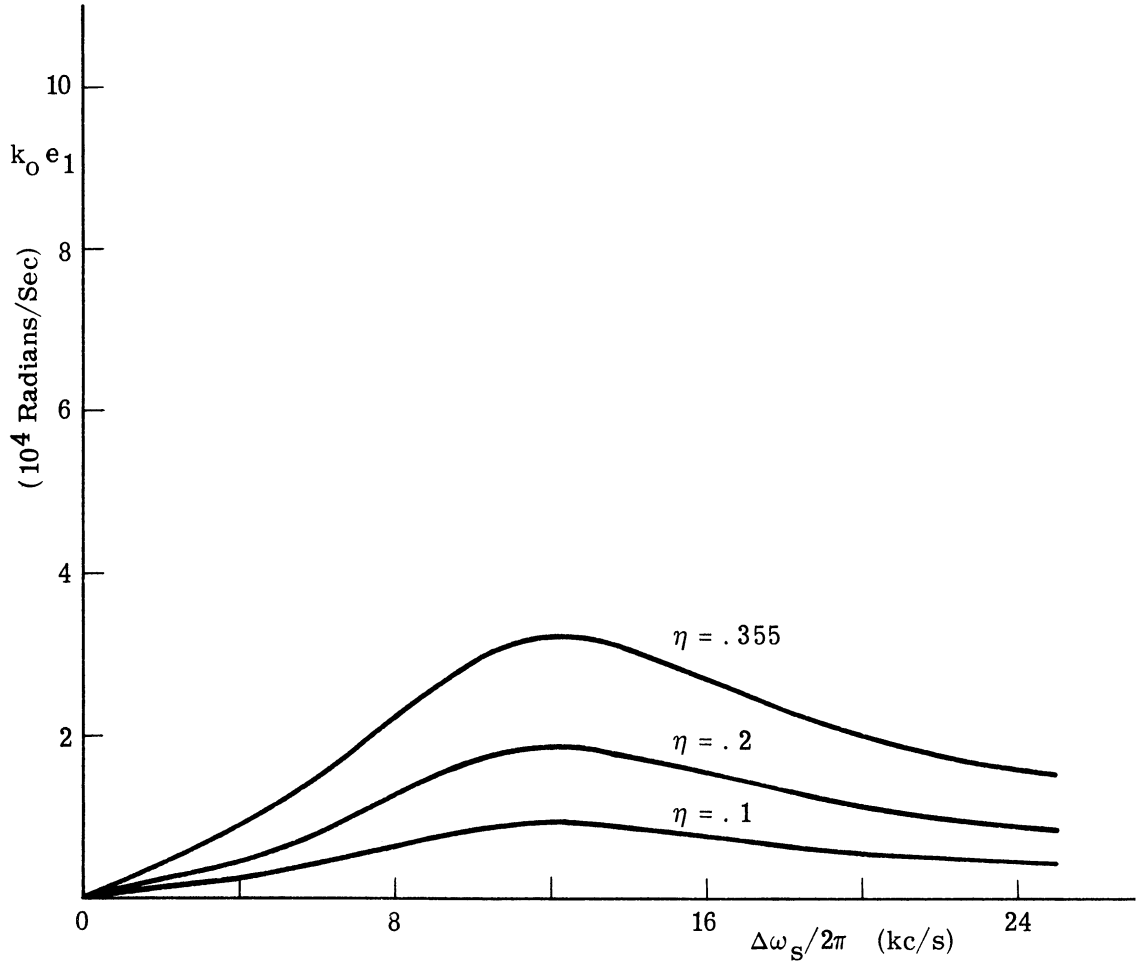

Fig. 4.8. System response for the single pole filter with G equal to 0.956 x 10^5 radians/second.

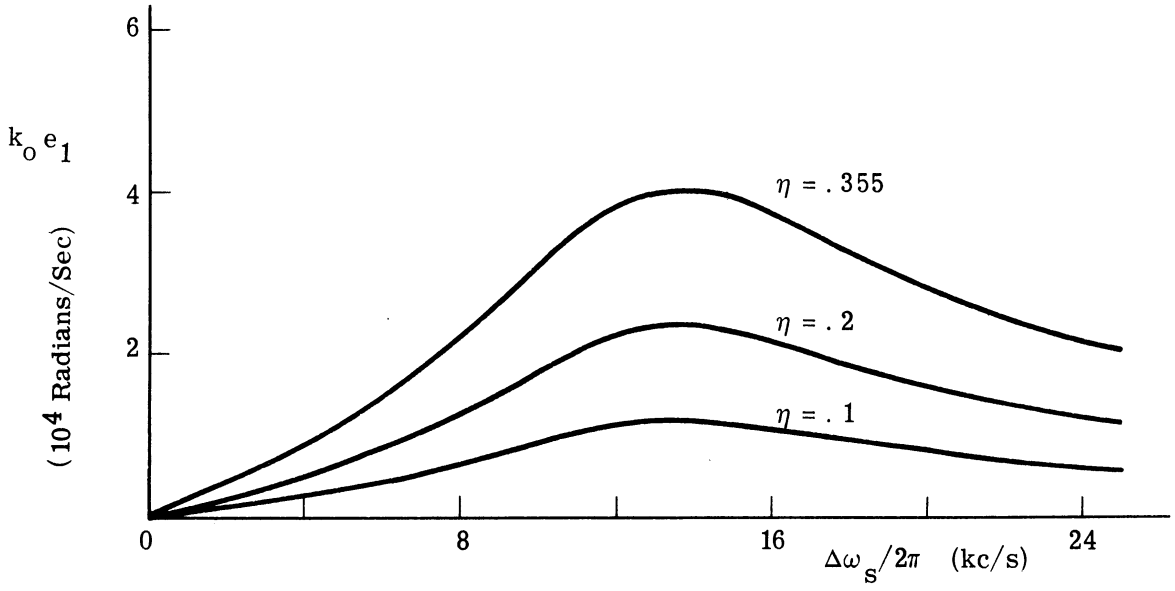

Fig. 4.9. System response for the single pole filter with G equal to 1.20 x 10^5 radians/second.

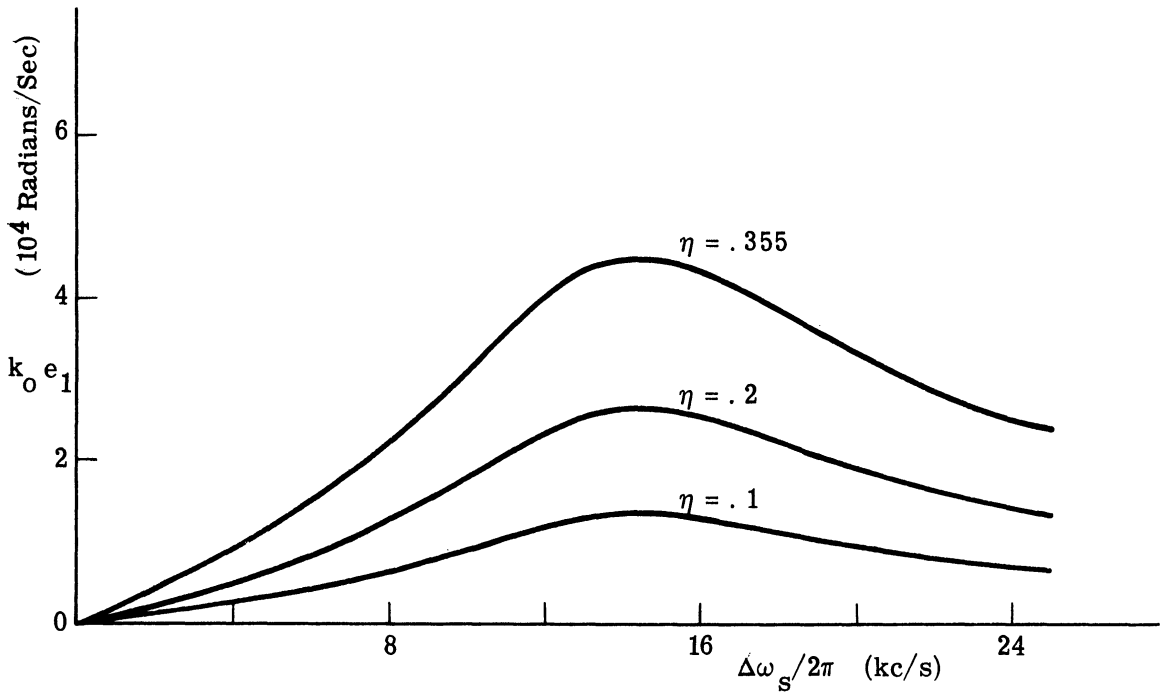

Fig. 4.10. System response for the single pole filter with G equal to 1.35×10^5 radians/second.

In the third example solution, the zero in the filter characteristic of the second example is replaced with a pair of complex conjugate poles. The filter transfer function is then given by

$$H(s) = \frac{1.984 \times 10^{15}}{(s+6.06\times10^4)(s+1.207\times10^5+j\ 1.348\times10^5)(s+1.207\times10^5-j\ 1.348\times10^5)} \quad (4.25)$$

This particular filter characteristic was originally chosen as an approximation to the composite lowpass filter characteristic of the experimental system shown in Fig. 5. Consequently, a relatively complete theoretical study of this case was performed and is presented here for its general interest. Subsequent experimental studies indicated, however, that the actual filter characteristic was not as accurately approximated in the example as was thought.

Once again, the square of the filter transfer characteristic magnitude, and the cotangent of the filter phase angle were computed and are plotted over a portion of their range in Fig. 4.15. It is interesting to compare the three sets of filter curves for these three examples. The magnitude curves are nearly identical, particularly the first

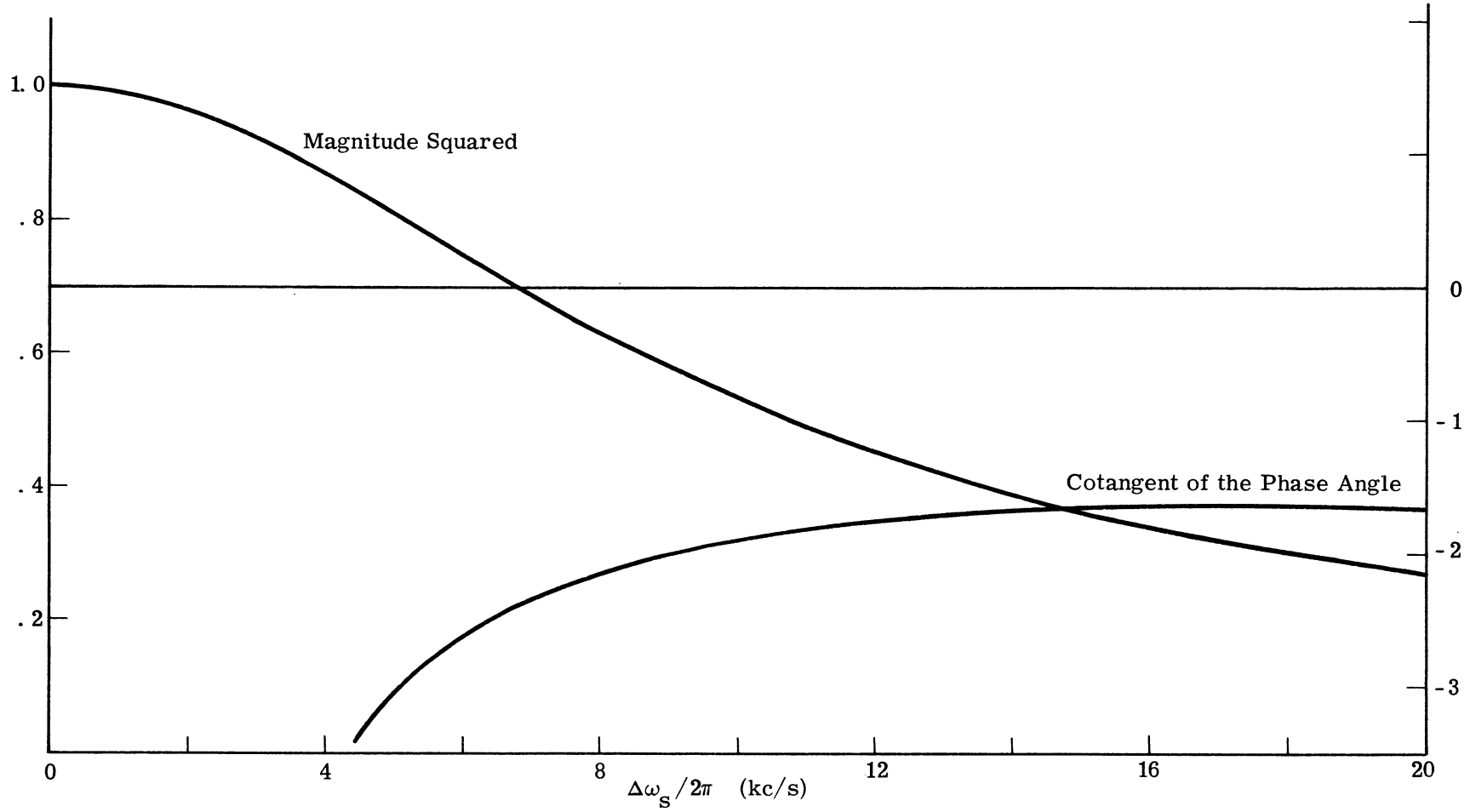

Fig. 4.11. Characteristics of the single pole-single zero filter.

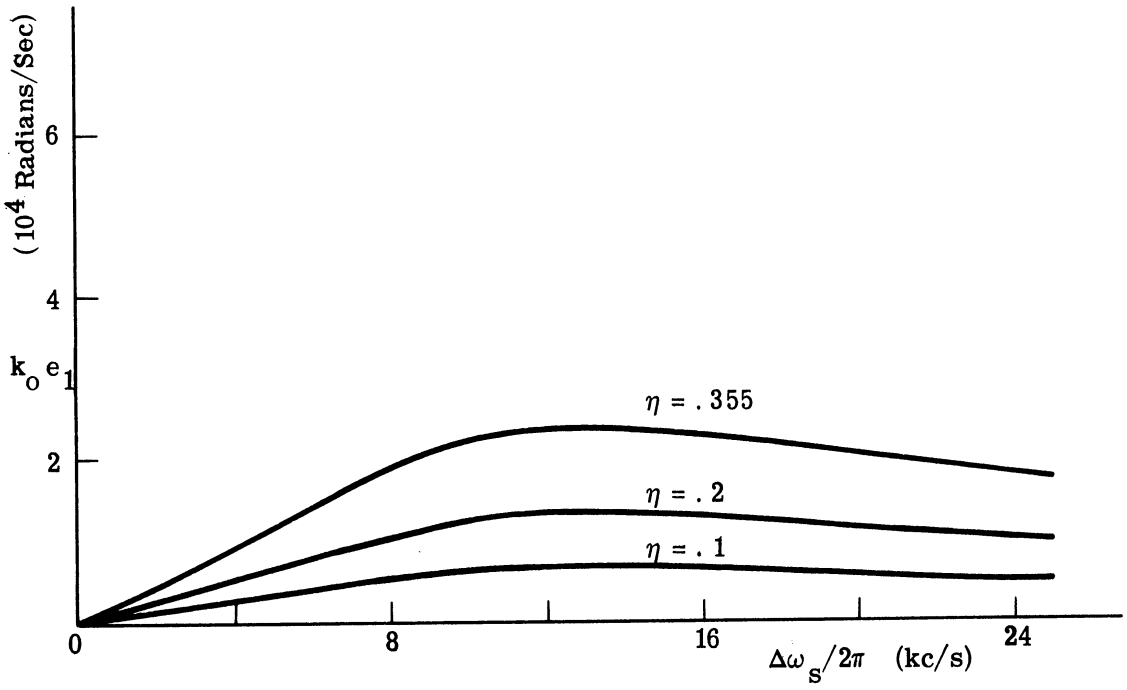

Fig. 4.12. System response for the single pole-single zero filter with G equal to 0.956 x 10^5 radians/second.

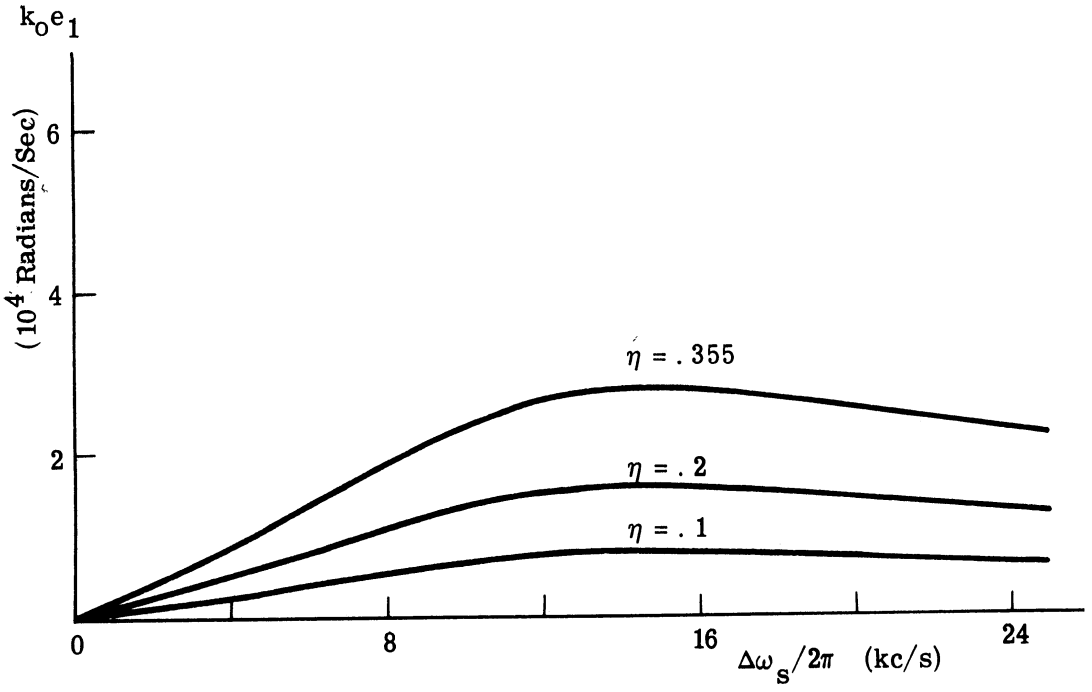

Fig. 4.13 System response for the single pole-single zero filter with G equal to 1.20 x 10^5 radians/second.

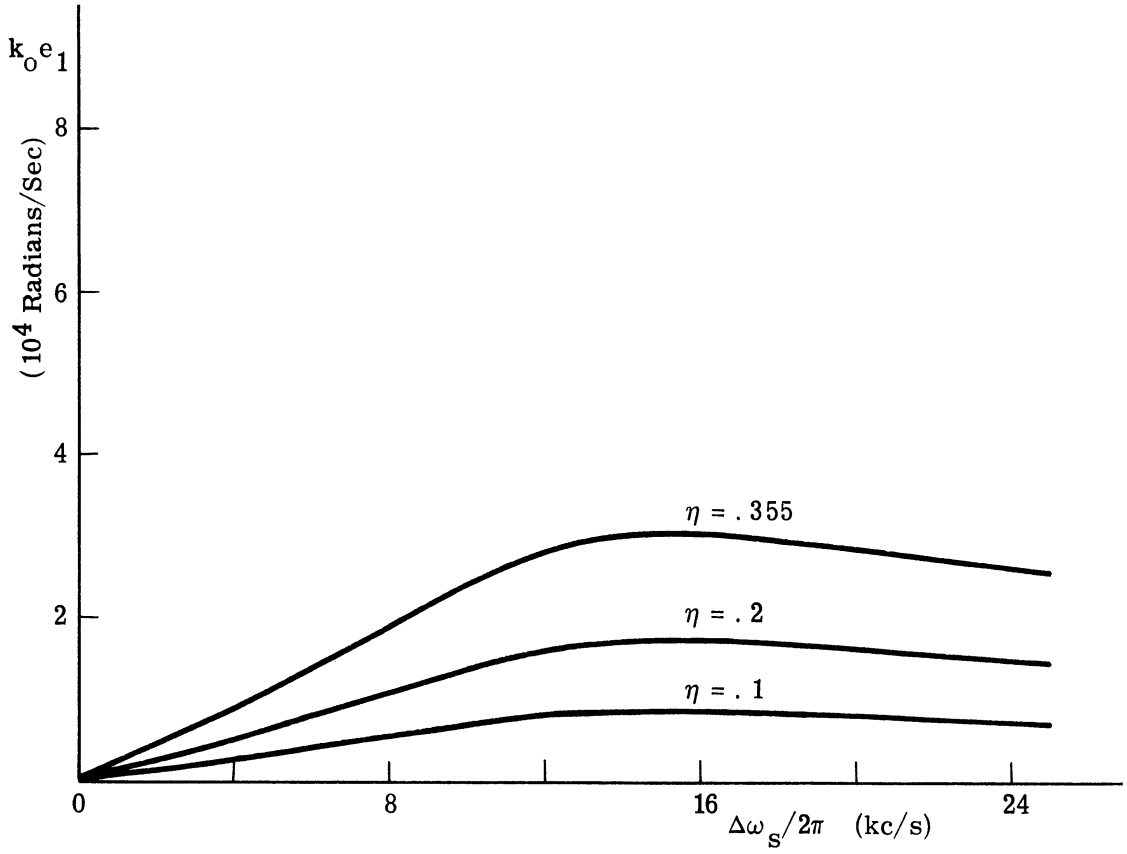

Fig. 4.14. System response for the single pole-single zero filter with G equal to 1.35×10^5 radians/second.

and third, while the phase curves differ considerably. In fact, in the present case, the phase shift is equal to $-\pi/2$ radians at a frequency of 12.9 kc. As a result, this system is potentially unstable. This means that the system gain must be limited in order for the forced oscillation analysis to apply.

The three values of gain selected for this example are the same as the values used in the first two examples. In this case, they correspond respectively to 3 db, 1 db, and 0 db less gain than is required for locked instability oscillations to exist. Figures 4.16-4.18, are again plots of $k_o e_1$ versus $\Delta\omega_s$, for $\Delta\omega_r$ equal to zero and for the values of η previously chosen. Again, only the first harmonic solution has been computed and graphed. These curves are much more peaked, and are considerably greater in amplitude, than in the earlier examples. The general appearance of the system response in this case is somewhat similar to that of the ideal-integrator case in the last section, particularly for the highest system gain.

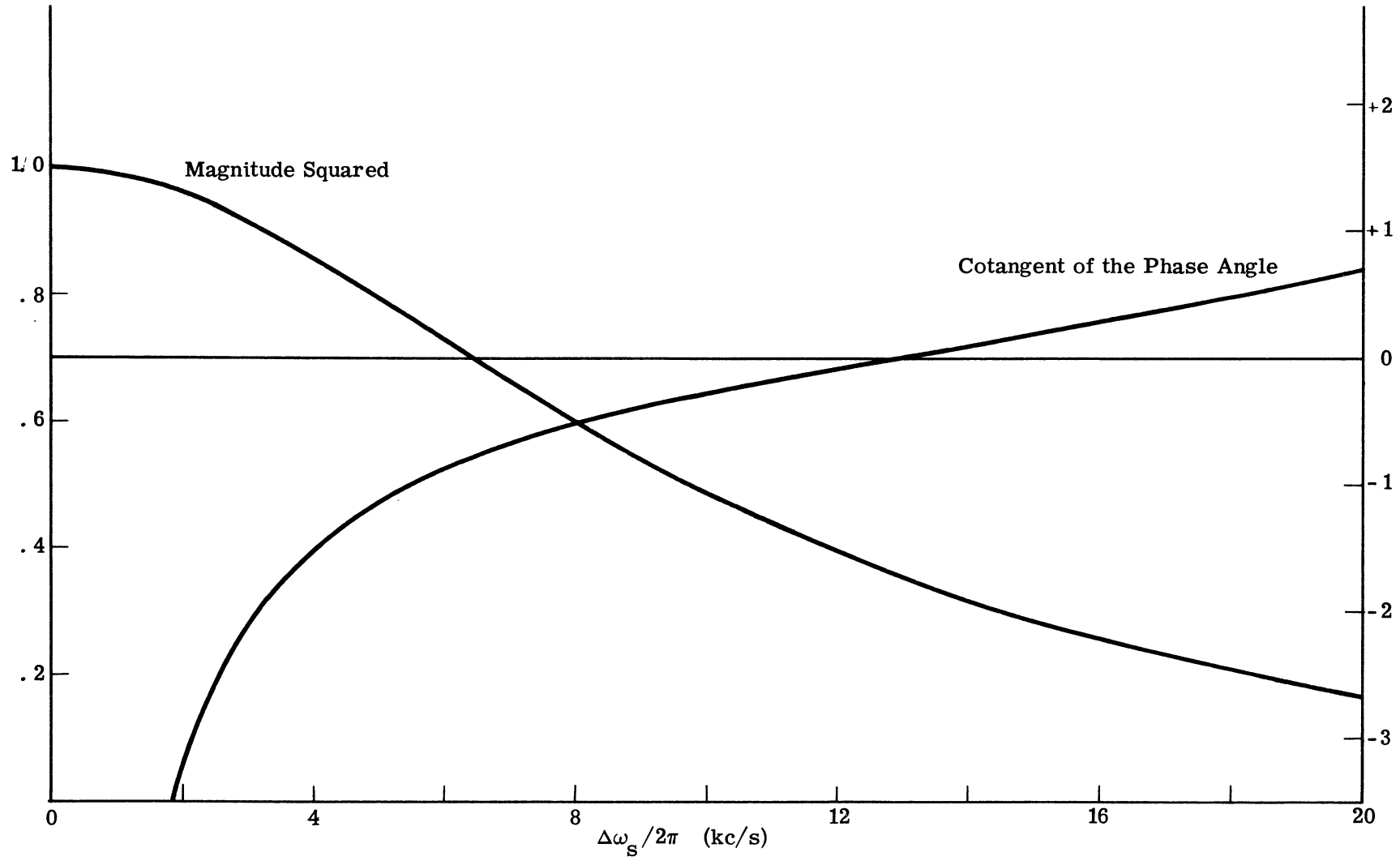

Fig. 4.15. Characteristics of the three pole filter.

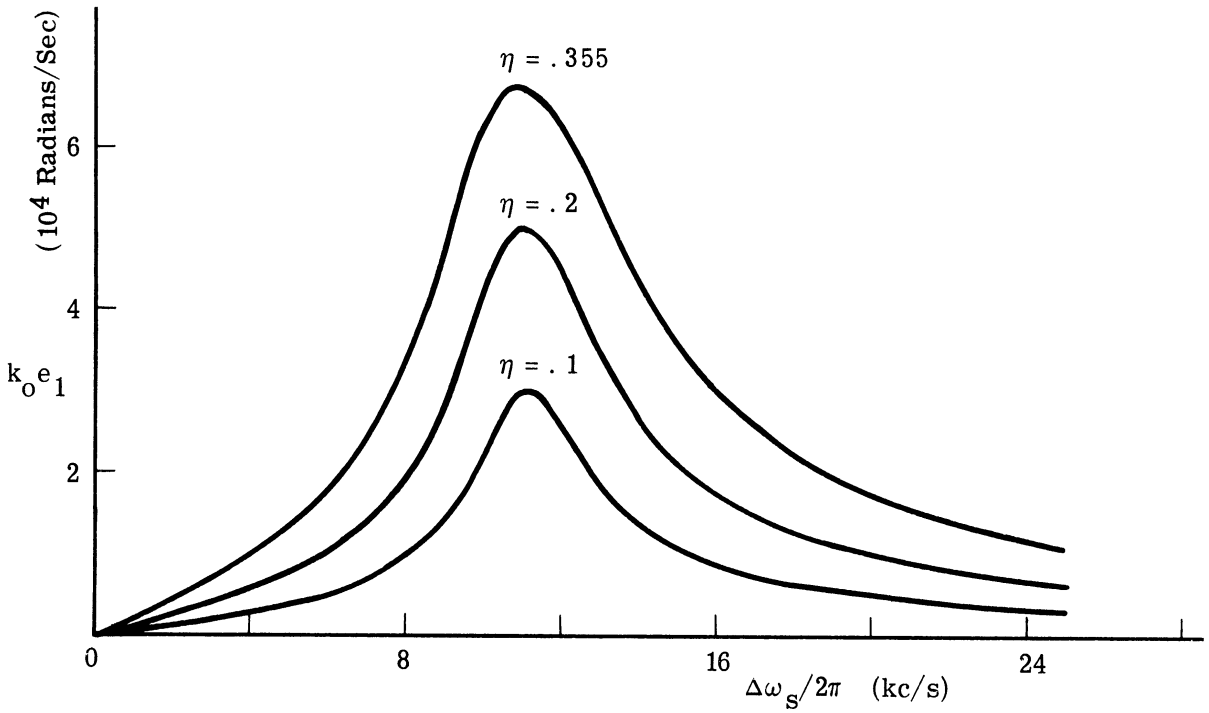

Fig. 4.16. System response for the three pole filter with G equal to 0.956×10^5 radians/second.

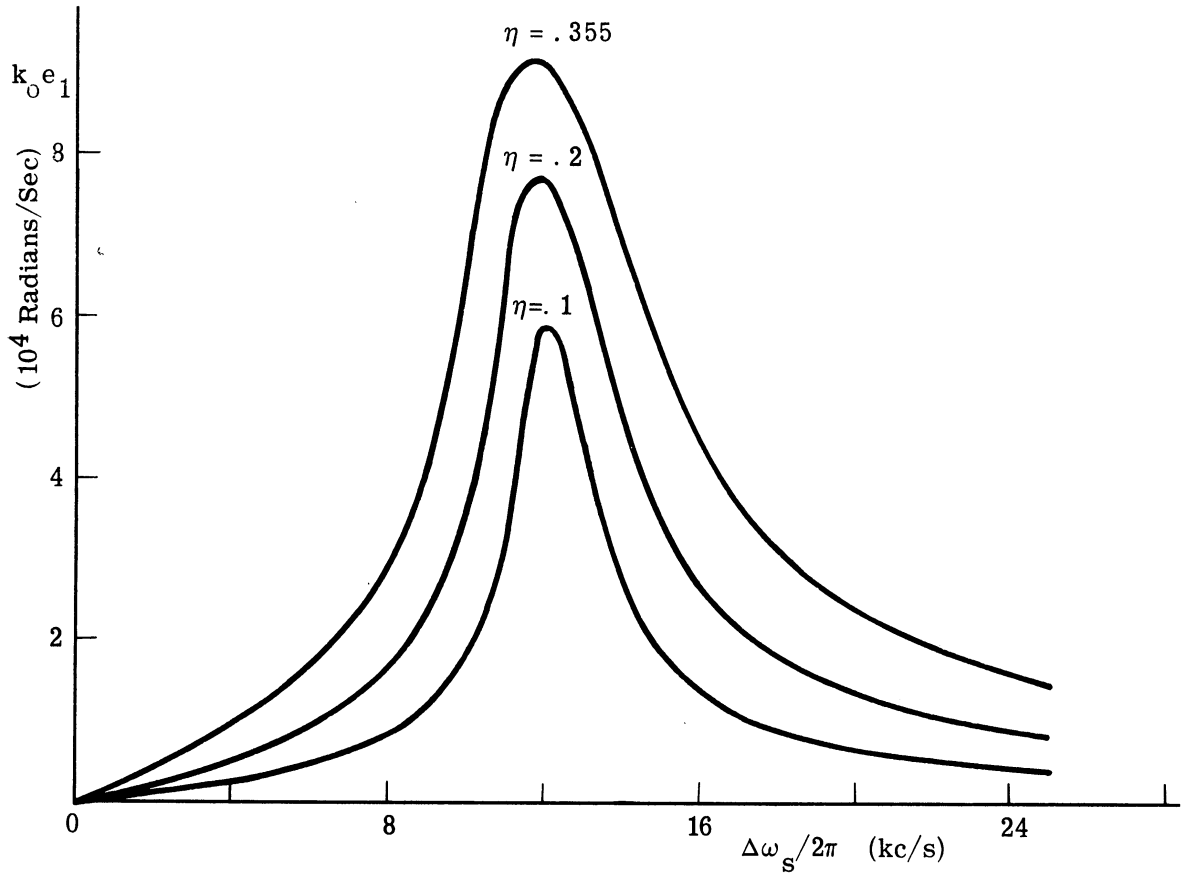

Fig. 4.17. System response for the three pole filter with G equal to 1.20×10^5 radians/second.

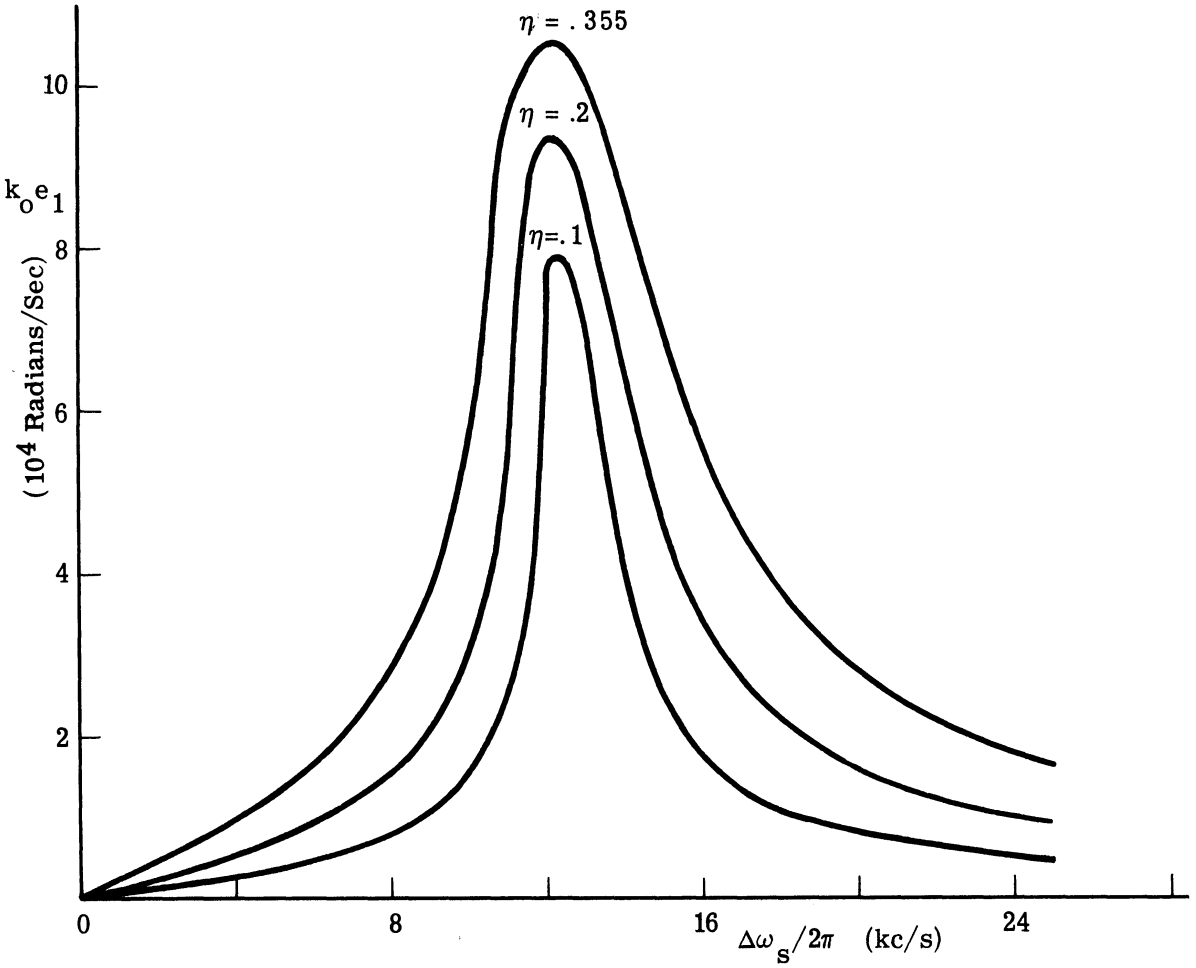

Fig. 4.18. System response for the three pole filter with G equal to 1.35×10^5 radians/second.

For this filter the variables $\Delta\theta_s$ and $\Delta\theta_r$ have also been plotted versus $\Delta\omega_s$, for $\Delta\omega_r$ equal to zero. Each of the two sets of curves shown in Figs. 4.19 and 4.20 is for the greatest value of system gain. Similar curves, of less amplitude, occur for lower values of system gain. Observe that $\Delta\theta_s$ has the general appearance of a step function, as was found for the ideal integrator. Also, $\Delta\theta_r$ is nearly equal to zero except in the immediate vicinity of 12.9 kc, the frequency at which the filter has a phase shift of $-\pi/2$ radians. Notice further that the required values ($\Delta\theta_s = \pi$ radians and $\Delta\theta_r = 0$ radian) of these two dependent variables at 12.9 kc has been found by the computer solution, which serves as a check on the computational method.

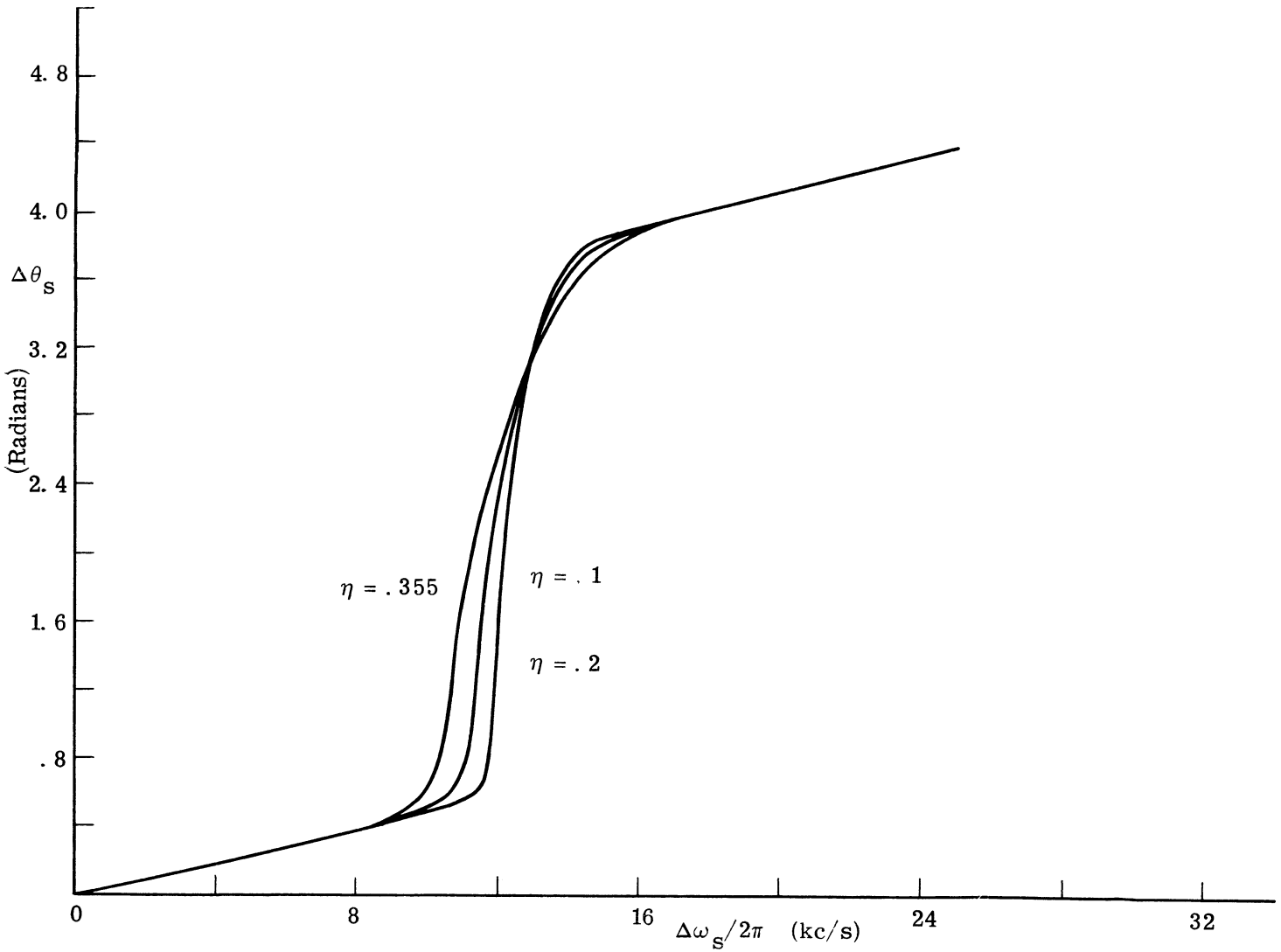

Fig. 4.19. $\Delta\theta_s$ characteristics for the three pole filter with G equal to 1.35×10^5 radians/second.

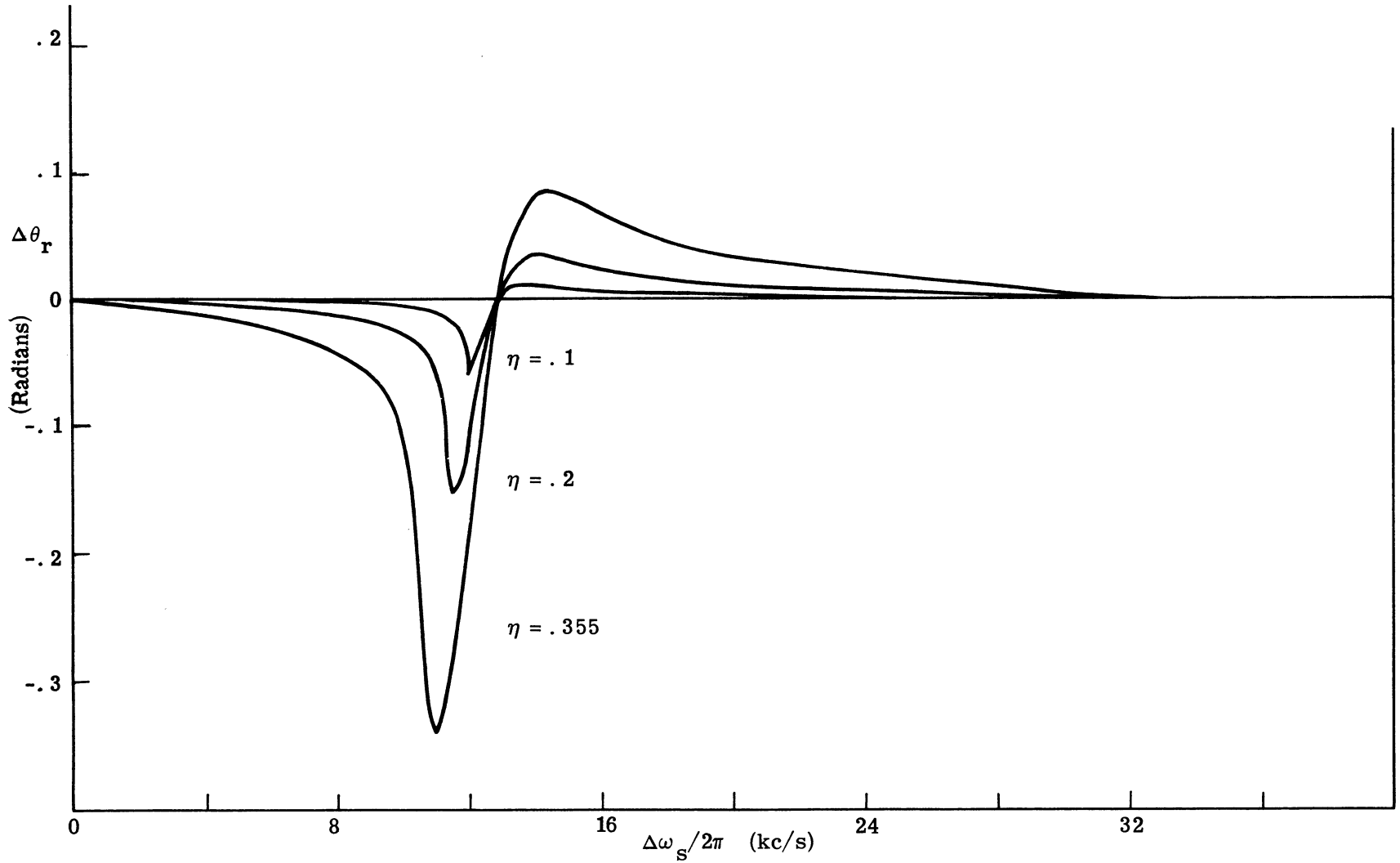

Fig. 4.20. $\Delta\theta_r$ characteristics for the three pole filter with G equal to 1.35×10^5 radians, second.

Figures 4.21-4.26 (each at a constant value of $\Delta\omega_s$) demonstrate the behavior of the three dependent variables as a function of $\Delta\omega_r$. All of these curves are for the intermediate value of system gain and for η equal to 0.2. In these curves β, rather than $k_o e_1$ (equal to $\Delta\omega_s \beta$), is shown. Since $\Delta\omega_s$ is a constant for each of these curves, $k_o e_1$ also can be found readily. Comparison of the $\Delta\theta_s$ curves should be performed cautiously since the scale for $\Delta\theta_s$ is not always identical between curves.

One observes from these curves that $\Delta\theta_r$ varies with $\Delta\omega_r$ in much the same way that it does when instability oscillations occur, i.e., with an almost inverse sine relationship. Nevertheless, $\Delta\theta_r$ deviates from this single input signal relationship whenever β is non-zero. Furthermore, $\Delta\theta_r$ generally is not equal to zero for $\Delta\omega_r$ equal to zero. This means that $\Delta\theta_r$ is not symmetric about the origin and, consequently, β and $\Delta\theta_s$ are not even functions. For relatively low values of η (such as $\eta = 0.2$), however, both β and $\Delta\theta_s$ are almost even and $\Delta\theta_r$ is almost odd about $\Delta\omega_r$ equal to zero and so little can be gained by also plotting these curves for negative values of $\Delta\omega_r$.

Finally, for this filter, Fig. 4.27 represents the system response plotted as a function of both positive $\Delta\omega_r$ and $\Delta\omega_s$ for η equal to 0.2 and G equal to 1.2×10^5 radians/sec, the intermediate gain value. From the previous discussion, it follows that this surface is essentially symmetric about the $k_o e_1$ - $\Delta\omega_s$ plane. It also can be shown that this surface is symmetric about the $k_o e_1$ - $\Delta\omega_r$ plane. For these reasons, it is sufficient to examine only the first quadrant. The maximum system response is seen to occur for $\Delta\omega_r$ equal to zero and for $\Delta\omega_s/2\pi$ equal to approximately 12 kc (see also Fig. 4.17). As $\Delta\omega_r$ increases, the peak decreases slightly, spreads out, and occurs at lower values of $\Delta\omega_s$.

The above description represents the general behavior of the harmonic solution for all filters. The peaking exhibited in Fig. 4.27 always exists but is of lesser magnitude for the inherently stable filters. To a great extent the over-all system response characteristics can be found from the $\Delta\omega_r$-equal-to-zero graphs shown extensively throughout this section.

In this section, the interrelations of the various system and input signal parameters to the system response have been presented with the aid of three examples, since any general direct interpretation of the coefficient equations appears impossible. One final interesting observation can be made from these three examples. For all filters and system

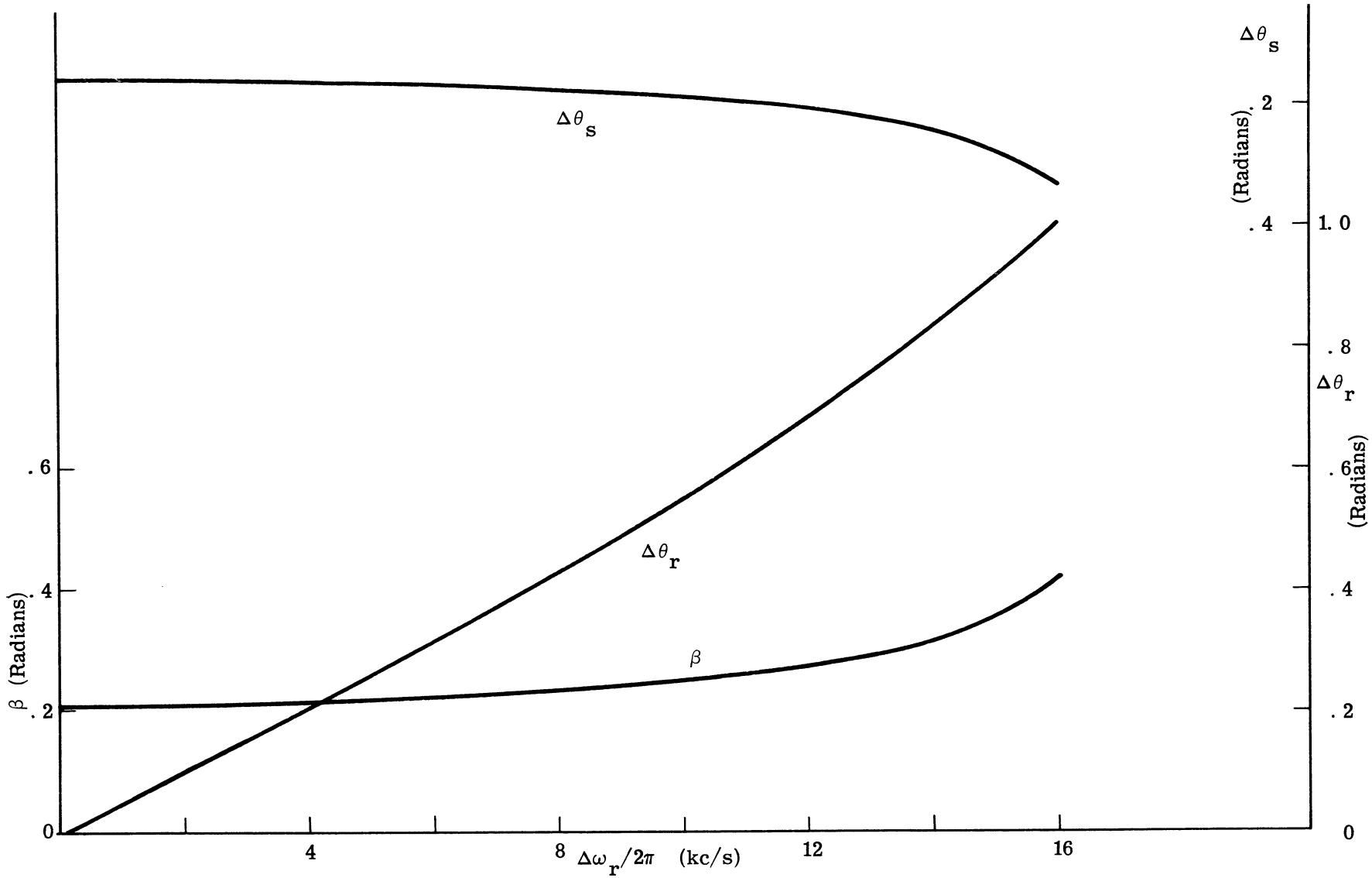

Fig. 4.21. System variables dependence on $\Delta\omega_r$ for $\Delta\omega_s/2\pi$ equal to 3 kc/sec.

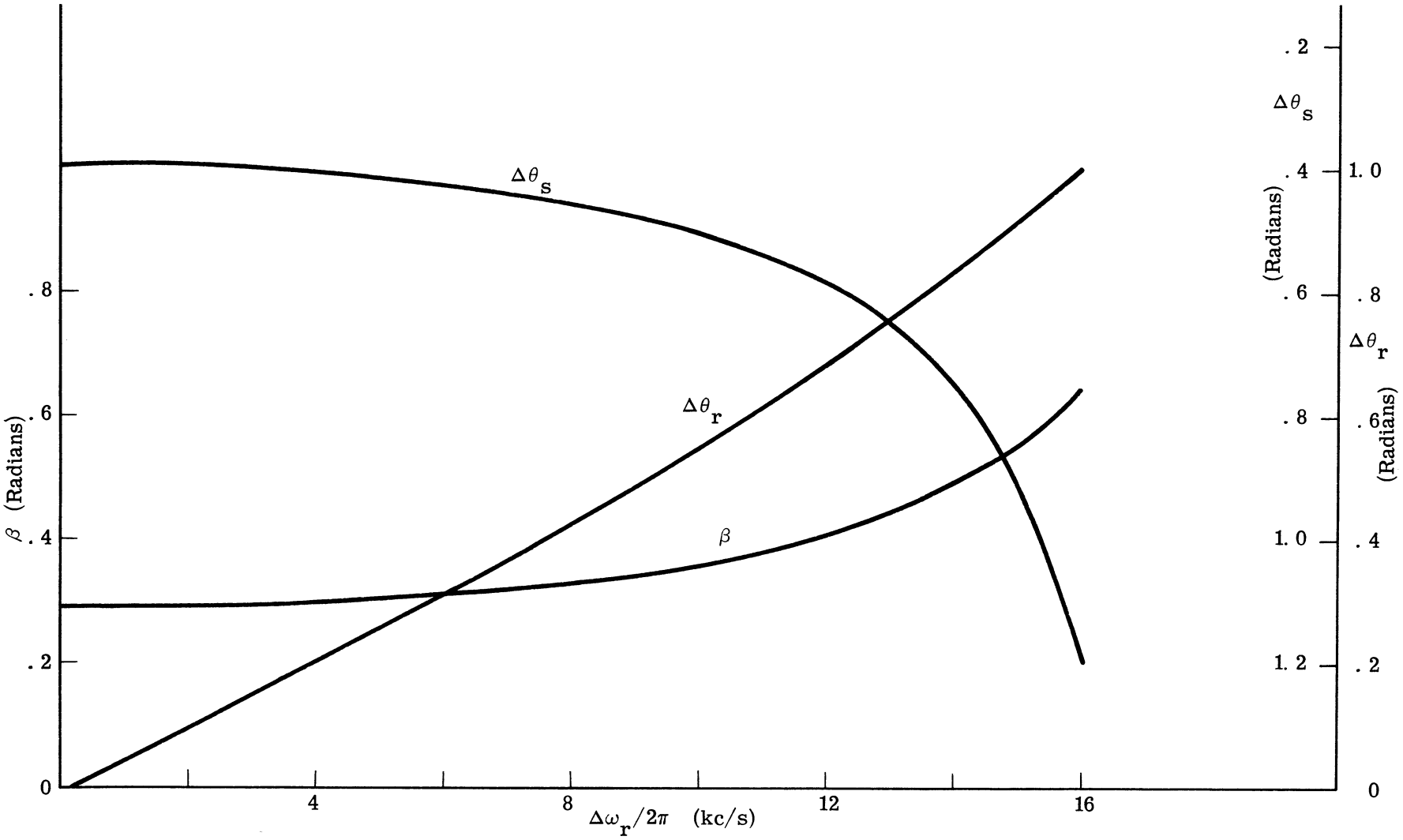

Fig. 4.22. System variables dependence on $\Delta\omega_r$ for $\Delta\omega_s/2\pi$ equal to 7 kc/sec.

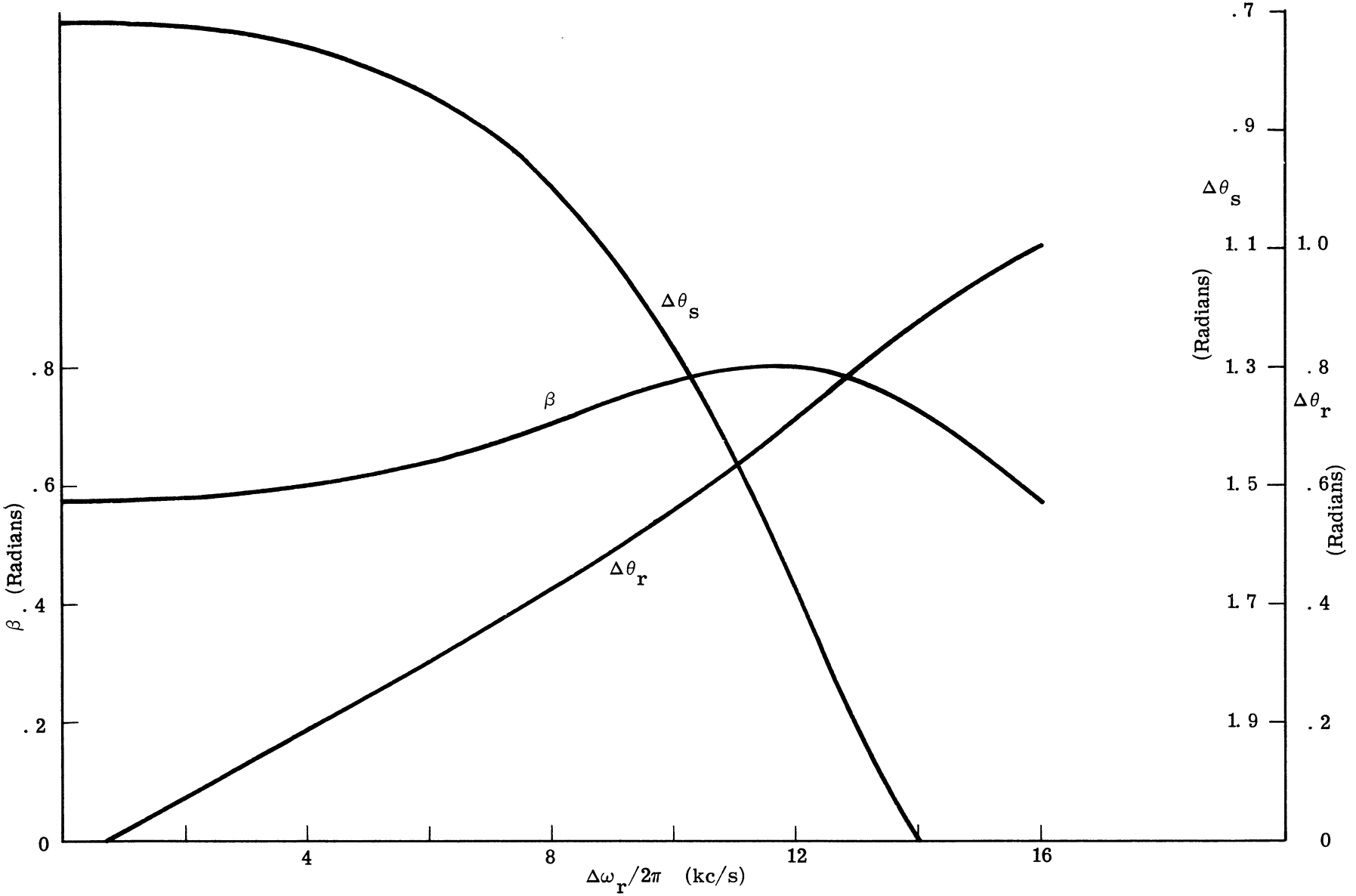

Fig. 4.23. System variables dependence on $\Delta\omega_r$ for $\Delta\omega_s/2\pi$ equal to 10 kc/sec.

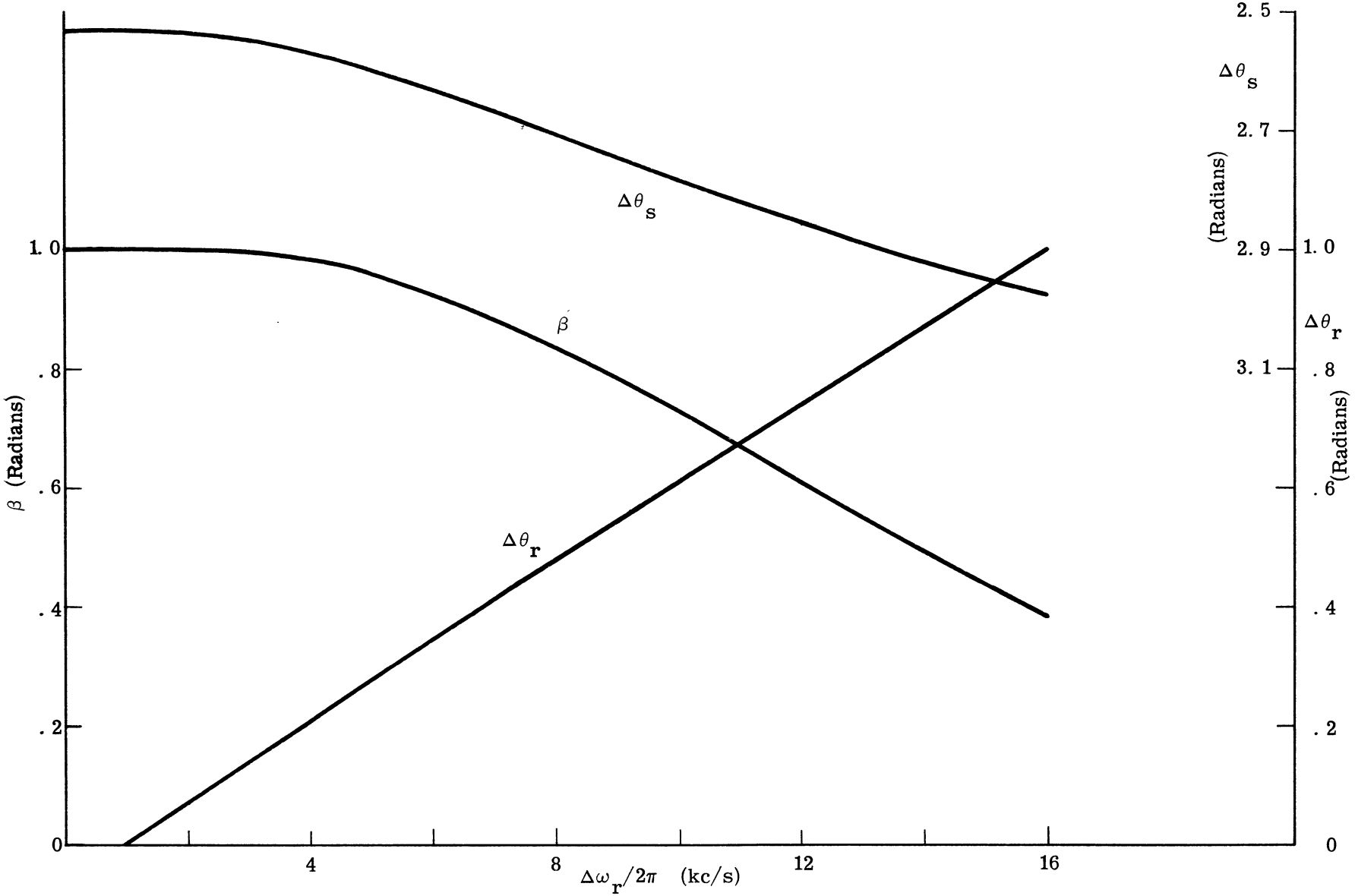

Fig. 4.24. System variables dependence on $\Delta\omega_r$ for $\Delta\omega_s/2\pi$ equal to 12 kc/sec.

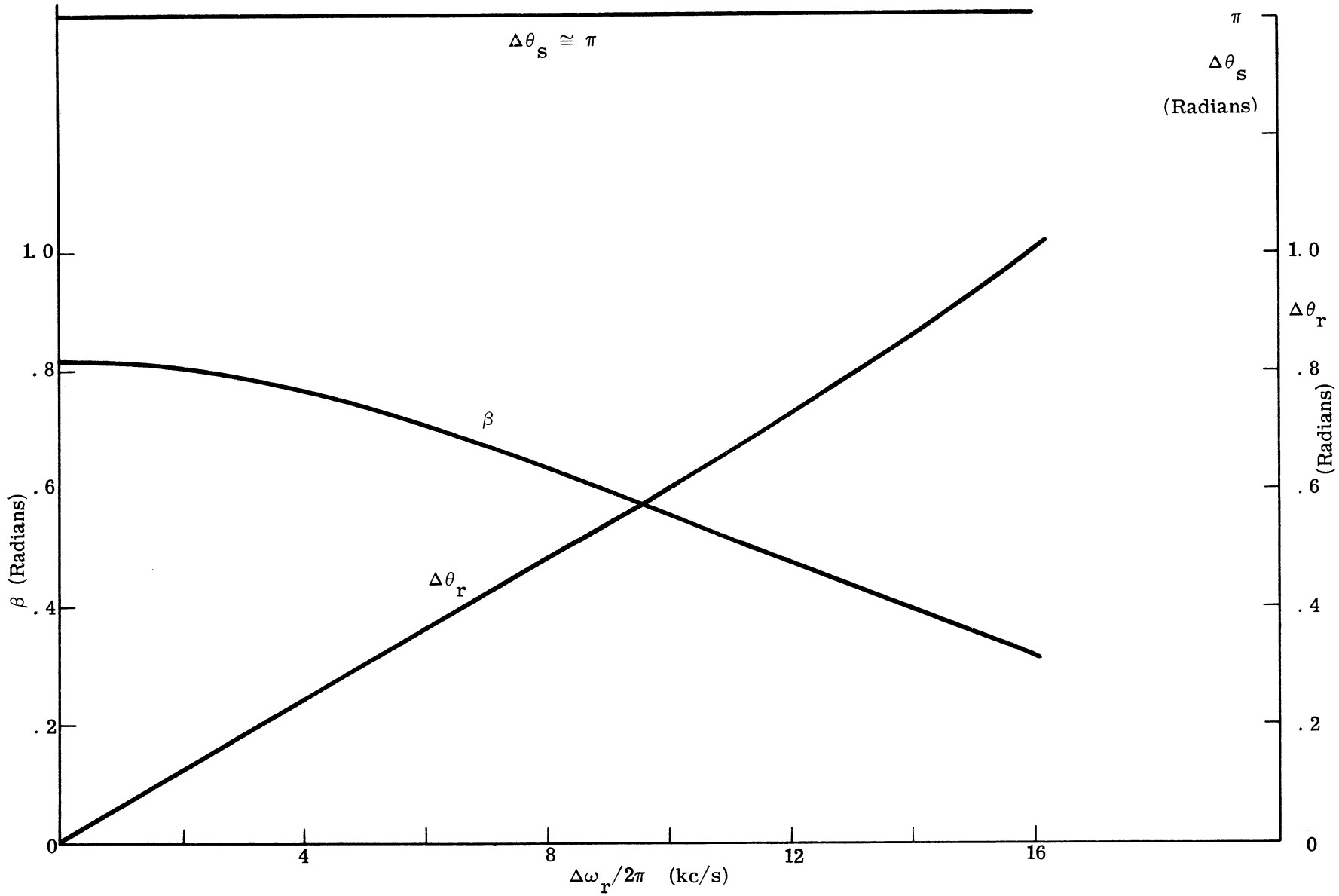

Fig. 4.25. System variables dependence on $\Delta\omega_r$ for $\Delta\omega_r/2\pi$ equal to 12.9 kc/sec.

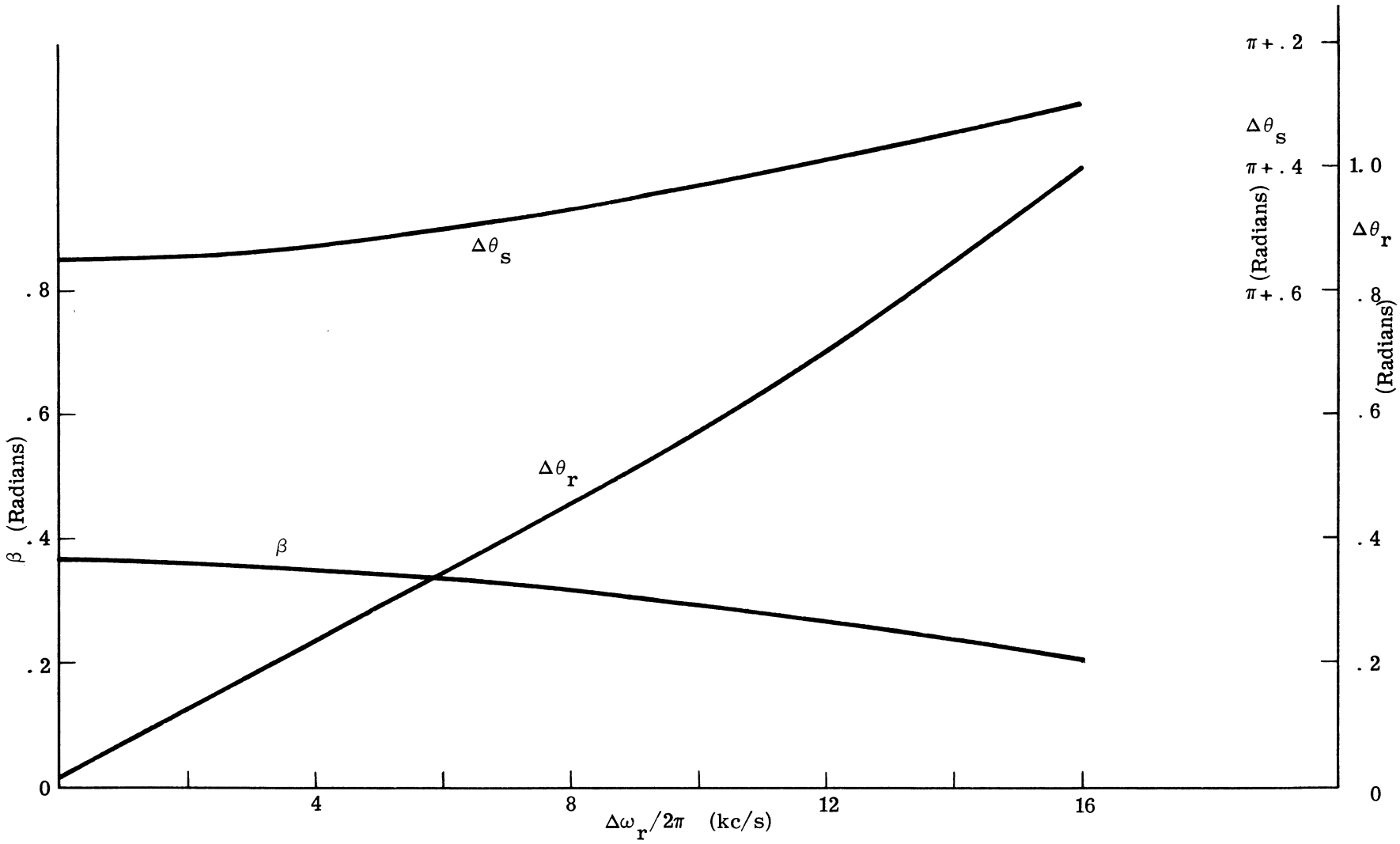

Fig. 4.26. System variables dependence on $\Delta\omega_r$ for $\Delta\omega_s/2\pi$ equal to 15 kc/sec.

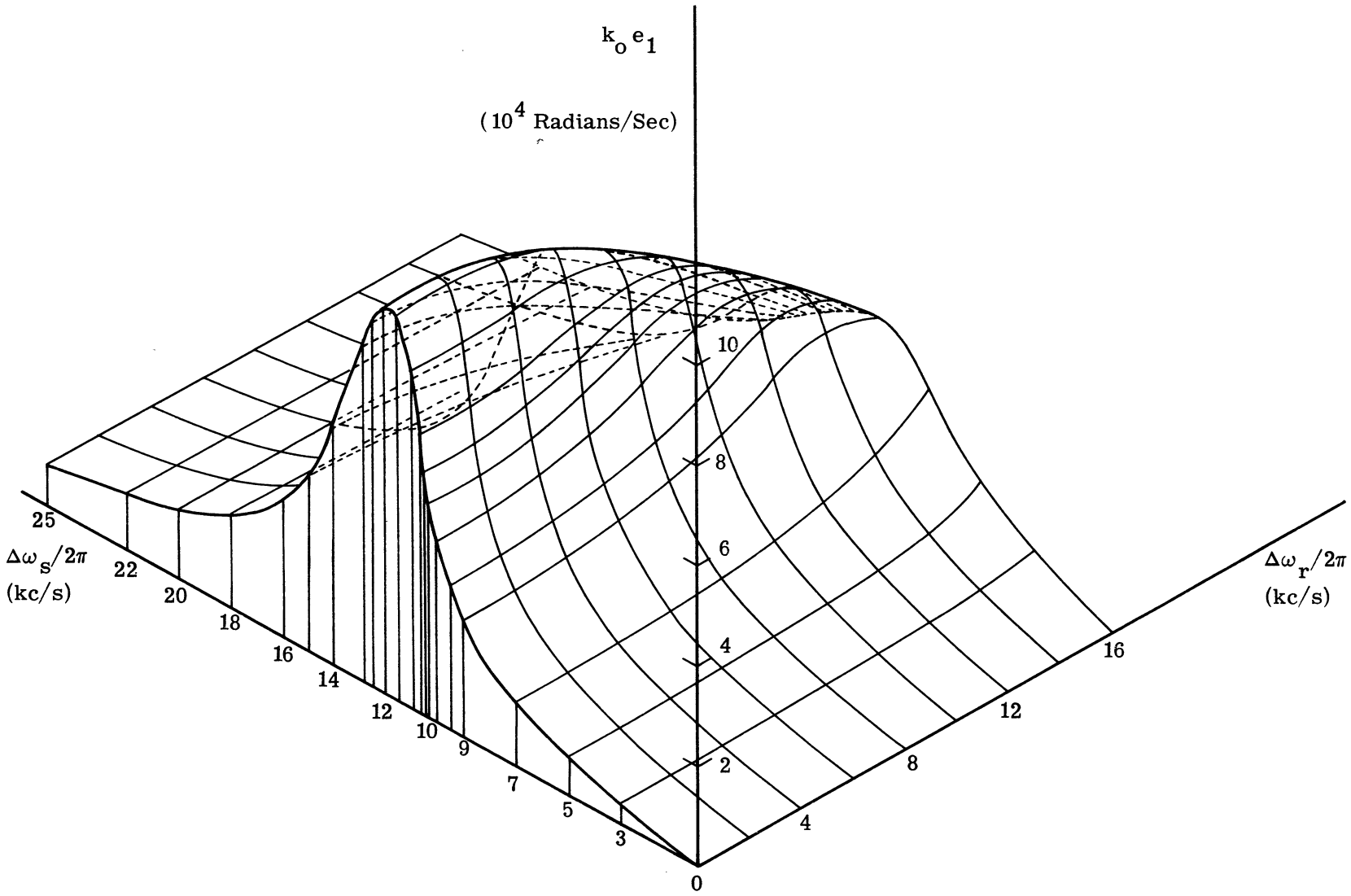

Fig. 4.27. System response as a function of $\Delta\omega_r$ and $\Delta\omega_s$.

gains evaluated, the system response amplitude is equal to $\eta\Delta\omega_s$ for small $\Delta\omega_s$, when $\Delta\omega_r$ is equal to zero. Granlund (Ref. 13) found an identical relation for the interference response in a conventional FM discriminator circuit.

4.5 Stability Analysis of the Forced Oscillations.

The validity of the analysis performed in Section 4.2 is primarily dependent on the existence of a stable, periodic, system response when the secondary interference signal is present. The stability theory for this forced case does not differ greatly from the locked oscillation case of Section 3.1.3. Once again, although the mathematical theory for answering the question of stability is available, the required calculations for each case are very lengthy. The general theory is presented briefly below. (For a more complete discussion see Section 3.1.3).

The orbital stability of the forced oscillations may be established by the first variation technique. The theory for this analysis (see Ref. 19) is described in terms of a system of n first-order differential equations. Let the column vector $\hat{\phi}(t)$ be a real solution of

$$\dot{\hat{x}} = \hat{F}(t,\hat{x}) \tag{4.26}$$

for $0 \leq t < \infty$, where the column vector $\hat{F}$ is analytic in $\hat{x}$ for each t. Then the first variation equation is

$$\dot{\hat{y}} = F_x[t,\hat{\phi}(t)]\,\hat{y} \quad , \tag{4.27}$$

where $F_x[t,\hat{\phi}(t)]$ is a matrix composed of the columns $\partial\hat{F}/\partial x_i (i=1,2,\ldots, n)$. In the event that $\hat{\phi}(t)$ is periodic of least period T, and $\hat{F}$ is periodic of period T in t, then Eq. 4.26 has a periodic coefficient matrix of period T. This is precisely the form assumed by the APC system equation when a secondary interference signal is present.

The following orbital stability theorem is proved in Ref. 19 for this case.

Theorem: If the characteristic exponents associated with the equation of first variation (Eq. 4.27) all have negative real parts, then the periodic solution $\phi(t)$ of Eq. 4.26 is asymptotically stable as t approaches infinity.

The application of the stability theory just outlined is identical to that carried out in Section 3.1.3 except that for an n-th order system it is necessary to find all n

characteristic exponents instead of n-1. Since each must be found separately, this increases the work for a system of given order.

4.6 Alternate Analytical Approach

In this section, the second, interference-susceptibility equation, Eq. 2.49, is examined further. This equation is equivalent to Eq. 2.46 (also Eq. 4.1), but it does differ substantially in form. The difference in form turns out to be a mixed blessing. The coefficient equations that result from this latter susceptibility equation are even more complex than those found in Section 4.2. On the other hand, an estimate of the system response can be made directly from this form for low values of $\Delta\omega_s$ and $\Delta\omega_r$.

When all but the first term of the sums in Eq. 2.49 are neglected, following the technique employed in the earlier work, it may be written as

$$\Delta\omega_r = -\beta\omega_f \cos(\omega_f t + \theta_1) + G\bar{H}(\omega)\sqrt{1 + \eta^2 + 2\eta\cos(\Delta\omega_s t)}\,\sin\left[\Delta\theta_r - \beta\sin(\omega_f t + \theta_1) + \tan^{-1}\frac{\eta\sin(\Delta\omega_s t)}{1 + \eta\cos(\Delta\omega_s t)}\right], \tag{4.28}$$

where β is defined by Eq. 3.23. The next step is to expand the two periodic functions of $\Delta\omega_s t$ into their respective Fourier series representations. It is then possible to obtain the desired coefficient equations.

The Fourier series expansion of the seemingly innocuous function, $\sqrt{1+\eta^2+2\eta\cos\Delta\omega_s t}$, is difficult. Since it is an even function, the expansion contains only cosine terms. The first three coefficients are derived in Appendix C. The results are

$$\sqrt{1 + \eta^2 + 2\eta\cos(\Delta\omega_s t)} = \frac{2}{\pi}(1 + \eta)\left\{E(k,\pi/2)\right.$$

$$+ \frac{2}{3}\left[F(k,\pi/2) + (k^2 - 2)\,D(k,\pi/2)\right]\cos(\Delta\omega_s t)$$

$$+ \frac{2}{15}\left[15k^2E(k,\pi/2) - 8(1 + k^2)\,F(k,\pi/2) + 16(1 - k^2 + k^4)\,D(k,\pi/2)\right]$$

$$\left.\cdot\cos(2\Delta\kappa_s t) + \ldots\right\}, \tag{4.29}$$

where

$$k = \frac{2\sqrt{\eta}}{1+\eta} \quad , \tag{4.30}$$

$$E(k,\pi/2) = \text{The complete elliptic integral of the second kind,} \tag{4.31}$$

$$F(k,\pi/2) = \text{The complete elliptic integral of the first kind,} \tag{4.32}$$

$$D(k,\pi/2) = [F(k,\pi/2) - E(k,\pi/2)]/k^2 \quad . \tag{4.33}$$

The higher order coefficients become progressively more complex expressions in terms of the first two kinds of elliptic integrals.

The second function in $\Delta\omega_s t$ has a relatively simple Fourier series representation. It is convenient to differentiate the function first.

$$\frac{d}{dt}\left[\tan^{-1}\frac{\eta \sin(\Delta\omega_s t)}{1+\eta\cos(\Delta\omega_s t)}\right] = \Delta\omega_s \frac{\eta\cos(\Delta\omega_s t)+\eta^2}{1+\eta^2+2\eta\cos(\Delta\omega_s t)} \tag{4.34}$$

The Fourier series expansion of this latter function also is given in Appendix C, with the result that for η^2 less than one,

$$\Delta\omega_s \frac{\eta\cos(\Delta\omega_s t)+\eta^2}{1+\eta^2+2\eta\cos(\Delta\omega_s t)} = -\Delta\omega_s \sum_{n=1}^{\infty}(-\eta)^n \cos(n\,\Delta\omega_s t) \quad . \tag{4.35}$$

Integration yields the desired series

$$\tan^{-1}\frac{\eta\sin(\Delta\omega_s t)}{1+\eta\cos(\Delta\omega_s t)} = -\sum_{n=1}^{\infty}\frac{(-\eta)^n}{n}\sin(n\,\Delta\omega_s t) \quad . \tag{4.36}$$

When the constant and fundamental terms of Eqs. 4.29 and 4.36 are substituted into Eq. 4.28, the harmonic solution becomes

$$\begin{aligned}\Delta\omega_r + \beta\,\Delta\omega_s \cos(\Delta\omega_s t + \theta_1) = \overline{GH}(\omega)\frac{2(1+\eta)}{\pi}\Bigg\{E \\ + \frac{2}{3}[F + (k^2-2)D]\cos(\Delta\omega_s t)\Bigg\}\sin[\Delta\theta_r \\ + (\eta - \beta\cos\theta_1)\sin(\Delta\omega_s t) - \beta\sin\theta_1\cos(\Delta\omega_s t)] \quad ,\end{aligned} \tag{4.37}$$

where

$$E = E(k,\pi/2), \quad F = F(k,\pi/2), \text{ and } D = D(k,\pi/2) \quad . \tag{4.38}$$

It is now possible to expand the sine function in terms of Bessel functions, and then equate coefficients as was done in Section 4.2. The result of this operation is an even more complex set of coefficient equations than the earlier ones, i.e., Eqs. 4.11, 4.16, and 4.17. Since these sets of equations should yield essentially the same result, this development will not be conducted further.

Some interesting relations can be found from Eq. 4.37. For low values of $\Delta\omega_s$ and $\Delta\omega_r$ the dependent variable θ_1 is essentially zero as can be determined from the analysis in the earlier section of this chapter. The product $G\overline{H}(\omega)$ is nearly equal to the real number G for low values of $\Delta\omega_s$ and for the commonly used lowpass filters. Finally, it may be shown that for small η

$$\frac{2(1+\eta)}{\pi}\left\{E + \frac{2}{3}[F + (k^2 - 2)D]\cos(\Delta\omega_s t)\right\} \equiv$$

$$1 + \eta + \frac{\eta}{1+\eta}\cos(\Delta\omega_s t) \quad . \tag{4.39}$$

Thus, for small $\Delta\omega_s$, $\Delta\omega_r$, and η, Eq. 4.37 takes the form

$$\Delta\omega_r + \beta\,\Delta\omega_s \cos(\Delta\omega_s t) = G\left[1 + \eta + \frac{\eta}{1+\eta}\cos(\Delta\omega_s t)\right]\sin[\Delta\theta_r$$

$$+ (\eta-\beta)\sin(\Delta\omega_s t)] \quad . \tag{4.40}$$

The Bessel function expansion of the sine term is

$$\sin[\Delta\theta_r + (\eta-\beta)\sin(\Delta\omega_s t)] = \sin(\Delta\theta_r)\cos[(\eta-\beta)\sin\Delta\omega_s t)]$$

$$+ \cos(\Delta\theta_r)\sin[(\eta-\beta)\sin(\Delta\omega_s t)]$$

$$= \sin(\Delta\theta_r)[J_o(\eta-\beta) + 2J_2(\eta-\beta)\cos(2\Delta\omega_s t) + \ldots]$$

$$+ \cos(\Delta\theta_r)[2J_1(\eta-\beta)\sin(\Delta\omega_s t) + \ldots] \quad . \tag{4.41}$$

Substitution of the first terms of this expansion into Eq. 4.40 yields

$$\Delta\omega_r + \beta\,\Delta\omega_s \cos(\Delta\omega_s t) = G\left[1+\eta+\frac{\eta}{1+\eta}\cos(\Delta\omega_s t)\right]$$

$$\cdot\left[\sin\Delta\theta_r J_o(\eta-\beta) + \cos\Delta\theta_r 2J_1(\eta-\beta)\sin(\Delta\omega_s t)\right] \quad . \tag{4.42}$$

From this last equation it follows, by equating the constant and periodic terms separately, that

$$\Delta\omega_r = G(1+\eta)\,J_o(\eta-\beta)\sin\Delta\theta_r \tag{4.43}$$

and

$$\beta\,\Delta\omega_s \cos(\Delta\omega_s t) = G(1+\eta)\cos\Delta\theta_r 2J_1(\eta-\beta)\sin(\Delta\omega_s t)$$

$$+\frac{G\eta}{1+\eta}\,J_o(\eta-\beta)\sin\Delta\theta_r\cos(\Delta\omega_s t) \quad . \tag{4.44}$$

The requirement for Eq. 4.44 to hold is that the first term on the right-hand side have a zero coefficient. This means that $J_1(\eta-\beta)$ must be zero which, in turn, implies that β is equal to η. Hence, from Eq. 4.43,

$$\sin\Delta\theta_r = \frac{\Delta\omega_r}{(1+\eta)\,G} \quad , \tag{4.45}$$

and from Eqs. 4.44 and 4.45,

$$\beta\,\Delta\omega_s = \frac{\eta\,\Delta\omega_r}{(1+\eta)^2} \cong \frac{\eta\,\Delta\omega_r}{1+2\eta} \quad . \tag{4.46}$$

Note that since Eq. 4.44 is not applicable when $\Delta\omega_s$ is equal to zero, Eq. 4.46 contains only the system response's dependence on $\Delta\omega_r$. Because β is essentially equal to η for low values of $\Delta\omega_r$ and $\Delta\omega_s$, one can write more generally

$$k_o e_1 = \beta\,\Delta\omega_s \cong \eta\,\Delta\omega_s + \frac{\eta\,\Delta\omega_r}{1+2\eta} \quad , \tag{4.47}$$

where the second term on the left-hand side has significance for only nonzero values of $\Delta\omega_s$.

These relations can be confirmed from the curves given in Section 4.4. Indeed, both Eq. 4.45 neglecting the η term and Eq. 4.47 with $\Delta\omega_r$ equal to zero previously were observed and remarked upon. The dependence of $k_o e_1$ on $\Delta\omega_r$ can be seen in Fig. 4.21, for example.

4.7 Case of System Insensitivity to Input Signal Amplitude

The third interference susceptibility equation (Eq. 2.50) developed in Section 2.3, pertains to APC systems designed to have a fixed system gain, i.e., systems which are insensitive to input signal amplitude. In this section, the coefficient equations appropriate to this case are developed. Once again, the complexity of these equations requires a computer solution.

Here, as before, only the first term of the sum expressions in Eq. 2.50 will be retained. Employing this simplification, the equation may be rewritten as

$$\Delta\omega_r' = -\beta\omega_f \cos(\omega_f t + \theta_1) + G'\overline{H}(\omega) \sin\left[\Delta\theta_r - \beta \sin(\omega_f t + \theta_1) + \tan^{-1}\frac{\eta \sin(\Delta\omega_s t)}{1+\eta\cos(\Delta\omega_s t)}\right]. \tag{4.48}$$

Substitution of the first term of the expansion given in Eq. 4.35 into Eq. 4.46 yields, for the harmonic solution,

$$\Delta\omega_r' + \beta\Delta\omega_s \cos(\Delta\omega_s t + \theta_1) = G'\overline{H}(\omega) \sin[\Delta\theta_r - \beta \sin(\Delta\omega_s t + \theta_1) + \eta \sin(\Delta\omega_s t)] \quad . \tag{4.49}$$

The Bessel function expansion of the sine factor is given by

$$\begin{aligned}
&\sin[\Delta\theta_r - \beta \sin(\Delta\omega_s t + \theta_1) + \eta \sin(\Delta\omega_s t)] \\
&= \sin(\Delta\theta_r) \cos[(\eta - \beta\cos\theta_1)\sin(\Delta\omega_s t) - \beta \sin\theta_1 \cos(\Delta\omega_s t)] \\
&+ \cos(\Delta\theta_r) \sin[(\eta - \beta\cos\theta_1)\sin(\Delta\omega_s t) - \beta \sin\theta_1 \cos(\Delta\omega_s t)] \\
&= \sin(\Delta\theta_r)\Big\{\cos[(\eta - \beta\cos\theta_1)\sin(\Delta\omega_s t)]\cos[\beta \sin\theta_1 \cos(\Delta\omega_s t)] \\
&\qquad + \sin[(\eta - \beta\cos\theta_1)\sin(\Delta\omega_s t)]\sin[\beta \sin\theta_1 \cos(\Delta\omega_s t)]\Big\}
\end{aligned}$$

$$+ \cos(\Delta\theta_r)\Big\{\sin[(\eta - \beta\cos\theta_1)\sin(\Delta\omega_s t)]\cos[\beta\sin\theta_1\cos(\Delta\omega_s t)]$$

$$- \cos[\eta - \beta\cos\theta_1)\sin(\Delta\omega_s t)]\sin[\beta\sin\theta_1\cos(\Delta\omega_s t)]\Big\}$$

$$= \sin(\Delta\theta_r)\Big\{[J_o(\alpha_1)+2J_2(\alpha_1)\cos(2\Delta\omega_s t)+\ldots][J_o(\alpha_2)-2J_2(\alpha_2)\cos(2\Delta\omega_s t)+\ldots]$$

$$+ [2J_1(\alpha_1)\sin(\Delta\omega_s t)+\ldots][2J_1(\alpha_2)\cos(\Delta\omega_s t)-\ldots]\Big\}$$

$$+ \cos(\Delta\theta_r)\Big\{[2J_1(\alpha_1)\sin(\Delta\omega_s t)+\ldots][J_o(\alpha_2)-2J_2(\alpha_2)\cos(2\Delta\omega_s t)+\ldots]$$

$$- [J_o(\alpha_1)+2J_2(\alpha_1)\cos(2\Delta\omega_s t)+\ldots][2J_1(\alpha_2)\cos(\Delta\omega_s t)-\ldots]\Big\}\,, \tag{4.50}$$

where

$$\alpha_1 = \eta - \beta\cos\theta_1\,, \tag{4.51}$$

$$\alpha_2 = \beta\sin\theta_1\,. \tag{4.52}$$

When only the principal constant and first harmonic terms of this expansion are retained, the sine factor becomes for small α_1 and α_2,

$$\sin[\Delta\theta_r - \beta\sin(\Delta\omega_s t + \theta_1) + \eta\sin(\Delta\omega_s t)] \equiv$$

$$\sin(\Delta\theta_r)\,J_o(\alpha_1)\,J_o(\alpha_2) + 2\cos(\Delta\theta_r)[J_o(\alpha_2)\,J_1(\alpha_1)\sin(\Delta\omega_s t) -$$

$$J_o(\alpha_1)\,J_1(\alpha_2)\cos(\Delta\omega_s t)]\,. \tag{4.53}$$

When this is used in Eq. 4.49, the result is

$$\Delta\omega_r' + (\eta - \alpha_1)\,\Delta\omega_s\cos(\Delta\omega_s t) - \alpha_2\,\Delta\omega_s\sin(\Delta\omega_s t)$$

$$= G'\overline{\Pi}(\omega)\Big\{\sin(\Delta\theta_r)\,J_o(\alpha_1)\,J_o(\alpha_2) + 2\cos(\Delta\theta_r)$$

$$\cdot\,[J_o(\alpha_2)\,J_1(\alpha_1)\sin(\Delta\omega_s t) - J_o(\alpha_1)\,J_1(\alpha_2)\cos(\Delta\omega_s t)]\Big\}\,. \tag{4.54}$$

The three coefficient equations follow from this result and Eq. 4.14; they are

$$\Delta\omega_r' = G' \sin(\Delta\theta_r)\, J_o(\alpha_1)\, J_o(\alpha_2) \quad , \tag{4.55}$$

$$\tan\Omega(\Delta\omega_s) = \frac{\dfrac{\alpha_2}{\eta-\alpha_1} - \dfrac{J_o(\alpha_2)J_1(\alpha_1)}{J_o(\alpha_1)J_1(\alpha_2)}}{1 + \dfrac{\alpha_2 J_o(\alpha_2)J_1(\alpha_1)}{(\eta-\alpha_1)J_o(\alpha_1)J_1(\alpha_2)}} \quad , \tag{4.56}$$

$$\Delta\omega_s^2[(\eta-\alpha_1)^2 + \alpha_2^2] = 4G'^2|\overline{H}(\Delta\omega_s)|^2 \cos^2(\Delta\theta_r)$$

$$\cdot\, [J_o^2(\alpha_1)J_1^2(\alpha_2) + J_o^2(\alpha_2)J_1^2(\alpha_1)] \quad . \tag{4.57}$$

These three coefficient equations can be solved using the same technique that was employed in Section 4.4 for the original set of equations. Although this has not been done, some insight into the nature of the solution can be found by examining the ideal-integrator case. On the basis of earlier work, it is thought that this particular example will give an exaggerated indication of the general character of the system response amplitude as a function of $\Delta\omega_s$.

When H(s) equals $1/\tau s$, then Eq. 4.54 reduces to (recall that $\Delta\omega_r'$ must be zero and so $\Delta\theta_r$ is equal to zero)

$$(\eta-\alpha_1)\cos(\Delta\omega_s t) - \alpha_2 \sin(\Delta\omega_s t) = \frac{2G_\infty'}{(\Delta\omega_s)^2\tau}[-J_o(\alpha_2)J_1(\alpha_1)$$

$$\cdot \cos(\Delta\omega_s t) - J_o(\alpha_1)J_1(\alpha_2)\sin(\Delta\omega_s t)] \quad . \tag{4.58}$$

Equating coefficients yields

$$(\eta-\alpha_1) = \frac{2G_\infty'}{(\Delta\omega_s)^2\tau} J_o(\alpha_2)J_1(\alpha_1) \quad , \tag{4.59}$$

$$\alpha_2 = \frac{2G_\infty}{(\Delta\omega_s)^2\tau} J_o(\alpha_1)J_1(\alpha_2) \quad . \tag{4.60}$$

A solution to this pair of equations is given by α_2 equal to zero and the single equation

$$\eta-\alpha_1 = -\frac{2G'_\infty}{(\Delta\omega_s)^2\tau} J_1(\alpha_1) \quad . \tag{4.61}$$

Since α_2 equals $\beta \sin \theta_1$, and β is assumed to be positive, this requires that θ_1 be equal to either zero or π radians. In those cases, α_1 must equal $\eta-\beta$ or $\eta+\beta$, respectively. Substitution of these values into Eq. 4.61 yields, respectively,

$$\frac{G'_\infty}{(\Delta\omega_s)^2\tau} = \frac{\beta}{2J_1(\beta\mp\eta)} \quad . \tag{4.62}$$

This equation is similar to Eq. 4.18 (for the harmonic solution Eq. 4.18 has n equal to one and $\Delta\omega_f$ equal to $\Delta\omega_s$) developed from the earlier analysis. Equation 4.62 is plotted in Fig. 4.28 for the lower two values of η. When this figure is compared with Fig. 4.1 (a plot of Eq. 4.18), the similarity is more prominent. A close inspection of Figs. 4.1 and 4.28 reveals jump discontinuities (see Fig. 4.6) which occur, respectively, at essentially the same abscissa values. (These discontinuities result from the existence of minimum abscissa values, for the right-hand branches of the curves.) The peak ordinate value (maximum β value), however, is slightly less in the case of system insensitivity to input signal amplitude.

Based on the above brief investigation, it appears that the use of a balanced phase detector or other mechanisms for eliminating dependence of the APC system gain on the input signal level does not materially affect the system response to a secondary signal. Recall that the above theory depends on the value of η existing at the input of the APC system's multiplier. The effect of a limiter, or other nonuniform signal processor preceding the APC system, must be considered separately.

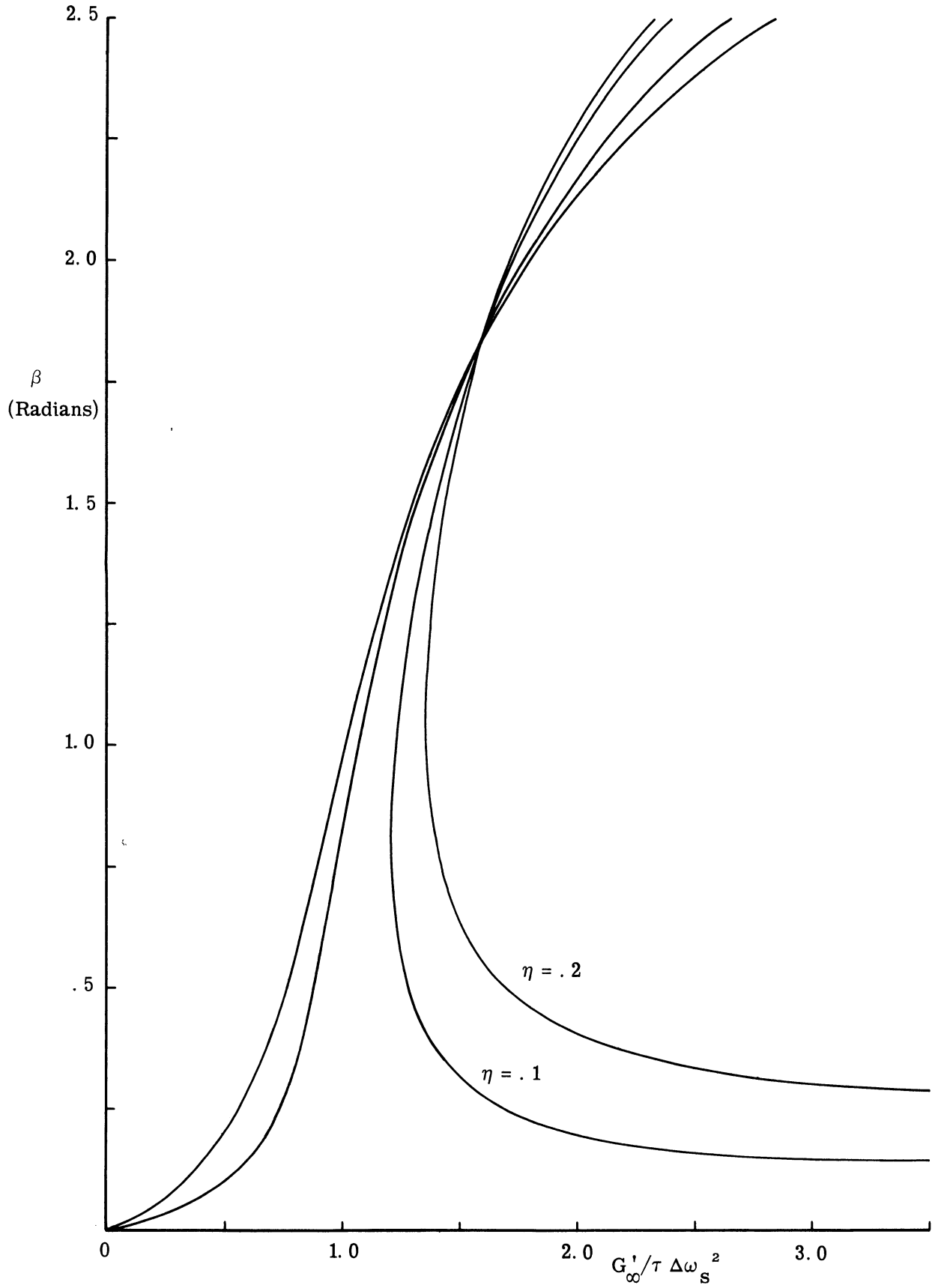

Fig. 4.28. The harmonic relation between β and $G'_\infty/\tau\Delta\omega_s^2$.

5. SUPPLEMENTARY EXPERIMENTAL PROGRAM

5.1 Summary of the Experimental Program

In Section 4, a general theoretical analysis of the APC system's response to a secondary interference signal was developed and interpreted. The purpose of this section is to examine a particular APC system and compare experimental findings with the theoretical predictions. Since the experimental work is not limited to a system response consisting of a single sinusoidal waveform, the data can be extended to include values of η near unity and system gains approaching the locked oscillation level. The latter information provides additional insight to the effect of secondary-signal interference.

An input-amplitude-sensitive APC system was constructed for the experimental program. The details of the system are described in Section 5.2. The experimental tests performed on the system are summarized with the aid of the block diagram shown in Fig. 5.1. This experimental configuration was used for checking both the locked instability oscillation analysis of Section 3 and the secondary signal interference analysis. In the former case, the signal generator supplying the secondary signal was turned off.

The following procedure was used for the experimental study of locked instability oscillation. The combination of reference signal generator level and attenuator setting was adjusted to yield a locked periodic oscillation (as opposed to the oscillations which occur just outside the locking range). This input signal amplitude was maintained as the reference signal frequency was varied across the entire passband of the APC system. The amplitude (both dc and ac) and frequency of the APC response were recorded for each reference frequency test point. Data were obtained for three levels of system gain. The results of these measurements have been presented in Section 3.2.

In measurements of the influence of a secondary signal, the following procedure was employed. A minimum attenuation of 20 db was maintained between the output of each signal generator and the APC system in order to insure adequate isolation of the two sources. At the beginning of each experimental run, the maximum attenuation available (a total of 80 db) was inserted at the output of the secondary signal generator. With the minimum attenuation of 20 db at the output of the reference signal generator, the output level and frequency of this generator were adjusted so the system verged on locked instability oscillations

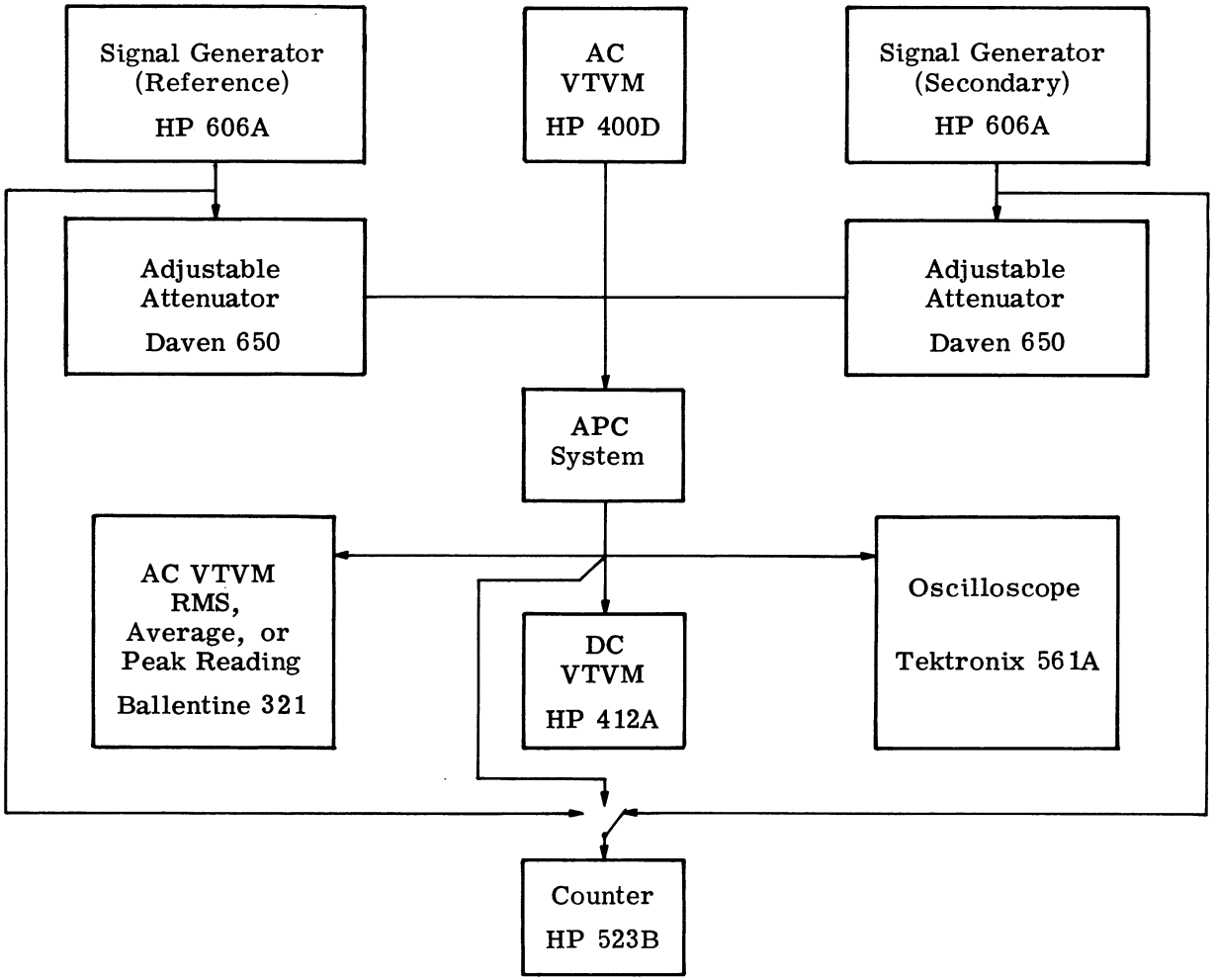

Fig. 5.1. Experimental test configuration.

with $\Delta\omega_r$ equal to zero; i.e., with the reference signal frequency equal to the open-loop system-oscillator frequency. An identical calibration procedure was then followed for the secondary signal generator.

The next step was to set up the particular values of G, $\Delta\omega_r$, and η required for the current run. The system gain, G, was adjusted by inserting the appropriate value of attenuation in the output of the reference signal generator; e.g., 21 db would represent a gain 1 db less than the gain required for oscillation. $\Delta\omega_r$ was set by tuning the reference signal generator frequency to the desired value with the aid of a counter. The value of η, the ratio between the secondary and reference signal levels, was set by inserting the required attenuation at the output of the secondary signal generator.

After these preliminary steps, the secondary signal generator frequency was varied across the passband of the APC system. The difference in the frequencies of the two signal generators, i.e., $\Delta\omega_s$, was recorded for each test point. The system response frequency, ac rms voltage level, and dc voltage level were recorded for these values of $\Delta\omega_s$. This entire procedure was carried out for several combinations of G, $\Delta\omega_r$, and η. Some experimental results are given in Section 5.3.

5.2 Experimental APC System

Before discussing the experimental data for the secondary interference signal case, it is convenient to consider briefly the circuit details of the APC system. This will further an understanding of the specific cause of system instability when an excessive input signal is present and of the particular response of the system to the secondary signal. Furthermore, the system's over-all lowpass filter transfer function is determined approximately for use in a theoretical comparison.

A study of the circuit diagram for the APC system, shown in Fig. 5.2, reveals that the required multiplication function is performed by a balanced phase detector. The resultant error signal is amplified by a differential amplifier and then filtered by a single-section RC filter. This lowpass filter is isolated with emitter-follower circuits. The filtered signal is then applied to the system oscillator, an astable multivibrator, in such a way as to control its frequency. The system oscillator output is approximately a square wave and is applied to one of the two inputs of the phase detector. The input signal is applied to the other detector input as indicated. In addition, an ac-coupled amplifier is provided for the system response signal. For experimental flexibility, a switch is included which can effectively remove the RC lowpass filter. (A photograph of this circuit is shown in Fig. 5.3.)

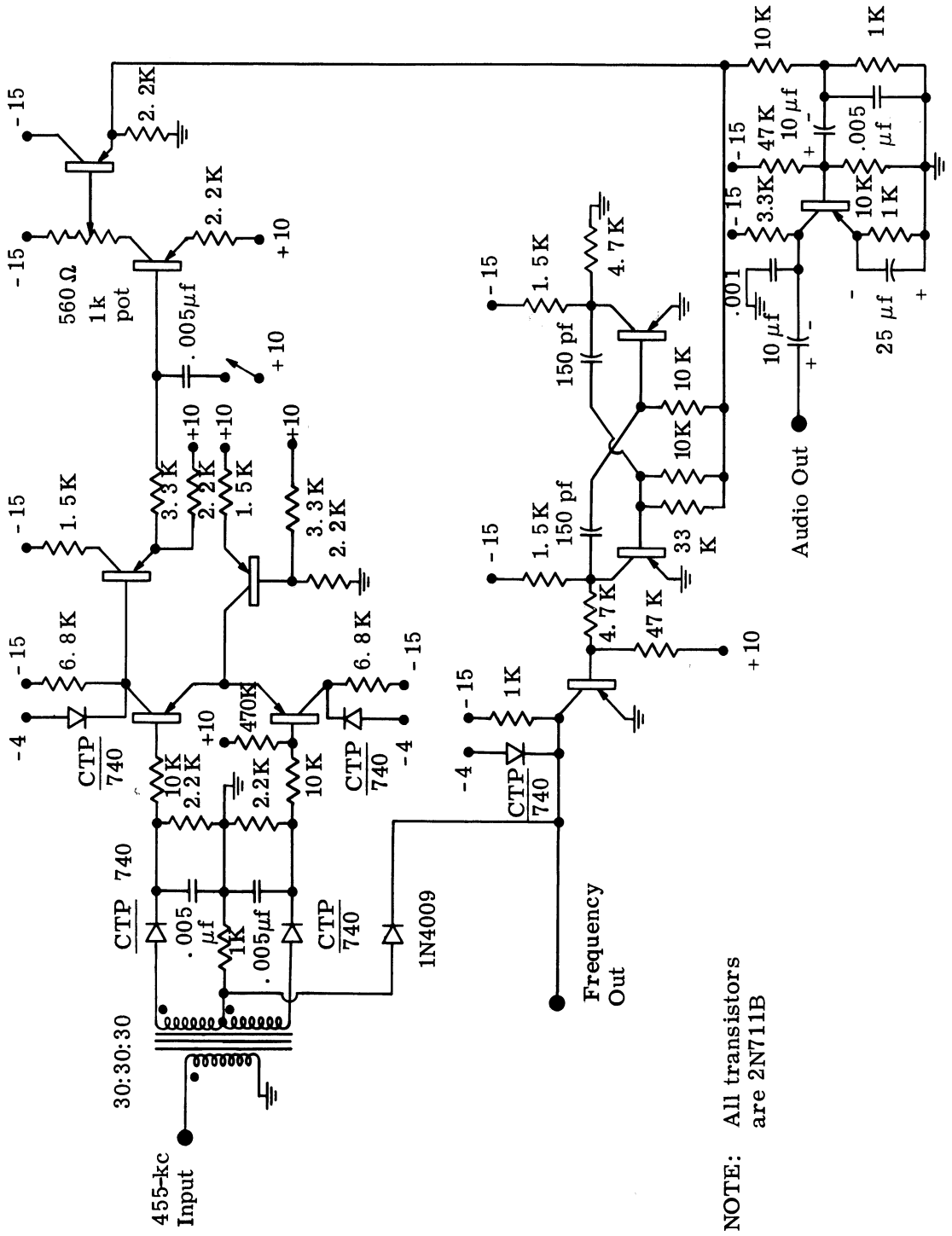

Fig. 5.2. APC system circuit diagram.

One of the important experimental parameters is k_o, the gain constant of the system oscillator measured in cycles (or radians) per second per volt. This parameter can be measured easily by applying a dc voltage to the oscillator input and noting the resultant frequency. The data points shown in Fig. 5.4 represent a series of these measurements, and the curve drawn through these points is a straight line approximation. The excellent frequency linearity of this astable multivibrator with voltage can be predicted by theory over an appropriate range of voltage. From this curve, the slope, k_o, is determined as 42.8 kc per volt.

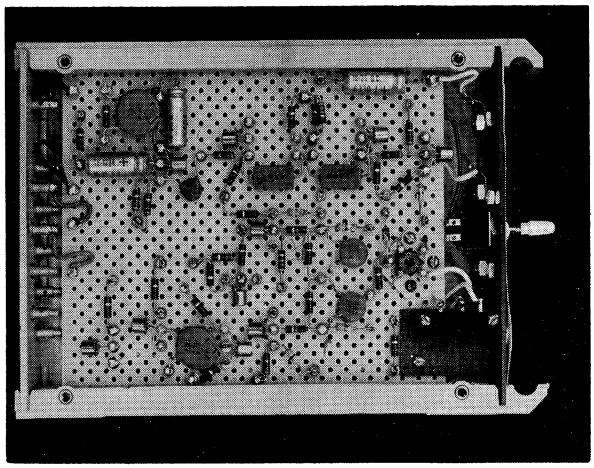

Fig. 5.3. The experimental APC system.

Another important circuit property is the over-all lowpass filter transfer function. If the stray capacitance of wiring and components is ignored, then the transfer function consists of a pair of isolated real poles. One of these is due to the RC filter of the system; the other is a consequence of the envelope detection circuit of the phase detector. More precisely, this latter pole is caused by the series diode resistance and effective secondary resistance of the transformer in the circuits coupling to the inputs of the differential amplifier. The presence of this second pole in the transfer function causes this system to be potentially unstable. Since the diode resistance depends on the input voltage level, so does the location of the pole. For this reason, it is difficult to assign directly by circuit analysis, or to determine experimentally, the appropriate time constant for this

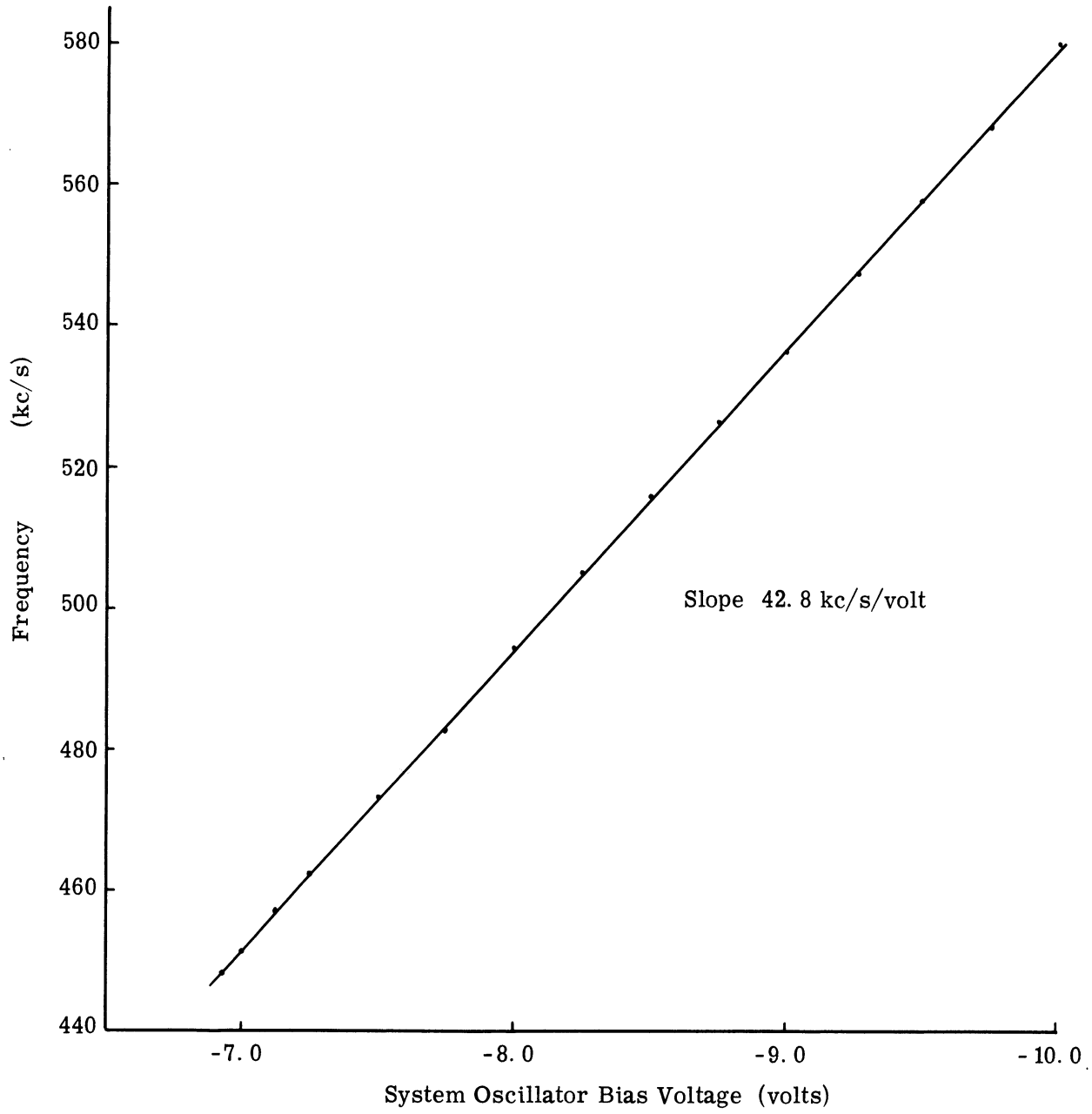

Fig. 5.4. System oscillator frequency versus voltage relation.

pole. An indirect determination follows.

Assuming that $\overline{H}(s)$ for this system has the form

$$\overline{H}(s) = \frac{1}{(1+\tau_1 s)(1+\tau_2 s)} \tag{5.1}$$

and recalling from the experimental work in Section 3.2 that $|\overline{H}(\omega_f)|$ is approximately equal to 0.43 when $\omega_f/2\pi$ is equal to 12.94 kc, then it follows that

$$0.43 = \frac{1}{\left|(1+j\tau_1 2\pi \times 12.94 \times 10^3)(1+j\tau_2 2\pi \times 12.94 \times 10^3)\right|} \quad . \tag{5.2}$$

At this frequency, the transfer function must introduce a phase shift of $-\pi/2$ radians. This requires that

$$\tau_1\tau_2 \, (2\pi \times 12.94 \times 10^3)^2 = 1 \quad . \tag{5.3}$$

Solving Eqs. 5.2 and 5.3 for τ_1 and τ_2 yields

$$\tau_1 = 7.02 \times 10^{-6} \text{ second} \quad ,$$

$$\tau_2 = 21.6 \times 10^{-6} \text{ second} \quad . \tag{5.4}$$

Where τ_2 is the time constant of the RC filter of the system and τ_1 is the time constant of the pole produced by the phase detector. A direct experimental evaluation of τ_2 can be made easily, as a check on the above result. This yields a value of 20.8×10^{-6} second.

Although it is unlikely that the transfer function given by Eq. 5.1, with the values of τ_1 and τ_2 indicated by Eq. 5.4, is an exact description of the actual filter characteristic, the model given is not unreasonable. It should be reiterated that it is difficult to measure experimentally the actual lowpass filter characteristics. This difficulty is caused by the phase detector (multiplier) circuit which introduces phase shift and attenuation in generating the control signal. This filtering action cannot be measured conveniently since the control signal does not exist explicitly in front of the diode circuits, and is modified by the detector filter at subsequent points. For this reason (in addition to the difficulty of experimentally evaluating $\overline{H}(s)$) the phase-detector gain constant, k_m, and hence the system gain, G, are also difficult to obtain directly. Certainly, one of the useful applications of the locked instability oscillation analysis is the indirect evaluation of G and $|\overline{H}(\omega_f)|$ from simple measurements.

5.3 Experimental and Comparative Theoretical Results

The experimental procedure outlined in Section 5.1 for the secondary-interference-signal case was employed to obtain the data shown graphically in Figs. 5.5-5.7. Each of these three sets of curves was made for a constant value of system gain and for $\Delta\omega_r$ equal to zero. The gains for these three sets are, respectively, 3 db, 1 db, and 0 db less than that required

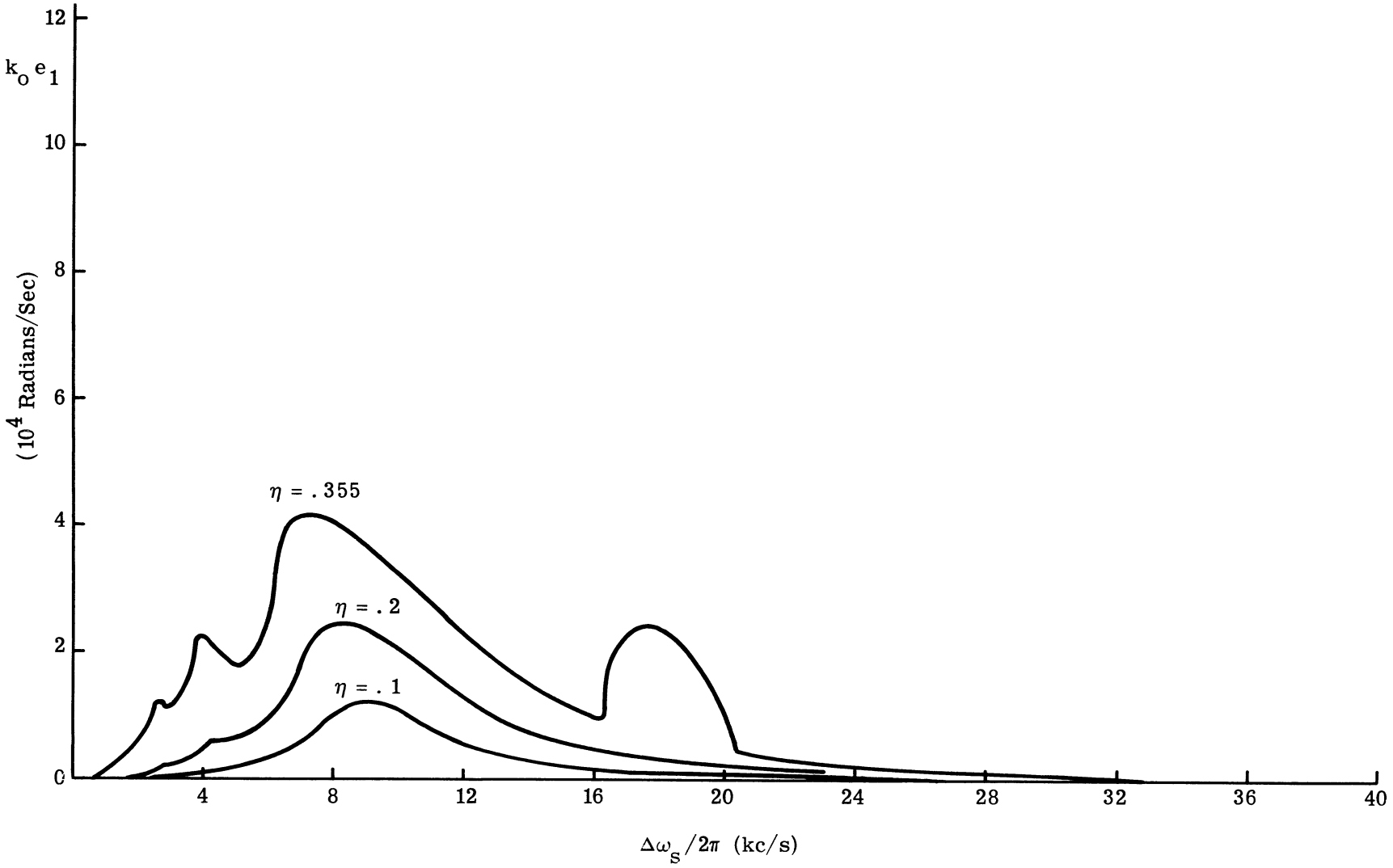

Fig. 5.5. System magnitude response for the experimental circuit with G equal to 1.355×10^5 radians/second.

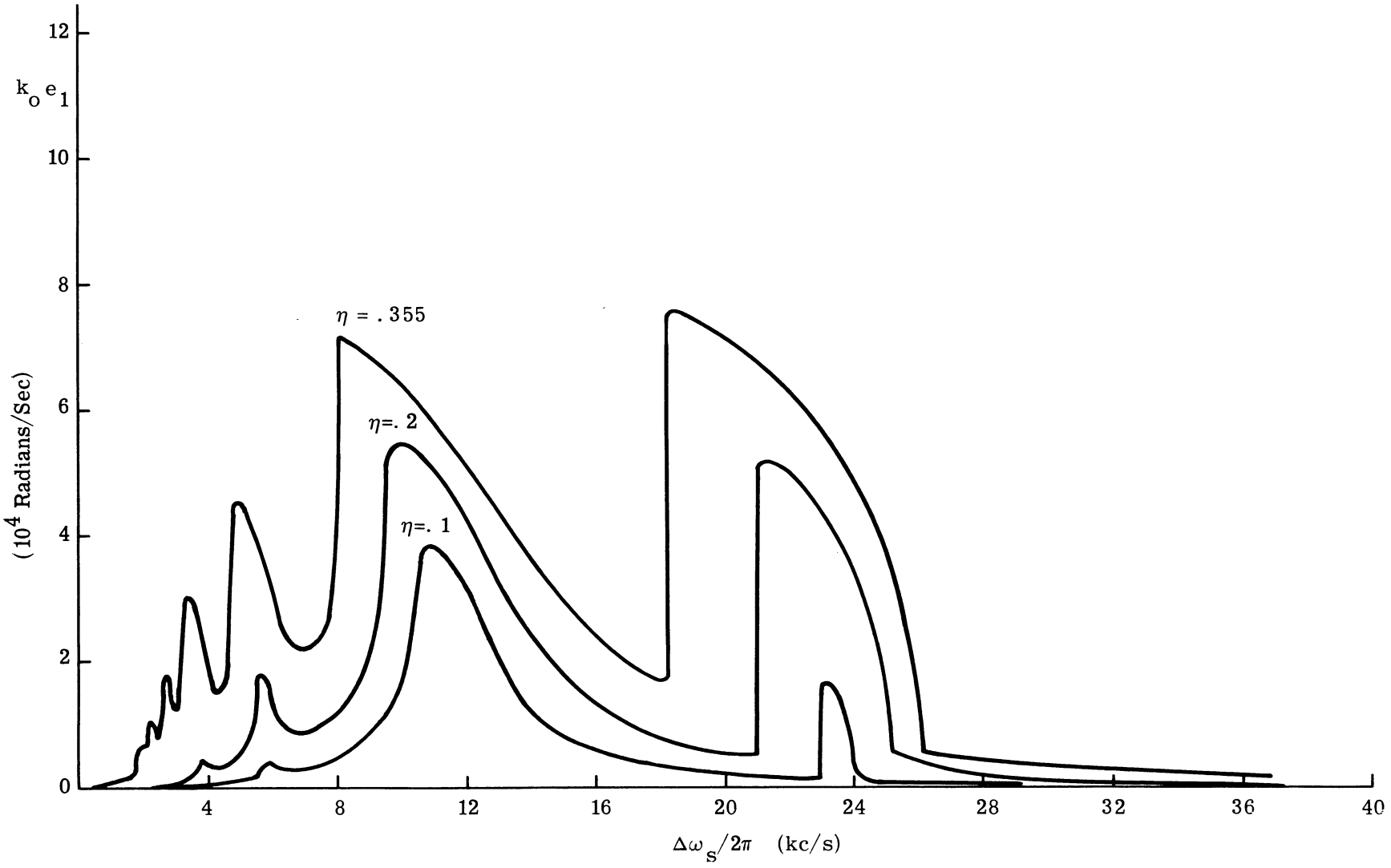

Fig. 5.6. System magnitude response for the experimental circuit with G equal to 1.685 x 10^5 radians/second.

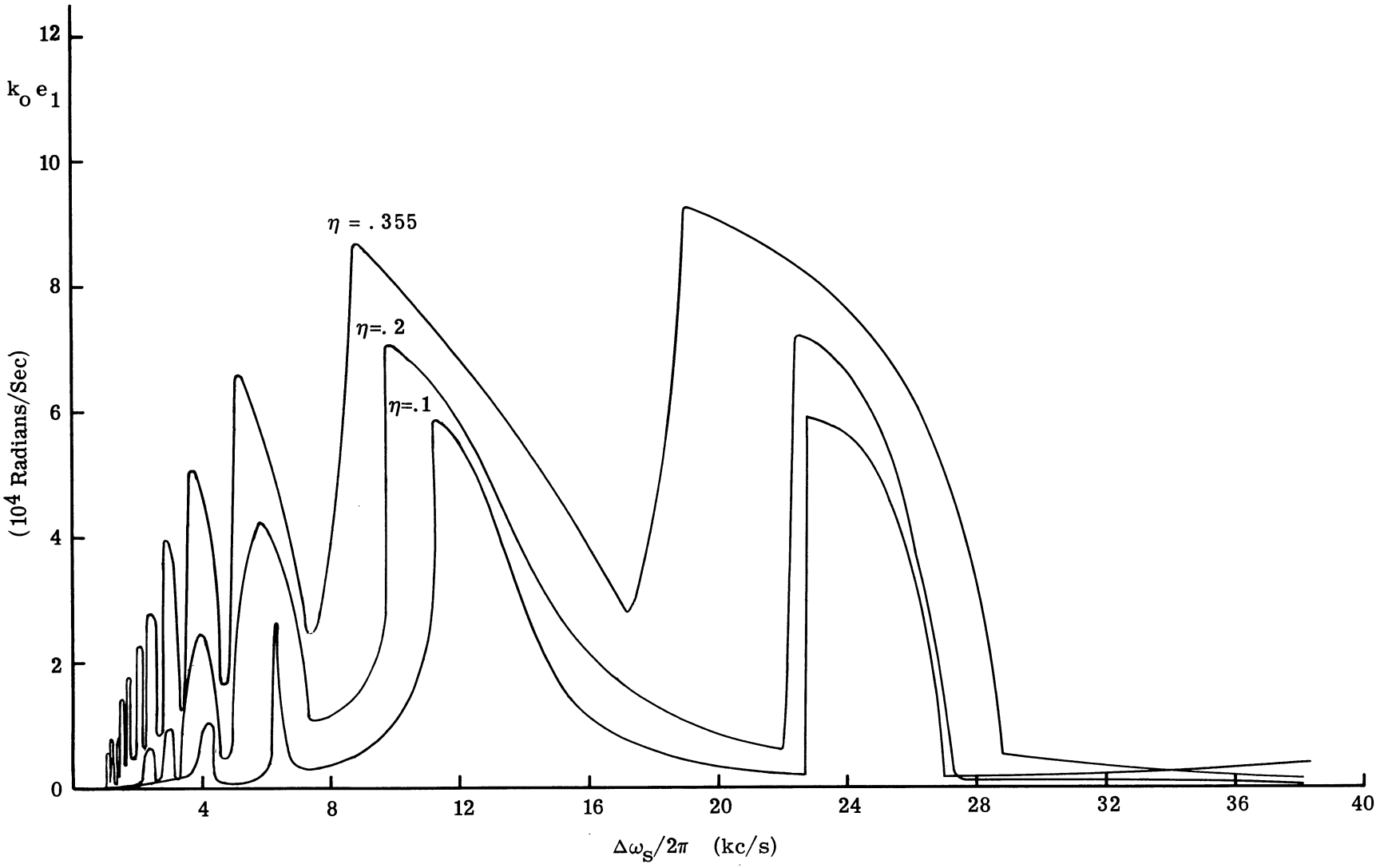

Fig. 5.7. System magnitude response for the experimental circuit with G equal to 1.89×10^5 radians/second.

for the initiation of locked oscillations. The ordinate and abscissa quantities, $k_o e_1$ and $\Delta\omega_s/2\pi$, are those used in Section 4 for the similar theoretical curves. The values of η used here are also the same as in Section 4.

In general, these curves reveal the presence of the harmonic, the first subharmonic, and a series of smaller ultraharmonic system response peaks. The harmonic response peak occurs on the various graphs between 7 and 11 kc. The first subharmonic response peak occurs at approximately twice the frequency of the harmonic peak. The frequency of system response within the subharmonic peak was found to equal $\Delta\omega_s/4\pi$, as expected. The absence of a second subharmonic response also agrees with the theoretical predictions. Although no attempt was made to analyze the ultraharmonic case theoretically, it is reasonable to expect that techniques similar to those used in this study could be applied. These peaks are relatively insignificant for the lower value of η and G. This changes dramatically, however, for the higher values of these parameters. Frequencies of system response within these peaks were, successively, $\frac{2\Delta\omega_s}{2\pi}$ kc, $\frac{3\Delta\omega_s}{2\pi}$ kc, etc.

The photographs in Figs. 5.8 - 5.10 show the system response for conditions as stated individually on each picture. For lower values of η the response is essentially sinusoidal. Nevertheless, it is clear that nonsinusoidal periodic waveforms occur for appreciably high values of η. These effects are pronounced for high values of G. For this reason, the applicability of the theoretical results developed in Section 4 is limited. The high-frequency ripple evident in these pictures is due to imperfect filtering of the system oscillator at the point of observation.

For the purposes of comparison, the analytical techniques developed in Section 4 were applied to a model of this experimental circuit. The system lowpass transfer function given by Eq. 5.1 (using the time constant values given in Eq. 5.4) was assumed for the model. The two filter quantities required by the Newton-Raphson method, i.e., the square of the magnitude of the transfer function and the cotangent of its phase angle, are plotted in Fig. 5.11. The harmonic solutions for the same values of gain used in Figs. 5.5-5.7 are shown respectively in Figs. 5.12-5.14. These latter curves evidence system behavior similar to that observed previously, but they have noticeably more amplitude than the experimental curves. An explanation of this may be that Eq. 5.1 does not adequately describe the actual

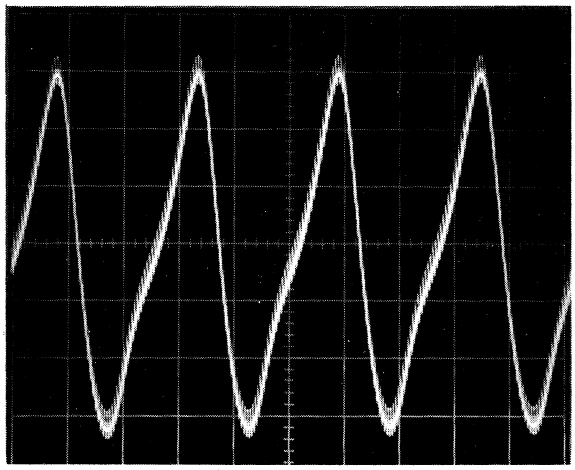

a) The harmonic peak for:
G=-1 db (relative to the gain required for system instability)
η=0.355
Frequency of oscillation (i.e., $\Delta\omega_s/2\pi$) = 7.92 kc/s
Vertical scale 0.1 volt/division
Horizontal scale 50 μsec/division

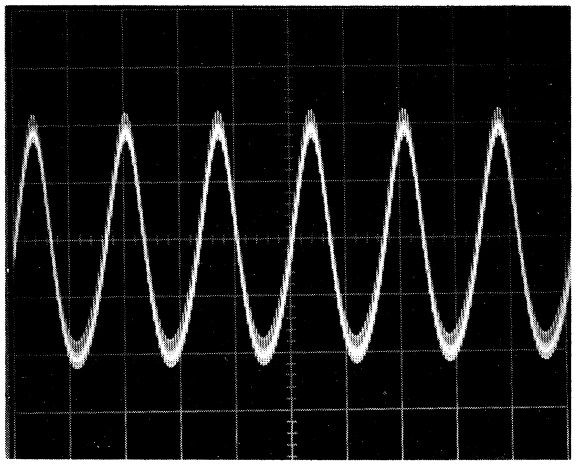

b) Halfway between the harmonic and first subharmonic peaks for the values of G and η used in (a)
Frequency of oscillation (i.e., $\Delta\omega_s/2\pi$) = 11.75 kc/s
Vertical and horizontal scales are identical

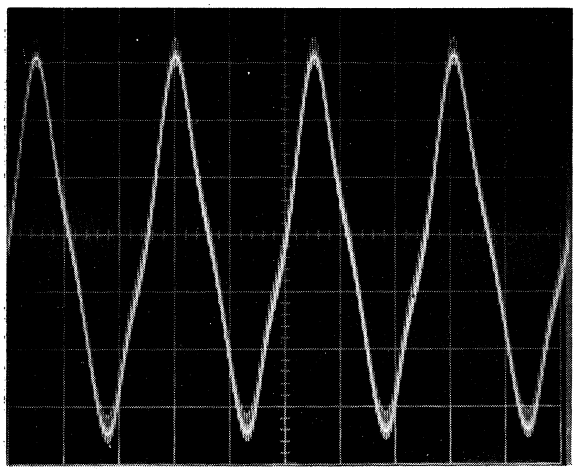

c) First subharmonic peak for the values of G and η used in (a) and (b)
Frequency of oscillation (i.e., $\Delta\omega_s/4\pi$) = 7.85 kc/s
Vertical and horizontal scales are identical

Fig. 5.8. Periodic forced system response waveforms.

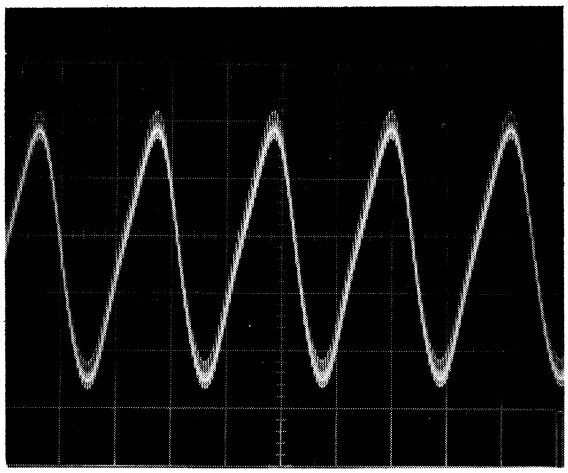

a) The harmonic peak for:
G = -1 db, η = 0.2
Frequency of oscillation
(i.e., $\Delta\omega_s/2\pi$) = 9.52 kc/s
Vertical scale 0.1 volt/division
Horizontal scale 50 μsec/division

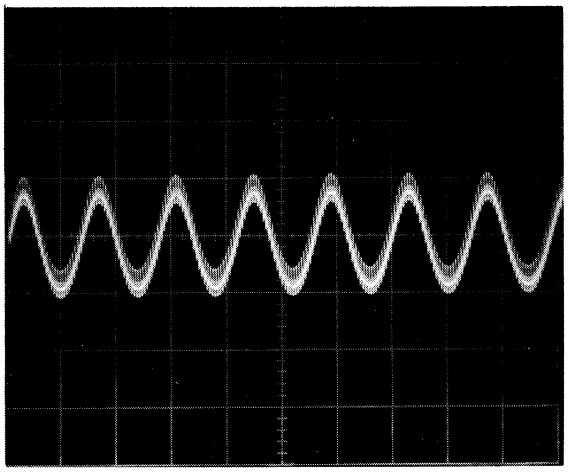

b) Halfway between the harmonic and first subharmonic peaks for the values of G and η used in (a)
Frequency of oscillation
(i.e., $\Delta\omega_s/2\pi$) = 14.30 kc/s
Vertical and horizontal scales are identical

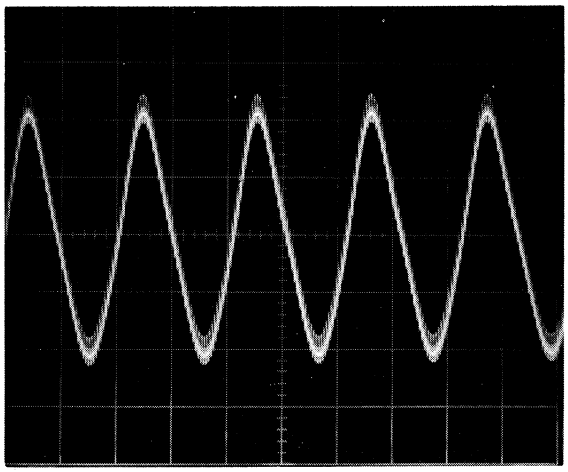

c) First subharmonic peak for the values of G and η used in (a) and (b)
Frequency of oscillation
(i.e., $\Delta\omega_s/4\pi$) = 9.52 kc/s
Vertical and horizontal scales are identical

Fig. 5.9. Periodic forced system response waveforms.

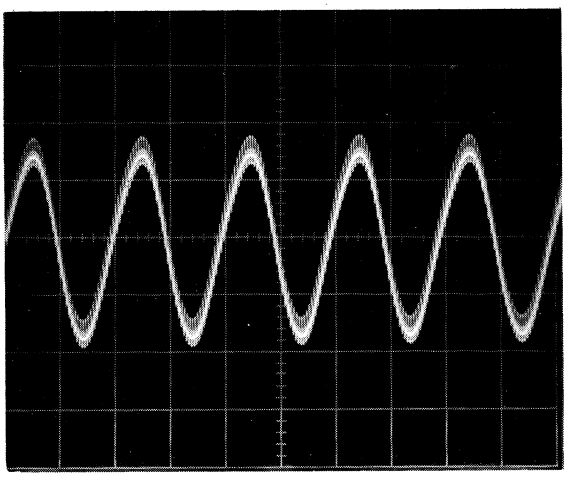

a) The harmonic peak for:
G = -1 db, η = 0.1
Frequency of oscillation
(i.e., $\Delta\omega_s/2\pi$) = 10.00 kc/s
Vertical scale 0.1 volt/
division
Horizontal scale 50 μsec/
division

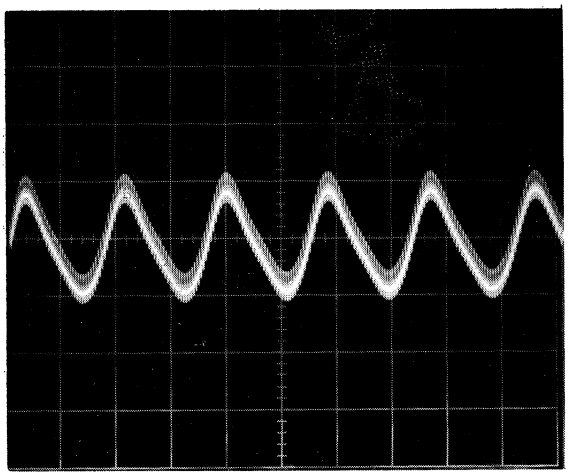

b) The first subharmonic peak
for the values of G and η
used in (a)
Frequency of oscillation
(i.e., $\Delta\omega_s/4\pi$) = 10.52 kc/s
Vertical and horizontal
scales are identical

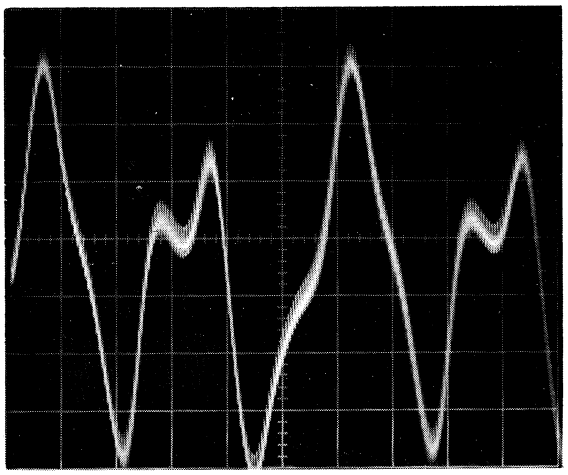

c) System response with $\Delta\omega_s/2\pi$
equal to and for:
G = -1 10.00 kc/s db, η = 0.56
Vertical and horizontal
scales are identical

Fig. 5.10. Periodic forced system
response waveforms.

system transfer function. From the work in Section 4.4 it can be seen that relatively slight changes in the phase angle of the transfer function can influence quite noticeably response characteristics. A second factor is that the actual response is nonsinusoidal for the higher values of η and G; this violates a basic theoretical assumption.

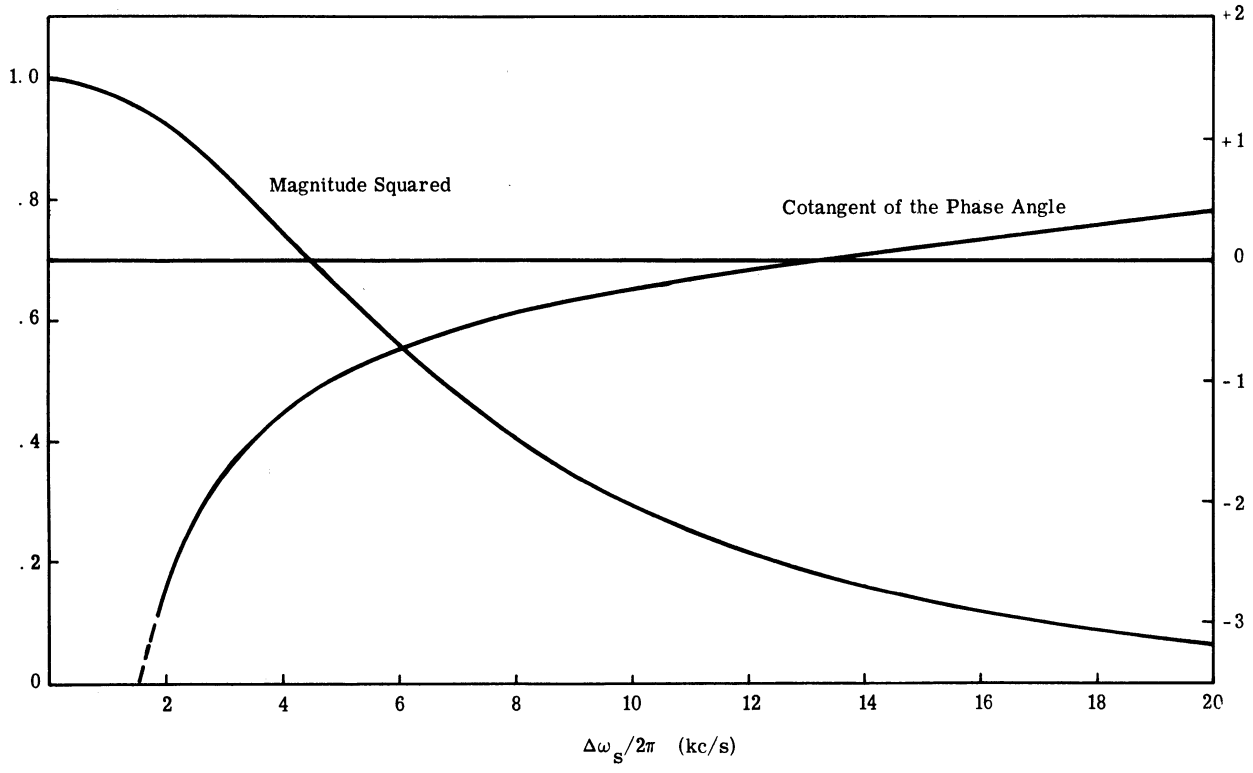

Fig. 5.11. Characteristics of the two-pole filter.

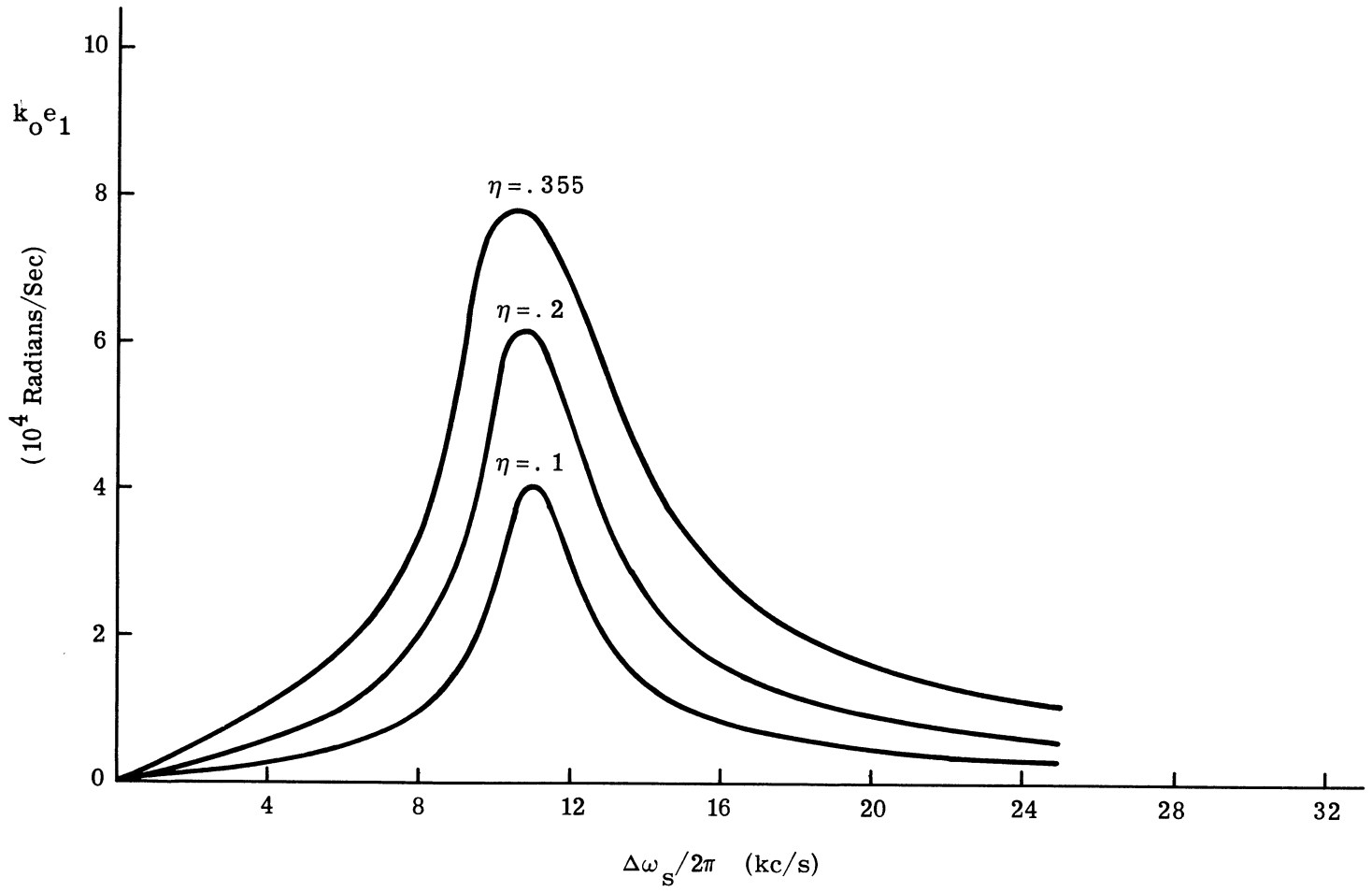

Fig. 5.12. System magnitude response for the two-pole filter with G equal to 1.335×10^5 radians/second.

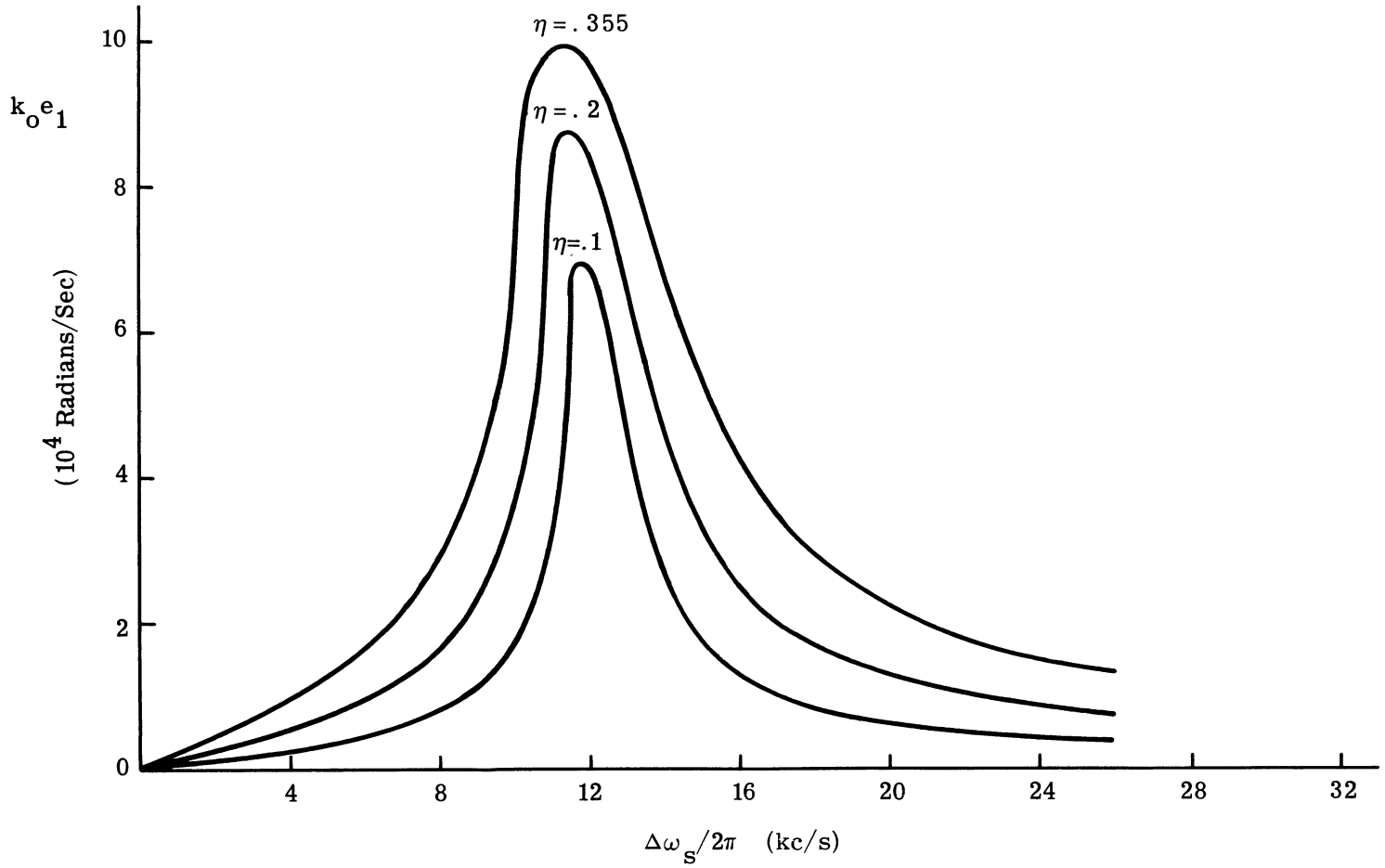

Fig. 5.13. System magnitude response for the two-pole filter with G equal to 1.685×10^5 radians/second.

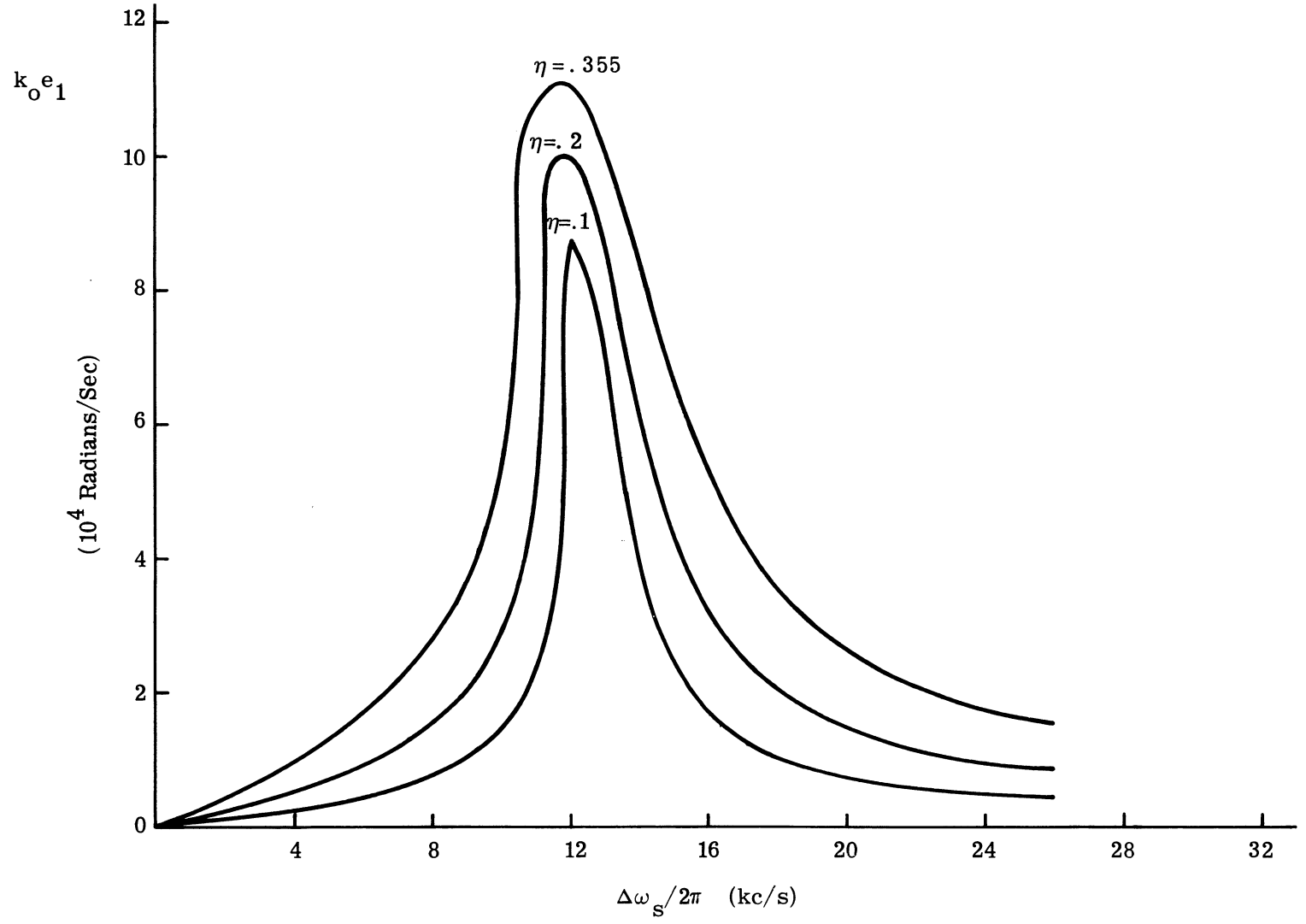

Fig. 5.14. System magnitude response for the two-pole filter with G equal to 1.89×10^5 radians/second.

6. CONCLUSIONS AND APPLICATIONS

Results of this study facilitate an understanding of the causes and effects of the locked, periodic responses of APC systems beyond that previously achieved. Two distinct types of periodic response were considered--locked instability and forced oscillations. The system designer is provided with the tools necessary to determine the possibility of either form of periodic response by his circuit, and with design guidelines for controlling these oscillations where needed. Several conclusions and applications based on the findings of this study are presented below.

The periodic response of an APC system to a single, constant-frequency input signal within the system's capture range has been referred to in this study as a locked instability oscillation. An APC system will exhibit locked instability oscillations only when the following two requirements are met:

1) The transfer function of the system's lowpass filter must introduce a phase shift of $-\pi/2$ radians at a finite frequency, and

2) The total system gain, including the attenuation through the lowpass filter, must exceed unity.

The frequency of oscillation, if it exists, will be the finite frequency at which the first requirement is met.

When locked instability oscillations exist, the magnitude of the periodic response is an even function of $\Delta\omega_r$, the difference between the input (reference) signal frequency and system oscillator's open-loop frequency. The response is maximum for $\Delta\omega_r$ equal to zero and decreases quite abruptly to zero for increasing $|\Delta\omega_r|$. The system phase error is an odd function of $\Delta\omega_r$ and has zero value for zero $\Delta\omega_r$. Except when $\Delta\omega_r$ is equal to zero, the static system phase error always exceeds in absolute value the error that would exist if no oscillations occurred. A typical example of both of these relationships was given in Fig. 3.3. It is generally true that as the system gain increases, the magnitude of the system response increases for any given value of $\Delta\omega_r$, and the range of $\Delta\omega_r$ over which the magnitude is nonzero also increases. The effect on the system phase error is also accentuated as the gain increases.

An additional, interesting aspect of the locked instability oscillation analysis is the ability to determine the system gain and the magnitude of the lowpass filter's transfer function at the frequency of oscillation. Both of these quantities can be found from three easily performed measurements. Since direct measurement of the gain and complete filter characteristics is often difficult, this indirect method is of considerable value. The three measurements needed are those of

1) The frequency of oscillation,

2) The maximum magnitude of oscillation, and

3) The value of $\Delta\omega_r$ at which the oscillations cease.

The specific relationships between these measured quantities and the quantities of interest were developed in Section 3.2 (see Eqs. 3.74-3.77).

The second type of periodic response considered in this study, i.e., forced oscillations, results when the APC system is subjected to two constant-frequency input signals.

In the particular problem analyzed, it is assumed that the greater amplitude input signal is the reference signal and that the other signal differs only slightly in frequency from the reference. It is then shown that the system exhibits a periodic response, i.e., a forced oscillatory response. Under the above conditions, the average frequency of the system oscillator is equal to the reference frequency for low-level periodic responses. (The frequency of the response oscillations should not be confused with the system oscillator frequency.) In contrast to locked stability oscillations which exist only for certain ranges of system parameters, all APC systems exhibit forced oscillations. The peak magnitude of the system response with forced oscillations is related, however, to the stability of the system. Based on the examples of Section 4.4, it can be seen that as the phase shift of the lowpass filter approaches and exceeds $-\pi/2$ radians, the response magnitude increases.

The general characteristics of the forced oscillations are considerably more complex than those of the locked instability oscillations. Three dependent variables are defined for this case--the magnitude of the response, the system phase error (between the reference signal and the system oscillator signal), and the phase relations between the periodic response and the input reference signals. The third variable is usually of little interest and will not be discussed here any further (see Section 4 for additional details). The four independent variables for any given APC system are:

1) G: The system gain,

2) η: The amplitude ratio between the secondary and reference signals,

3) $\Delta\omega_r$: The difference in the radian frequencies of the reference and open-loop system oscillator signals, and

4) $\Delta\omega_s$: The difference in the radian frequencies of the secondary and reference signals.

In general, the magnitude of the system response will be zero whenever $\Delta\omega_s$ is zero, provided that the sum of the input signals does not cause system instability (for systems sensitive to input-signal amplitude). Further, it has been shown that the response magnitude is essentially equal to $\eta\Delta\omega_s$ for small $\Delta\omega_s$. Grandlund found this same behavior for the FM discriminator preceded by a wideband limiter (see Ref. 13). For this reason, it is expected that an APC system designed to operate properly as an FM demodulator will exhibit the same effectiveness against co-channel interference as does the limiter-discriminator combination.

As $\Delta\omega_s$ is increased further, the magnitude of the system response tends to peak in one or more places. The number of peaks and the degree of peaking are a function of the other three independent variables as well as of the lowpass filter characteristic of the system (as discussed previously). Usually, there are two dominant peaks--the harmonic and first subharmonic response peaks. The radian frequency of the response oscillation within these two peaks is, respectively, $\Delta\omega_s$ and $\Delta\omega_s/2$. Since the first subharmonic peak occurs for values of $\Delta\omega_s$ approximately twice those of the harmonic peak, the frequency of system response in these peaks is nearly the same. The harmonic response prevails for values of $\Delta\omega_s$ immediately below and above the first subharmonic peak. The consequent changes of oscillation mode may be, but are not necessarily, quite abrupt. The system response waveform is nearly sinusoidal in both of these peaks for low values of η and G. The existence of any significant higher-order subharmonic peaks was neither predicted by the theory nor observed experimentally.

A number of lesser peaks may exist with values of $\Delta\omega_s$ below that for occurence of the harmonic peak. These ultraharmonic peaks occur in increasing numbers as η is increased, for any fixed value of G. The radian frequencies at which these peaks occur are 1/2, 1/3, 1/4, etc., times the values of $\Delta\omega_s$ for which the harmonic peak exists. The frequencies of system response within these peaks are, respectively, $2\Delta\omega_s$, $3\Delta\omega_s$, $4\Delta\omega_s$, etc. Here the response waveform was quite complex for the experimental system evaluated (see Section 5). Certainly, the existence of these ultraharmonic peaks jeopardizes the co-

channel performance of an APC system. The tendency toward this peaking decreases as G is decreased. Furthermore, it is expected that the magnitude of these peaks can also be decreased through choice of a suitable, relatively stable lowpass filter (such as the single zero-single pole filter of Section 4.4).

The dependence of the system response magnitude on $\Delta\omega_r$ is, in turn, quite dependent on $\Delta\omega_s$. An example of this relation, for the harmonic peak with η and G fixed, was given in Fig. 4.27. In general, the harmonic peak decreases in amplitude, and occurs at lower values of $\Delta\omega_s$, as $\Delta\omega_r$ increases. Furthermore, this peak broadens with increasing $\Delta\omega_r$. The first subharmonic peak tends to decrease in relative size and to disappear eventually for increasing $\Delta\omega_r$, as do the ultraharmonic peaks. In general, the effect of increasing η and/or G is to accentuate the characteristics already discussed.

Modification of the phase error of the system by the presence of the forced oscillations is similar to that in the case of locked instability oscillation. There are some differences, however, in the two cases. For example, the phase error is not generally equal to zero when $\Delta\omega_r$ is zero, although it does not deviate greatly from zero for even moderate values of η and G. The phase error remains an odd function of $\Delta\omega_r$ (essentially the inverse sine of $\Delta\omega_r/G$), and is almost independent of $\Delta\omega_s$. These results have been verified both theoretically and experimentally.

As previously stated, this study serves, a) to provide the designer a means for analyzing his system with regard to its susceptibility to a locked periodic response, and b) to provide guidelines for the control of the locked periodic response. An example of the former is given by the work of Sections 3.2 and 5. From the theoretical work developed in this study, along with the analysis technique described in Appendix A, it is possible to determine analytically the system response characteristics for at least the harmonic and subharmonic response peaks. Likewise, the degree of locked instability oscillation, if any, can be determined for any given value of system gain.

Specific applications where the guidelines are useful are in the design of receivers to reduce co-channel interference and of frequency synthesizers utilizing APC systems. It was mentioned previously that an APC system might effect co-channel rejection of a second FM signal similar to that of the limiter-discriminator circuit. Another related application of an APC system was recently discussed by Bridges and Zalewski (see Ref. 22), who proposed a technique to reduce co-channel interference in AM double-sideband systems--which may employ two APC systems. Each APC system is required to lock to one of the two received carrier signals and reject the other. These carrier signals are assumed to be at

nearly the same frequency. Since the object of the two APC systems is to provide a copy of their respective carriers without any (or, at most, with a minimum of) additional spectral components, results of this study dictate that considerable care must be taken in the design of the two lowpass filters in the system. Specifically, a particularly stable filter is needed to minimize the forced response peaks--at the possible expense of system holding range.

In the design of a particular form of frequency synthesizer (see Ref. 23), APC systems are used to extract a single harmonic component from a reference frequency comb of many, harmonically related signals. It is desirable that the APC system bandwidth approach in value the harmonic separation of adjacent comb components, in order to insure that the system will lock to the desired signal. Beyond this objective, other spectral energy in the output of the APC oscillator should be minimized. Care and compromise in the design of the system filter are required to achieve these two conflicting objectives.

APPENDIX A

NEWTON-RAPHSON METHOD FOR SIMULTANEOUS NON-LINEAR EQUATIONS

The Newton-Raphson method is an iterative technique for the solution of simultaneous non-linear equations. The following brief description is abstracted from Ref. 24. We seek the solution(s) of the system

$$\hat{f}(\hat{x}) = 0 \quad , \tag{A.1}$$

where

$$\hat{x} = \text{column vector } [x_1, x_2, \ldots, x_n] \quad , \tag{A.2}$$

and

$$\hat{f} = \text{column vector } [f_1(\hat{x}), f_2(\hat{x}), \ldots, f_n(\hat{x})] \quad , \tag{A.3}$$

consisting of n real equations in the n real unknowns, $\hat{x}$. Now define the matrix

$$M(\hat{x}) = [f_{ij}(\hat{x})] \qquad 1 \leq i, j \leq n \quad , \tag{A.4}$$

with elements

$$f_{ij}(\hat{x}) = \frac{\partial f_i(\hat{x})}{\partial x_j} \quad . \tag{A.5}$$

Thus, det $M(\hat{x})$ is the Jacobian of the system (A.1) evaluated for the vector $\hat{x}$. With these definitions in mind, and with the starting vector

$$\hat{x}_o = \text{column vector to} [x_{10}, x_{20}, \ldots, x_{n0}] \quad , \tag{A.6}$$

the Newton-Raphson method is given by the iterative equation

$$\hat{x}_{k+1} = \hat{x}_k + \hat{\delta x}_k, \qquad k = 0, 1, 2, 3, \ldots \ , \tag{A.7}$$

where $\hat{\delta x}_k$ is the solution vector for the set of simultaneous linear equations given by

$$M(\hat{x}_k)\hat{\delta x}_k = -\hat{f}(\hat{x}_k) \ . \tag{A.8}$$

It can be proven (see Ref. 24) that if the elements of $M(\hat{x})$ are continuous in a neighborhood of a point $\hat{x}'$ such that

$$\hat{f}(\hat{x}') = 0 \ , \tag{A.9}$$

and if det $M(\hat{x}')$ is nonzero and $\hat{x}_o$ is "near" $\hat{x}'$, then

$$\lim_{k\to\infty} \hat{x}_k = \hat{x}' \ . \tag{A.10}$$

Since the system (A.1) may have several solutions, the requirement that $\hat{x}_o$ be near $\hat{x}'$ guarantees that the selected starting vector will converge to the desired solution.

APPENDIX B

IMPLEMENTATION OF THE NEWTON-RAPHSON METHOD

The Newton-Raphson method described in Appendix A easily may be programmed for the solution of a particular set of equations on a digital computer. The only possible programming complication lies in executing the required solution of a set of simultaneous linear equations (i.e., the solution of Eq. A.8). Since many efficient routines are available for this specific problem, even this usually entails only selecting an appropriate library subroutine.

A flow chart of the program used for the calculations in Sections 4.4 and 5.3 is given in Fig. B.1. This program was designed to solve for the three unknowns β, $\Delta\theta_r$, and $\Delta\theta_s$, as functions of $\Delta\omega_r$ and $\Delta\omega_s$ for fixed values of η and G, all for a given lowpass filter. The starting vector β_o, $\Delta\theta_{ro}$, and $\Delta\theta_{so}$, is supplied for the first values of $\Delta\omega_r$ and $\Delta\omega_s$ analyzed. After the first solution is obtained, $\Delta\omega_r$ is incremented and the solution of the first point is used as the new starting vector. This continues until the maximum desired value of $\Delta\omega_r$ is reached. Then $\Delta\omega_r$ is reset to its initial value and $\Delta\omega_s$ is incremented. Here, the starting vector is the solution to the point with the initial value of $\Delta\omega_r$ and the previous value of $\Delta\omega_s$. For this value of $\Delta\omega_s$, $\Delta\omega_r$ again is run through all of its values. The program continues until the final values of $\Delta\omega_s$ and $\Delta\omega_r$ are reached.

For each point on the $\Delta\omega_r$ - $\Delta\omega_s$ plane, the solution vector is printed and so is the product, $\beta\Delta\omega_s$. This latter value is proportional to the magnitude of the system response. Based on the experience of running this program on an IBM 7090 computer, it was possible to calculate approximately 125 points per minute. (Each point represents a new value of $\Delta\omega_r$ and, when incremented, $\Delta\omega_s$.) Typically, between three and four iterations were required for each point when it was specified that each of the variables, δx_{k_1}, δx_{k_2}, and δx_{k_3} at any given iteration was less than one percent of the respective values of the elements of $\hat{x}_k$.

The $M(\hat{x})$ elements required by the Newton-Raphson method are determined from the coefficient equations derived in Section 4.2; namely, Eqs. 4.11, 4.16, 4.17. These are rewritten here in the format of Appendix A.

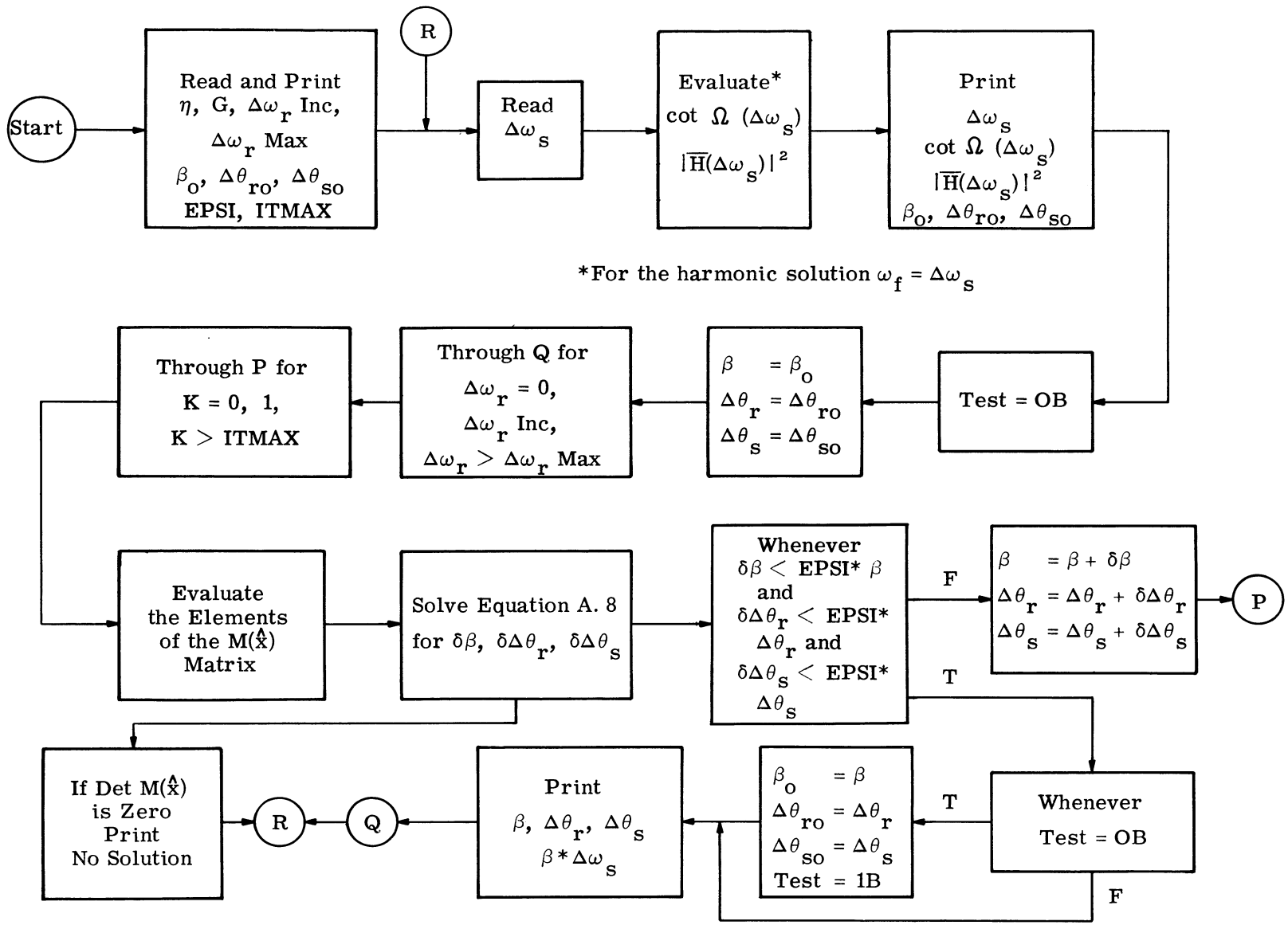

Fig. B.1. Flow chart of the Newton-Raphson method program.

$$f_1(\hat{x}) = \Delta\omega_r - G[J_o(\beta)\sin(\Delta\theta_r) + \eta J_n(\beta)\sin(\Delta\theta_s)], \tag{B.1}$$

$$f_2(\hat{x}) = \cot(\omega_f) - \frac{\eta J_{n-1}(\beta)\sin(\Delta\theta_s)}{\eta J_{n-1}(\beta)\cos(\Delta\theta_s) - 2J_1(\beta)\cos(\Delta\theta_r)}, \tag{B.2}$$

$$f_3(\hat{x}) = \beta^2\omega_f^2 - G^2|\overline{H}(\omega_f)|^2[4J_1^2(\beta)\cos^2(\Delta\theta_r) - 4J_1(\beta)\cos(\Delta\theta_r)\cdot\eta J_{n-1}(\beta)\cos(\Delta\theta_s) + \eta^2 J_{n-1}^2(\beta)], \tag{B.3}$$

where $\hat{x}$ = column vector $[\beta, \Delta\theta_r, \Delta\theta_s]$. (B.4)

The respective partial derivatives (the matrix required elements) can be expressed as:

$$f_{11}(\hat{x}) = -G\{J_1(\beta)\sin(\Delta\theta_r) + \eta\sin(\Delta\theta_s)[\frac{n}{\beta}J_n(\beta) - J_{n-1}(\beta)]\}, \tag{B.5}$$

$$f_{12}(\hat{x}) = G J_o(\beta)\cos(\Delta\theta_r), \tag{B.6}$$

$$f_{13}(\hat{x}) = \eta G J_n(\beta)\cos(\Delta\theta_s), \tag{B.7}$$

$$f_{21}(\hat{x}) = \frac{2\eta\sin(\Delta\theta_s)\cos(\Delta\theta_r)[J_o(\beta)J_{n-1}(\beta) - \frac{n}{\beta}J_1(\beta)J_{n-1}(\beta) + J_1(\beta)J_n(\beta)]}{[\eta J_{n-1}(\beta)\cos(\Delta\theta_s) - 2J_1(\beta)\cos(\Delta\theta_r)]^2}, \tag{B.8}$$

$$f_{22}(\hat{x}) = \frac{-2\eta J_1(\beta)J_{n-1}(\beta)\sin(\Delta\theta_s)\sin(\Delta\theta_r)}{[\eta J_{n-1}(\beta)\cos(\Delta\theta_s) - 2J_1(\beta)\cos(\Delta\theta_r)]^2}, \tag{B.9}$$

$$f_{23}(\hat{x}) = \frac{\eta^2 J_{n-1}^2(\beta) - 2\eta J_1(\beta)J_{n-1}(\beta)\cos(\Delta\theta_s)\cos(\Delta\theta_r)}{[\eta J_{n-1}(\beta)\cos(\Delta\theta_s) - 2J_1(\beta)\cos(\Delta\theta_r)]^2}, \tag{B.10}$$

$$f_{31}(\hat{x}) = G^2|\overline{H}(\omega_f)|^2\{8\cos^2(\Delta\theta_r)J_1(\beta)[J_o(\beta) - \frac{1}{\beta}J_1(\beta)] - 4\eta\cos(\Delta\theta_r)\cdot\cos(\Delta\theta_s)J_{n-1}(\beta)[J_o(\beta) - \frac{1}{\beta}J_1(\beta)] - 4\eta\cos(\Delta\theta_r)\cos(\Delta\theta_s)J_1(\beta)\cdot[\frac{n-1}{\beta}J_{n-1}(\beta) - J_n(\beta)] + 2\eta^2 J_{n-1}(\beta)[\frac{n-1}{\beta}J_{n-1}(\beta) - J_n(\beta)]\} - 2\beta\omega_f^2, \tag{B.11}$$

$$f_{32}(\hat{x}) = 4G^2|\overline{H}(\omega_f)|^2 J_1(\beta)\sin(\Delta\theta_r)[\eta J_{n-1}(\beta)\cos(\Delta\theta_s) - 2J_1(\beta)\cos(\Delta\theta_r)], \tag{B.12}$$

$$f_{33}(\hat{x}) = 4\eta G^2|\overline{H}(\omega_f)|^2 J_1(\beta)J_{n-1}(\beta)\cos(\Delta\theta_s)\cos(\Delta\theta_r). \tag{B.13}$$

Equations B.5-B.13 constitute the nine elements required for the 3 x 3 $M(\hat{x})$ matrix in Eq. A.8 for the original three coefficient equations. Equations B.1-B.3 constitute the elements of the $\hat{f}(\hat{x})$ vector also required by Eq. A.8. In the program, all twelve of thse elements must be evaluated at each iteration in order to solve for the correction elements in $\delta\hat{x}_k$.

APPENDIX C

DERIVATION OF SOME FOURIER COEFFICIENTS

In Section 4.6, the Fourier series expansion of two periodic functions are required. The appropriate coefficients for these series are developed below. The first function to be considered is the radical expression, $\sqrt{1 + \eta^2 + 2\eta \cos \Delta\omega_s t}$, with period $2\pi/\Delta\omega_s$. The constant η is positive and less than unity. This function is even with respect to t and has a nonzero average value.

The appropriate cosine series coefficients are given by

$$a_k = \frac{2}{\pi} \int_0^{\pi} \sqrt{1 + \eta^2 + 2\eta \cos x} \cos kx \, dx, \; k = 0, 1, 2 \ldots \; , \tag{C.1}$$

where

$$x = \Delta\omega_s t. \tag{C.2}$$

With the aid of the identity

$$\cos x = 1 - 2 \sin^2\left(\frac{x}{2}\right) \; , \tag{C.3}$$

the a_o coefficient becomes

$$a_o = \frac{4}{\pi} \int_0^{\pi} \sqrt{1 + 2\eta + \eta^2 - 4\eta \sin^2\left(\frac{x}{2}\right)} \, dx/2 \; , \tag{C.4}$$

or

$$a_o = \frac{4}{\pi} \int_0^{\pi/2} \sqrt{(1 + \eta)^2 - 4\eta \sin^2 y} \, dy \tag{C.5}$$

with the change of variables

$$y = x/2 \; . \tag{C.6}$$

Let

$$k^2 = \frac{4\eta}{(1+\eta)^2} \quad . \tag{C.7}$$

Then Eq. C.5 may be written as

$$a_o = \frac{4(1+\eta)}{\pi} \int_o^{\pi/2} \sqrt{1 - k^2 \sin^2 y}\, dy = \frac{4(1+\eta)}{\pi} E(k,\pi/2) \quad , \tag{C.8}$$

where $E(k,\pi/2)$ is the complete elliptic integral of the "second kind." Although $E(k,\pi/2)$ is a function of k (and hence η) it will be helpful to write it simply as E in the following development. Thus, the leading coefficient in the cosine series is just

$$a_o/2 = \frac{2(1+\eta)}{\pi} E \quad . \tag{C.9}$$

For small η this may be expanded in the form

$$a_o/2 = (1+\eta)\left[1-\eta-\frac{3}{4}\frac{\eta^2}{(1+\eta)^2} - \ldots\right] \tag{C.10}$$

which shows that the average value of this function for small η is similar to unity.

The calculation of the coefficient a_1 is carried out in much the same way. With the changes of variables (C.2, C.6 and C.7) and the identity (C.3), a_1 may be written as

$$a_1 = \frac{4(1+\eta)}{\pi} \int_o^{\pi/2} \sqrt{1 - k^2 \sin^2 y}\,(1 - 2 \sin^2 y)\, dy \tag{C.11}$$

or

$$a_1 = \frac{4(1+\eta)}{\pi} \left[E - 2 \int_o^{\pi/2} \sin^2 y \sqrt{1 - k^2 \sin^2 y}\, dy \right] \tag{C.12}$$

The integral of Eq. C.12 may be evaluated with the aid of the identity

$$\int_o^{\pi/2} \sin^2 y \sqrt{1 - k^2 \sin^2 y}\, dy = \int_o^{\pi/2} \frac{\sin^2 y(1 - k^2 \sin^2 y)\, dy}{\sqrt{1 - k^2 \sin^2 y}} \quad . \tag{C.13}$$

With the aid of Ref. 25 the two terms of the right-hand side may be expressed by

$$\int_0^{\pi/2} \frac{\sin^2 y\, dy}{\sqrt{1-k^2 \sin^2 y}} = \frac{1}{k^2} [F(k,\pi/2) - E] \tag{C.14}$$

and

$$\int_0^{\pi/2} \frac{\sin^4 y\, dy}{\sqrt{1-k^2 \sin^2 y}} = \frac{2}{3k^2} (1+k^2) \frac{(F(k,\pi/2) - E)}{k^2} - \frac{1}{3k^2} F(k,\pi/2) \quad , \tag{C.15}$$

where $F(k,\pi/2)$ is the complete elliptic integral of the "first kind", abbreviated to F below. Combining these expressions yields

$$a_1 = \frac{4(1+\eta)}{3k^2\pi} [(2 - k^2) E + 2(k^2 - 1)F] \quad . \tag{C.16}$$

For small η it may be shown that a_1 is similar to η.

The higher order coefficients may be found in exactly the same way. For example a_2 is easily placed in the form

$$a_2 = \frac{4(1+\eta)}{\pi} \int_0^{\pi/2} \sqrt{1 - k^2 \sin^2 k} \, (1 - 8 \sin^2 y + 8 \sin 4y)\, dy \quad , \tag{C.17}$$

from which it is not difficult but somewhat tedious to show that

$$a_2 = \frac{4(1+\eta)}{15\pi} [15k^2 E - 8(1 + k^2)F + 16(1 - k^2 + k^4)D] \quad , \tag{C.18}$$

where D is defined as

$$D = \frac{F - E}{k^2} \quad . \tag{C.19}$$

The second function for which the Fourier coefficients must be found is $\Delta\omega_s \frac{\eta\cos(\Delta\omega_s t) + \eta^2}{1+\eta^2+2\eta\cos(\Delta\omega_s t)}$. In this case it is easy to derive the general coefficient. Once again this function is even with respect to t, but has no constant term. This may be seen from its integral (Eq. 4.34) which has no term increasing linearly with t. The desired coefficients are given by

$$a_k = \frac{2\eta\Delta\omega_s}{\pi} \int_0^{\pi} \frac{\cos x+\eta}{1+\eta^2+2\eta\cos x} \cos kx\, dx, \quad k = 1, 2, \ldots \quad , \tag{C.20}$$

where again

$$x = \Delta\omega_s t \quad . \tag{C.21}$$

With the aid of the following two definite integrals found in Ref. 25,

$$\int_o^{\pi} \frac{\cos kx dx}{1+\eta^2+2\eta\cos x} = \frac{\pi(-\eta)^k}{1-\eta^2} \quad \text{for} \quad \eta^2 < 1 \tag{C.22}$$

and

$$\int_o^{\pi} \frac{\cos x \cos kx dx}{1+\eta^2+2\eta\cos x} = \frac{\pi}{2} \frac{1+\eta^2}{1-\eta^2} (-\eta)^{k-1} \quad \text{for} \quad \eta^2 < 1 \quad , \tag{C.23}$$

Eq. C.20 takes the form

$$a_k = \frac{2\eta\Delta\omega_s}{\pi}\left[\frac{\pi}{2} \frac{1+\eta^2}{1-\eta^2} (-\eta)^{k-1} + \eta \frac{\pi(-\eta)^k}{1-\eta^2}\right] , \tag{C.24}$$

which can be simplified algebraically to

$$a_k = -(-\eta)^k \Delta\omega_s \quad . \tag{C.25}$$

REFERENCES

1. G. W. Preston and J. C. Tellier, "The Lock-In Performance of an AFC Circuit," Proc. IRE, Vol. 41 (1953), pp. 249-251.

2. W. J. Gruen, "Theory of AFC Synchronization," Proc. IRE, Vol. 41 (1953), pp. 1043-1048.

3. R. Jaffe and E. Rechtin, Design and Performance of Phase-Lock Loops Capable of Near-Optimum Performance Over a Wide Range of Input Signal and Noise Levels, Progress Report No. 20-243, Jet Propulsion Laboratory, Dec., 1954.

4. A. J. Viterbi, Acquisition and Tracking Behavior of Phase-Locked Loops, External Publication No. 673, Jet Propulsion Laboratory, July, 1959.

5. H. T. McAleer, "A New Look at the Phase-Locked Oscillator," Proc. IRE, Vol. 47 (1959), pp. 1137-1143.

6. T. J. Rey, "Automatic Phase Control: Theory and Design," Proc. IRE, Vol. 48 (1960), pp. 1760-1771.

7. C. S. Weaver, "Thresholds and Tracking Ranges in Phase-Locked Loops," IRE Trans. SET, Sept. 1961, pp. 60-70.

8. A. K. Rue and P. A. Lux, "Transient Analysis of a Phase-Locked Loop Discriminator," IRE Trans. SET, Dec. 1961, pp. 105-111.

9. D. L. Schilling, The Response of an Automatic Phase Control System to FM Signals and Noise, Research Report No. PIBMRI-1040-62, Polytechnic Inst. of Brooklyn, June 1962.

10. J. A. Develet, Jr., "A Threshold Criterion for Phase-Lock Demodulation," Proc. IEEE, Vol. 51 (1963), pp. 349-356.

11. A. J. Viterbi, "Phase-Locked Loop Dynamics in the Presence of Noise by Fokker-Planck Techniques," Proc. IEEE, Vol. 51 (1963), pp. 1737-1753.

12. H. L. VanTrees, "Functional Techniques for the Analysis of the Nonlinear Behavior of Phase-Locked Loops," Proc. IEEE, Vol. 52 (1964), pp. 894-911.

13. J. Granlund, Interference in Frequency-Modulated Reception, Technical Report No. 42, Mass. Inst. of Tech., Jan., 1949.

14. T. S. George, "Analysis of Synchronization Systems for Dot-Interlace Color Television," Proc. IRE, Vol. 39 (1951), pp. 124-131.

15. D. Richman, "Color-Carrier Reference Phase Synchronization Accuracy in NTSC Color Television," Proc. IRE, Vol. 42 (1954), pp. 106-288.

16. L. H. Enloe, "Decreasing the Threshold in FM by Frequency Feedback," Proc. IRE, Vol. 50 (1962), pp. 18-30.

17. C. S. Weaver, "Increasing the Dynamic Tracking Range of a Phase-Locked Loop," Proc. IRE, Vol. 48 (1960), pp. 952-953.

18. Reference Data for Radio Engineers, (International Telephone and Telegraph Corp., 1956).

19. E. A. Coddington and N. Levinson, Theory of Ordinary Differential Equations, (New York: McGraw-Hill Book Company, Inc., 1955).

20. F. R. Moulton, Differential Equations (New York: Dover Publications, 1958).

21. J. J. Stoker, Nonlinear Vibrations in Mechanical and Electrical Systems, (New York: Interscience Publishers, Inc., 1950).

22. J. E. Bridges and R. A. Zalewski, "Orthogonal Detection to Reduce Common Channel Interference," Proc. IEEE, Vol. 52 (1964), pp. 1022-1028.

23. T. W. Butler, Jr. and E. M. Aupperle, "Solid-State Discrete-Frequency Synthesizer," IRE Trans. Inst., Sept. 1962, pp. 67-71.

24. B. Carnahan, H. A. Luther, and J. O. Wilkes, Applied Numerical Methods, Vol. I, (New York: John Wiley and Sons, Inc., 1964).

25. I. M. Ryshiki and I. S. Gradstein, Summen-, Produkt-, und Integral-Tafeln Tables, (Berlin: VEB Deutscher Verlag Der Wissenschaften, 1957).

DISTRIBUTION LIST

No. of Copies	
20	DDC Cameron Station, Bldg. 5 ATTN: TISIA 5010 Duke Street Alexandria, Virginia
3	AFAL Wright-Patterson AFB, Ohio ATTN: AVWW (Deception)
2	Research and Technology Division Wright-Patterson AFB, Ohio ATTN: SEPI SEPIR
1	Dr. B. F. Barton, Director Cooley Electronics Laboratory The University of Michigan Ann Arbor, Michigan
40	Project File Cooley Electronics Laboratory The University of Michigan Ann Arbor, Michigan